Relativity
and
Electron Correlation
in
Chemistry

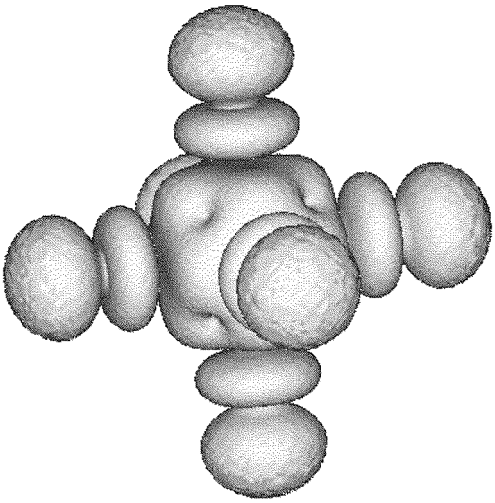

L. Visscher

Relativity and Electron Correlation in Chemistry

RIJKSUNIVERSITEIT GRONINGEN

Relativity and Electron Correlation in Chemistry

PROEFSCHRIFT

ter verkrijging van het doctoraat in de
Wiskunde en Natuurwetenschappen
aan de Rijksuniversiteit Groningen
op gezag van de
Rector Magnificus Dr S. K. Kuipers
in het openbaar te verdedigen op
vrijdag 10 september 1993
des namiddags te 2.45 uur precies

door

Lucas Visscher

geboren op 23 juni 1966
te Meppel

Promotor: Prof. Dr W. C. Nieuwpoort

Referent: Dr P. J. C. Aerts

Groningen, 20 juli 1993

Voorwoord

Nu het proefschrift zo goed als gereed is, is het tijd voor een woord van dank aan al degenen die in meer of mindere mate hebben bijgedragen aan het onderzoek dat de basis vormt voor dit werk.

Allereerst wil ik mijn promotor Wim Nieuwpoort bedanken voor de ruimte die hij mij bood om mijn eigen ideëen uit te werken en voor de verhelderende discussies over de fysica achter de methoden.

Ik wil mijn referent Patrick Aerts bedanken voor de introduktie op het terrein van de relativistische quantumchemie, al onze "gebalanceerde" discussies en natuurlijk ook voor het kritisch lezen van de vroege versies van dit proefschrift.

Dank ook aan de professoren Haas en Snijders omdat ze snel tijd vrij wisten te maken voor het lezen en beoordelen van het manuscript.

I would like to thank Knut Faegri for his careful reading of the manuscript and for the good cooperation and discussions over the years. I thank you and Odd Gropen also for organising the pleasant Oslo and Tromsø workshops that gave me lots of new ideas.

I like to thank Ajaya Mohanty and Ken Dyall for their hospitality during my visit to the States. Ken, I'm looking forward to come to California to do some new research together.

A special word of thank goes to Trond Saue. Without your enthousiasm and collaboration the chapter on PtH would not have been here in this form. I also thank you for your appearance as paranimf at the promotion.

Ook een speciaal woord van dank voor mijn andere paranimf, Olivier Visser. De door jou geschreven programma's en onze discussies over computers en methoden hebben in belangrijke mate bijgedragen aan dit proefschrift.

Hirzo Merenga wil ik graag bedanken voor het opvoeren van het boemeltje MFDSCF tot een op TGV snelheid convergerend programma.

De leden van de vakgroep Theoretische Chemie wil ik uiteraard ook bedanken voor de goede sfeer tijdens de promotie periode. Mijn voormalige kamergenoot Bauke Kooistra bedank ik voor alle time-reversed conversaties, mijn andere voormalige kamergenoot Theo Thole voor zijn geheel eigen kijk op mijn onderzoek, mijn huidige kamergenoot Bert de Jong voor het uittesten van DIRRCI's limieten, Johan Heijnen voor het in goede staat houden van de harde en softe waar, Ria Broer voor het me wegwijs maken in de wereld van vaste stof clusterberekeningen en last but not least Alex de Vries die van een pauze echt een pauze wist te maken.

Tenslotte wil ik uiteraard ook jou, Tineke, bedanken voor je steun gedurende de gehele promotieperiode en in het bijzonder die tijdens de laatste hectische maanden.

Acknowledgement

This investigation was supported by The Netherlands Foundation for Fundamental Research on Matter (FOM) with financial aid from The Netherlands Organisation for Scientific Research (NWO).

Part of the calculations were performed on the Dutch CRAY-YMP/464 supercomputer using a grant from the National Computing Facilities Foundation (NCF).

Voor mijn vader
Ter nagedachtenis aan mijn moeder

"Atomics is a very intricate theorem and can be worked out with algebra but you would want to take it by degrees because you might spend the whole night proving a bit of it with rulers and cosines and similar other instruments and then at the wind-up not believe what you had proved at all. If that happened you would have to go back over it till you got a place where you could believe your own facts and figures as delineated from Hall and Knight's Algebra and then go on again from that particular place till you had the whole thing properly believed and not have bits of it half-believed or a doubt in your head hurting you like when you loose the stud of your shirt in bed."

The Third Policeman, Flann O'Brien.

Contents

Parts of this thesis have been, or will be, published separately. The references are :

Chapter 3 : L. Visscher, O. Visser, P. J. C. Aerts, W. C. Nieuwpoort and H. Merenga, to be published in MOTECC 1994 (Escom : Leiden).

Chapter 4 : L. Visscher, P. J. C. Aerts, O. Visser, W. C. Nieuwpoort, Int. J. Quantum Chem. : Quantum Chem. Symp. **25**, 131 (1991).

Chapter 5 : L. Visscher, T. Saue, W. C. Nieuwpoort, K. Faegri, O. Gropen, accepted for publication in J. Chem. Phys.

1. General Introduction

1.1. Physical motivation of the research

Molecules and crystals that contain heavy elements, in particular 5d transition metals and rare earths, are of growing interest in chemistry and physics. For instance the diversity of gold chemistry[1], the catalytic activity of platinum[2] and the luminescence of lanthanide-doped crystals[3] can be mentioned as examples of recent studies. Whereas spectra and other properties of light atoms and molecules can be satisfactory explained in a non-relativistic quantum mechanical model, one has to consider the theory of relativity if one deals with elements that belong to the lower regions of the periodic table.

In chemistry the most well known shortcoming of the non-relativistic quantum theory is the ad hoc introduction of electron spin and the neglect of spin-orbit coupling. The coupling between the spin and orbital momentum breaks the strict spin selection rules that follow from non-relativistic quantum theory. The influence of this coupling on spectra may be profound. In the spectrum of mercury for instance we find that the strong line at 2537 Å arises from the "spin-forbidden" $^3P_1 \rightarrow {}^1S_0$ transition[4]. The effects on chemical bonding are also non-negligible since the l-shells of the atoms are splitted into $j = l \pm 1/2$ subshells. In the 6p series for instance one finds a separation between the $p_{1/2}$ and the $p_{3/2}$ subshell that is of the order of an electronvolt[5]. This large energy difference prohibits formation of strong σ-bonds with these elements since σ-bonds require participation (hybridisation) of both $p_{1/2}$ and $p_{3/2}$ orbitals[6].

Other important but not directly observable manifestations of relativity are the mass-velocity correction and the Darwin correction[7]. These terms lead to the "relativistic contraction" of the s- and p-shells and to expansion of the d- and f-shells. A consequence of this contraction is for instance the stabilisation of the 6s shell that leads to a considerable increase of the electron affinity of platinum and gold.

Many more examples of chemical consequences of relativity may be found in the literature[4,5,6,8,9,10]. The phrase "relativistic effects" that is often used in this context is a bit misleading since the effects that were described above are of course unphysical. The atoms do not really contract since there is no "non-relativistic atom" just like there is no "relativistic atom". The contraction is the difference between the outcome of different models and has nothing to do with a real physical process.

However, the success and widespread use of the non-relativistic quantum mechanical model in chemistry makes it worthwhile to investigate its limits and analyse its deviations from more precise models. The purpose of this work is to derive and use a formalism that enables such an investigation. The method is based on the Dirac

equation that describes the motion of an electron in accordance with both the theory of special relativity and the theory of quantum mechanics.

1.2. Relativistic ab initio calculations

The starting point of non-relativistic quantum chemistry is the Schrödinger equation that describes the motion of electrons and nuclei. This many-particle equation cannot be solved exactly and ways to obtain approximate solutions must be found.

In the so-called *ab initio* type of methods one attempts to solve the many-particle Schrödinger equation with a minimum of experimental information. The only parameters that are used are fundamental physical constants like the masses and charges of the electron and nuclei. The quality of the outcome depends on the validity of the approximations that were made to make the problem computationally feasible and on the numerical accuracy that can be attained.

The motion of the nuclei and the electrons can be separated in the Born-Oppenheimer[11] approximation by assuming that the time-scale of electronic movement is much smaller than that of nuclear movement. We then obtain with a many-electron equation in which the interaction with the nuclei is represented by an electric field. A commonly used approximation scheme for this many-electron equation is the Hartree-Fock method that reduces it to an effective one-electron equation. The many-electron wave functions that are formed from the solutions of the latter equation differ from the exact solutions of the hamiltonian by the absence of terms that account for the correlation between the motion of electrons with different spin. This correlation, which may be of key importance in the determination of the ground state or structure of a molecule, can be treated by a number of accurate, but computationally more demanding, post Hartree-Fock methods. Well known methods[12] are the Multi Configurational Self Consistent Field (MCSCF) method, the Configuration Interaction (CI) method and the Coupled Cluster (CC) method. Alternatively, instead of using one of these explicitly correlated methods, one may employ Density Functional[13] methods that implicitly account for electron correlation.

In the past decades these *ab initio* methods based on the Schrödinger equation have been successfully applied to the calculation of physical and chemical properties of a variety of (small) molecules. Computer codes that may be used for such *ab initio* calculations have become widely available and are becoming a standard and easy to use tool in chemical research.

In most codes relativity is, however, either not treated, or treated by the use of relativistic effective potentials. In the latter case the core electrons are replaced by an effective potential that is fitted to the solutions of atomic relativistic calculations. In addition some of the scalar relativistic terms may be incorporated. The remaining

term, the spin-orbit coupling, can be treated as a perturbation in the final stage of the calculations. This approach gives reasonable results for many molecules, but it may break down when the magnitude of the spin-orbit coupling and other relativistic effects becomes comparable in magnitude to the LS-multiplet splittings. This is often the case in molecules that contain heavy atoms. In such cases the use of perturbation theory is questionable and verification of the outcome by means of a method that includes relativistic effects from the outset is desirable.

In 1928 Dirac proposed his famous equation[14] that describes the motion of an electron in accordance with both the laws of special relativity and quantum mechanics. The many-electron generalisation of his one electron equation, the Dirac-Coulomb-Breit[15] equation is nowadays the starting point for most explicit relativistic calculations.

The relativistic analogue of the Hartree-Fock method, the Dirac-Fock-(Breit) method was first formulated by Swirles[16] in 1935. For atoms excellent computer programs[17,18] have been constructed that efficiently use the spherical symmetry of the atom to solve the resulting differential equations by numerical integration. The typical timings for such calculations are in the order of minutes on a mainframe computer and calculations may thus be performed in a routine fashion.

For molecules the situation is more difficult. In general, the lack of symmetry prohibits reduction of the problem to an effective one or two-dimensional equation. Therefore numerical integration is no longer feasible and basis set expansion techniques like the ones that are used in non-relativistic molecular Hartree-Fock calculations become more favourable. Computer codes[19,20,21,22,23] which actually apply this technique to molecules of general shape are recently developed but do still demand large computer resources. One of the early codes (MOLFDIR) was developed in Groningen by Aerts[24] (closed-shell Dirac-Fock) and later extended by Visser[25] (open-shell Dirac-Fock and small CI calculations).

Like the non-relativistic Hartree-Fock method, the Dirac-Fock method does not include electron correlation. It is hence not suited to give precise quantitative descriptions of the electronic structure of the complex open-shell systems, that one often encounters in transition metal or rare earth compounds. More sophisticated methods that go beyond the mean field approximation and do include electron correlation are thus desirable. The relativistic direct CI method that is described in this thesis is an example of such a method.

1.3. Outline of this thesis

The first two chapters give the physical background of the relativistic CI method. The fundamental aspects of the relativistic treatment of many electron systems will be discussed in chapter 2. After the introduction of the Dirac and Dirac-Coulomb-(Breit/Gaunt) hamiltonians we consider expansion of these hamiltonians in a basis of a limited number of determinantal functions. A graphical method to represent such many-electron function spaces is given and used to define different types of CI spaces.

Chapters 3 and 4 are dedicated to the technical details of the method. In chapter 3 we describe the Dirac-Fock-CI method and its implementation in the MOLFDIR package. Chapter 4 deals with the problems that arise in the construction of contracted basis functions for the small component parts of the one-electron spinors.

Applications of the relativistic CI-method to a number of molecules are presented in chapters 5 and 6. In chapter 5 results of our calculations on the PtH molecule with the Dirac-Fock and the relativistic CI method are compared with results of other types of calculations and with experimental measurements of this molecule. The change of the d-d excitation spectra in the series CoF_6^{2-}, RhF_6^{2-} and IrF_6^{2-} is considered in chapter 6. Calculations on these complex ions have been performed at the non-relativistic and at the relativistic level of theory to study the influence of relativity in different rows of the periodic table.

Chapter 7 summarises the work presented in this thesis and gives some suggestions for further research. The last part of the thesis is an appendix in which the calculation of CI-matrix elements with the aid of graphical representations of CI-spaces is demonstrated.

References

1) "The chemistry of gold", R. J. Puddephatt, (Elsevier Science Publishers: Amsterdam 1978).

2) F. R. Hartley, "Chemistry of the Platinum Group Metals", (Elsevier Science Publishers: Amsterdam 1991).

3) R. Visser, J. Andriessen, P. Dorenbos, C. W. E. van Eijk, J. Phys.: Cond. Mat. (1993).

4) K. S. Pitzer, Acc. Chem. Res. **12**, 271 (1979).

5) J. P. Desclaux, At. Data Nucl. Data Tables **12**, 314 (1973).

6) P. A. Christiansen, W. C. Ermler, K. S. Pitzer, Ann. Rev. Chem. **36**, 407 (1985).

7) The basic theory can be found in numerous textbooks, see for instance A. Messiah, Quantum Mechanics **I** and **II**, (North-Holland Publishing Company: Amsterdam 1961).

8) P. Pyykkö, Chem. Rev. **88**, 563 (1988).

9) P. Pyykkö, Adv. Quantum Chem. **11**, 353 (1978).

10) P. Pyykkö, Relativistic Theory of Atoms and Molecules, Lecture Notes in Chemistry **41**, (Springer: Berlin 1986).

11) M. Born, J.R. Oppenheimer, Ann. der Phys. **84**, 457 (1927).

12) A good review of methods is given in: R. McWeeny, "Methods of Molecular Quantum Mechanics. 2nd Ed.", (Academic Press: London 1989).

13) P. Hohenberg and W. Kohn, Phys. Rev. B **3**, 864 (1964).

W. Kohn and L. J. Sham, Phys. Rev. B **4**, 1133 (1965).

14) P.A.M Dirac, Proc. Roy. Soc. A, **117**, (1928), 610; Proc. Roy. Soc. A, **118**, (1928), 351.

15) G. Breit, Phys. Rev. , **34**, (1929), 553.

16) B. Swirles, Proc. Roy. Soc. London A, **152**, (1935), 625.

17) K.G Dyall, I. P. Grant, C. T. Johnson, E. P. Plummer and F. Parpia, Computer Phys. Commun. **50**, 375 (1998).

18) J. P. Desclaux, Comput. Phys. Comm. **9**, 31 (1975).

19) The MOLFDIR program package, chapter 3.

20) K. G. Dyall, in "Relativistic and Electron Correlation Effects in Molecules and Solids", ed. G. L. Malli, (Plenum: New York 1993).

21) S. Okada and O. Matsuoka, J. Chem. Phys. **91**, 4193 (1989).

22) A. K. Mohanty and E. Clementi, Int. J. Quantum Chem. **39**, 487 (1990).

23) T. Saue, Thesis, University of Oslo (1991).

24) P. J. C. Aerts, Ph. D. Thesis, University of Groningen (1986).

25) O. Visser, Ph. D. Thesis, University of Groningen (1992).

2. Many electron systems

2.1. Abstract

In this chapter some aspects of the relativistic description of many-electrons systems will be discussed. We consider briefly the one-electron Dirac equation that describes the motion of an electron in an electromagnetic field in accordance with both the theory of special relativity and the theory of quantum mechanics. From the Dirac hamiltonian we construct the Dirac-Coulomb hamiltonian that can be used for calculations on many-electron systems like atoms and molecules.
The many-electron wave functions that are the eigensolutions of this equation can be obtained by the Dirac-Fock-CI method. In the remaining part of this chapter we will focus on the many-electron expansion space that is used in these methods. We will introduce a graphical representation of such spaces and consider the reductions of the full many-electron space that must be made to make the problem computationally feasible.

2.2. The Dirac equation for the free electron

This relativistic single particle equation was proposed in 1928 by Dirac[1] and is usually written in a covariant form which illustrates the symmetry of space and time in an elegant way

$$i\gamma^{\mu}\partial_{\mu}\,\psi = mc^2\,\psi \qquad (1)$$

where m is the rest mass of the particle, c is the speed of light and the γ^{μ} are the four Dirac matrices that fulfil the following commutation rules

$$\left[\gamma^{\mu},\,\gamma^{\nu}\right]_{+} = 2g^{\mu\nu} \qquad (2)$$

with $g^{\mu\nu}$ the metric tensor ($g^{00} = 1$, $g^{11} = g^{22} = g^{33} = -1$, other elements 0).
Since we shall use time independent potentials only in the following derivations, we can split off the explicit time dependence and use the time-independent version of the equation

$$\left(c\,\alpha\;\mathbf{p} + \beta mc^2\right)\psi = \varepsilon\,\psi \qquad (3)$$

by defining $\beta = \gamma^0$ and $\alpha_k = \gamma^0\gamma^k$ (k =1, 3). The α and β matrices are 4 by 4 matrices which are in the usual form given by

$$\alpha_x = \begin{pmatrix} 0_2 & \sigma_x \\ \sigma_x & 0_2 \end{pmatrix} \quad \alpha_y = \begin{pmatrix} 0_2 & \sigma_y \\ \sigma_y & 0_2 \end{pmatrix} \quad \alpha_z = \begin{pmatrix} 0_2 & \sigma_z \\ \sigma_z & 0_2 \end{pmatrix} \quad \beta = \begin{pmatrix} I_2 & 0_2 \\ 0_2 & -I_2 \end{pmatrix} \qquad (4)$$

the σ's are the 2x2 Pauli matrices; I_2 and 0_2 are the 2x2 identity and null matrix respectively. This 4-component spinor equation, which describes the free electron, is in accordance with the special theory of relativity. The properties and the physical interpretation of this equation can be found in standard textbooks[2,3,4] and will not be discussed extensively here. Some important points should, however, be summarised at this stage.

The spectrum of the Dirac equation is unbounded, both from above and from below. Two types of eigensolutions occur for the free-electron case: solutions that have eigenvalues above mc^2 and solutions with eigenvalues below $-mc^2$. The appearance of a continuum of negative energy solutions gives rise to conceptual difficulties. There is no "ground state" of lowest energy, like there is in non-relativistic theory, which suggests that the electrons may fall down into the negative energy continuum and attain an infinitely low energy.

Dirac circumvented this problem by defining the vacuum as the situation in which all states with negative eigenvalues are occupied and all states with positive energy eigenvalues are unoccupied. This means that additional electrons may not occupy the negative states due to the Pauli exclusion principle. Excitation of an electron from a negative energy state to a positive energy state implies the creation of a hole in the filled continuum "sea of electrons" and a new electron. The negative energy eigensolutions are then interpreted as solutions for such hole particles with charge +e, positrons, while the positive energy eigensolutions describe particles with electric charge -e, electrons. This interpretation is, however, not without problems either, because one has to deal with the interaction of electrons with the infinite negative background charge from the filled sea of electrons. This leads to infinities in actual calculations of electron properties with this theory. The problems were ultimately solved by the theory of renormalised quantum electrodynamics that was developed in the late forties[5].

In chemistry the problems connected with the treatment and interpretation of the positron solutions are less prominent. The pair creation process that gives rise to such particles requires energies of the order of $2mc^2$, which is well beyond the energy range that applies for ordinary chemical processes.

To stress the partitioning of the spectrum and the different nature of the electron and positron solutions the 4-component equation is often written as a 2-component equation for 2-component spinors

$$\begin{pmatrix} mc^2.I_2 & c\,\sigma\ \mathbf{p} \\ c\,\sigma\ \mathbf{p} & -mc^2.I_2 \end{pmatrix}\begin{pmatrix} \psi^L \\ \psi^S \end{pmatrix} = \varepsilon\begin{pmatrix} \psi^L \\ \psi^S \end{pmatrix} \qquad (5)$$

It can be shown that for the positive energy solutions the upper 2-component spinor has an amplitude of order c larger than the lower 2-component spinor. It is hence called the large component, while the lower 2-component spinor is called the small component.

2.3. Interaction terms

In our description of the electronic structure of molecules we will use the Born-Oppenheimer[6,7] approximation. The electron-nuclei interaction is then represented by a static field φ

$$\begin{pmatrix} (mc^2 - e\varphi).I_2 & c\,\sigma\ \mathbf{p} \\ c\,\sigma\ \mathbf{p} & (-mc^2 - e\varphi).I_2 \end{pmatrix}\begin{pmatrix} \psi^L \\ \psi^S \end{pmatrix} = \varepsilon\begin{pmatrix} \psi^L \\ \psi^S \end{pmatrix} \qquad (6)$$

The positive potential created by the nuclei leads to the appearance of bound electron states. To compare the electron eigenvalues with the values found in non-relativistic theory we will shift the spectrum by $-mc^2$

$$\begin{pmatrix} -e\varphi.I_2 & c\,\sigma\ \mathbf{p} \\ c\,\sigma\ \mathbf{p} & (-e\varphi - 2mc^2).I_2 \end{pmatrix}\begin{pmatrix} \psi^L \\ \psi^S \end{pmatrix} = \varepsilon\begin{pmatrix} \psi^L \\ \psi^S \end{pmatrix} \qquad (7)$$

This single particle equation can be solved exactly for a spherical-symmetric potential. Unfortunately, the hydrogen(like) atom is the only system in chemistry that can be treated with this model. The next step is therefore to find a many-particle equation that can be used for many-electron atoms and molecules. To this end we have to find an appropriate electron-electron interaction operator.

The Coulomb operator is not invariant under Lorentz operations and is hence not a valid relativistic operator by itself. It can, however, be shown by the use of quantum electrodynamics to be the first term of an expansion of the complete interaction. This complete interaction cannot be written in closed form but has to be obtained by (diagrammatic) perturbation theory. In this way invariance corrections to the Coulomb operator may be obtained to (in principle) any order. In practice usually only the next term in the expansion is kept[8] which, in the so-called low frequency limit, yields an

operator first derived by Breit[9]. Combining the Coulomb and the Breit interaction we obtain

$$g_{ij}^{\text{Coulomb + Breit}} = \frac{1}{r_{ij}} - \frac{1}{2}\left(\frac{(\alpha_i . \alpha_j)}{r_{ij}} + \frac{(\alpha_i . \mathbf{r}_{ij})(\alpha_j . \mathbf{r}_{ij})}{r_{ij}^3}\right) \qquad (8)$$

The Breit interaction can be interpreted as consisting of 2 terms: a term that represents the magnetic interaction between the electrons and a term representing the retardation due to the finite velocity of the interaction. The magnetic term was also derived by Gaunt in 1929[10] and is called the Gaunt interaction.

$$g_{ij}^{\text{Coulomb + Gaunt}} = \frac{1}{r_{ij}} - \frac{(\alpha_i . \alpha_j)}{r_{ij}} \qquad (9)$$

If we abbreviate the electron-electron interaction operator by g_{ij} we can now write a general many-electron hamiltonian

$$H = \sum_{i}^{N} h_i + \frac{1}{2}\sum_{i \neq j}^{N} g_{ij} \qquad (10)$$

and a corresponding many-electron equation

$$H\ \Psi(r_1, r_2, .., r_n), = E\ \Psi(r_1, r_2, .., r_n) \qquad (11)$$

This many-electron equation will be called the Dirac-Coulomb-(Gaunt/Breit) equation depending on the operator g_{ij} that is used. The many-electron Dirac-Coulomb-(Gaunt/Breit) hamiltonian is, like the original Dirac operator, unbound.

2.4. Definition of the 1-electron spinor space

To solve equation (11) we will approximate the many-electron wave function Ψ by a sum of antisymmetrised products (Slater determinants) of orthonormal single particle functions ψ

$$\Psi(r_1,r_2,..,\ r_n) \quad \sum_I \Phi_I\ (r_1,r_2,..,\ r_n)\ C_I \tag{12}$$

$$\Phi_I\ (r_1,\ r_2,\ldots,r_n) = (n!)^{-\ 1/2}\det|\ \psi_{I1}(r_1)\ \psi_{I2}(r_2)\ \ldots\psi_{In}(r_n) \tag{13}$$

The functions ψ will be taken to belong to the positive energy part of an appropriate single particle spectrum. With this choice the Dirac-Coulomb operator is truncated and we are left with an operator that is bounded from below. In this description the contributions of the states with electron-positron pairs are neglected, an approach that is therefore sometimes called the no-pair approximation[11].

The problem with the method is the determination of the appropriate one-electron spinor space. It is easily verified that each choice of potential φ in equation (7) yields a different division of the total spinor space into an electron and a positron part. The electron-electron interaction further complicates the problem, since in this case no unique choice of single particle functions exists. For every choice of model function (like a single determinant) we have the problem that the potential will depend on the model wave function itself and changes if we optimise the occupied spinors.

We use the Dirac-Fock method to generate single particle spinor spaces. In this method the division of the one-particle space into a positron and an electron part is determined variationally. In the formalism the effect of the electron-electron interaction is approximated by subjecting each electron to the mean field exerted by the others. A detailed description of the Dirac-Fock method and its implementation in the MOLFDIR program package will be given in chapter 3.

2.5. Graphical representation of the many-electron expansion space

We will now use the one-particle spinor basis that was obtained by solving the Dirac-Fock equations to write the hamiltonian in a second quantised form. With the introduction of the electron creation operator a_i^+ and annihilation operator a_j we can write our hamiltonian in the following form

$$H = \sum_{i,j} \langle\ i|\ \hat{h}\ |\ j\ \rangle\ a_i^+ a_j + \sum_{i,j,k,l} \left(ij|\ \hat{g}\ |\ kl\right)\ a_i^+ a_j^+ a_k a_l \tag{14}$$

Using the generators of the unitary group $E_{ij} = a_i^+ a_j$ and the anticommutation relation $[a_i^+, a_j]_+ = \delta ij$ the hamiltonian can also be written as

$$H = \sum_{i,j} \langle i | \hat{h} | j \rangle E_{ij} + \sum_{i,j,k,l} (ij | \hat{g} | kl) \left(E_{ij} E_{kl} - E_{il} \delta_{jk} \right) \qquad (15)$$

At this point no assumption is made about the range of the indices i, j, k and l, other than that they should run over positive energy solutions only. The corresponding many electron space is infinite but not complete since it lacks contributions from determinants with one or more occupied positron states.

Restriction of the range of the one-particle spinors to a finite number also projects the many-electron function space onto a space of finite dimension. This space is called the Full-CI space. It is usually further reduced to make the problem computationally feasible. We will now introduce a graphical representation of the many-electron space that is very useful in the discussion of such reductions of the Full CI space to different types of CI spaces. A general description of such graphical methods to represent many-electron function spaces may be found in the book by Duch[12].

If we use a finite set of m one-electron spinors to describe a system with n electrons we can make $\binom{m}{n}$ antisymmetric product functions or determinants (13). Graphically all possible determinants with 3 electrons in 6 one-electron spinors can pictured as paths in a graph (figure 1).

Figure 1 : Graphical representation of a CI space.

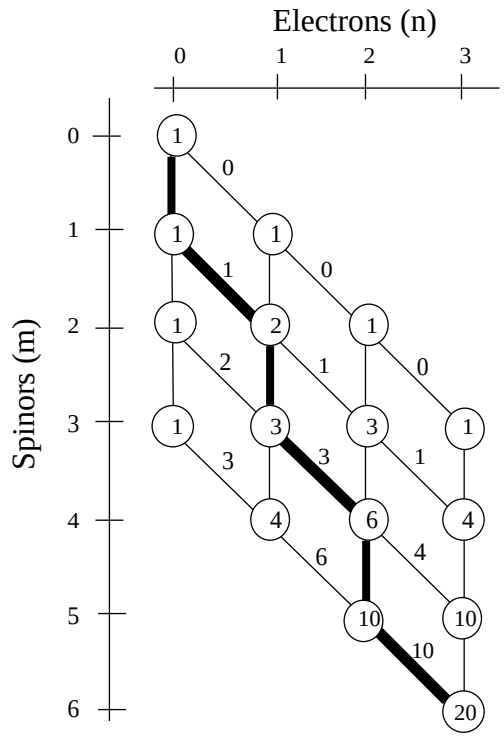

An occupied spinor m_1 is represented by an arc connecting vertex (m_1-1, n_1-1) to vertex (m_1, n_1), an unoccupied spinor is represented by an arc connecting vertex (m_1-1, n_1) to (m_1, n_1). The determinant |246| is thus represented by the thick line in the graph (figure 1).
This graphical representation provides a convenient way of ordering the determinants. We define the vertex weight $W(m_1, n_1)$ as the number of different paths that lead from the top of the graph to this vertex. It is easy to see that this weight can be calculated recursively using the formula

$$W(m_1, n_1) = W(m_1\text{-}1, n_1\text{-}1) + W(m_1\text{-}1, n_1) \qquad (16)$$

By definition we take the weight of the starting vertex W(0,0) to be 1. We now define arc weights in the following way

- All vertical arcs (connecting vertices with the same number of electrons) have zero weight.
- The weight $Y(m_1, n_1)$ of the arc which connects the vertices (m_1-1, n_1-1) and (m_1, n_1) is equal to $W(m_1\text{-}1, n_1)$.
- If vertex (m_1-1, n_1) lies outside the graph its weight and the weight of $Y(m_1, n_1)$ are zero.

The arc weights for the (6 spinor, 3 electron) system are indicated in figure 1. The zero weights of the vertical arcs are omitted for clarity. A unique index of a path through the graph (a determinant) can now be defined as

$$I = 1 + \sum_{k}^{n} Y(m_k, k) \qquad (17)$$

This so-called reverse lexical ordering gives the upper path |123| index 1 and the lower path |456| index 20. If we have a situation in which one determinant will dominate the CI wave function then it is convenient to number the active spinor set in such a way that the occupied spinors of this determinant precede the unoccupied spinors. This gives this determinant index 1 while determinants that differ in many places from it, and are likely to contribute little to the CI wave function, have the highest indices.

2.6. The Restricted Active Space formalism

The size of the Full-CI space increases factorially with the number of spinors. It is therefore usually not feasible to perform calculations in which all determinants from this space are allowed to contribute to the many-electron wave function.

In non-relativistic calculations several ways to reduce the size of a full-CI space to more tractable dimensions are used. Starting point is usually the Hartree-Fock (or Dirac-Fock, in our case) wave function. This wave function consists of a single determinant, for which an optimum set of orbitals (spinors) is calculated. This reduction of the many-electron function space implies that explicit electron-electron correlation other than the exchange correlation is ignored. Methods that go beyond this optimised single determinantal description are therefore called correlated methods.

Correlation energy is defined as the difference between the energy expectation value of the single-determinantal (Dirac-Fock) wave function and a many-determinantal wave function. It is sometimes useful to analyse the contributions to the correlation energy in terms of a static and a dynamical part[13].

The static correlation energy arises from the occurrence of near-degeneracies in the many-electron spectrum. For a good description of one state from such a near-degenerate set, all the other states of the degenerate set should also be included within the many-electron space, a requirement that is incompatible with a single determinantal space. This part of the correlation energy can usually be accounted for by extension of the space with a small number of determinants. The wave function is then written as a short linear combination of determinants that all have rather large coefficients.

The remaining part is called the dynamical electron correlation and shows up as the contribution of many determinants with small coefficients in the wave function. An important part of this correction has to do with the interaction of electrons at short distances, the so-called cusp region. In this region the Coulomb repulsion between the electrons gives rise to terms containing r_{12} in the many-electron wave function. Explicit inclusion of such two-electron terms is not possible in our many-electron basis that is built from products of one-electron spinors. These terms can, however, be relatively well approximated by inclusion of determinants that are doubly excited relative to the reference determinant.

We now focus on the CI spaces that may be defined on the basis of these considerations. We will show that the Restricted Active Space (RAS) formalism[14] provides a very general and convenient way to handle different choices of CI spaces.

In the RAS method we divide our spinors into a core set with low spinor energies, that is completely filled, an active set that does have variable occupation in the different determinants and a set of high-lying virtual spinors that do not significantly contribute to any state of practical interest. This division is shown graphically in figure 2.

Figure 2 : Graphical representation of a constrained CI space.

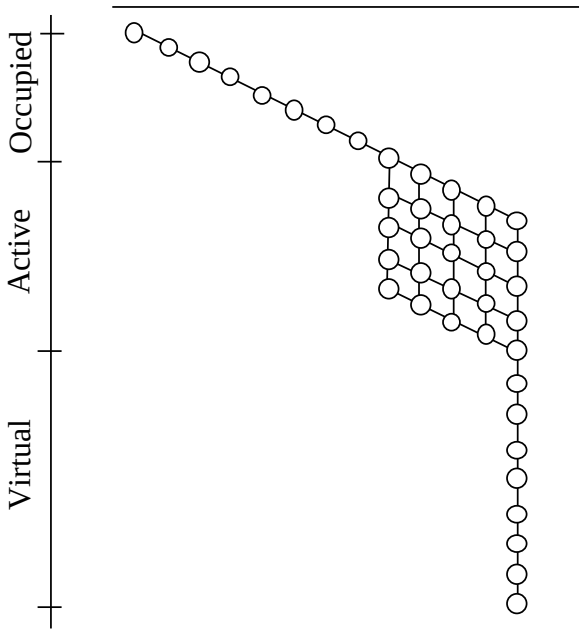

In the remainder we will only draw the active part of the graphs since there is only one way of passing through the inactive core and through the unoccupied region and the contribution of these parts of the graph to the index of a path is zero.
In the RASCI method we subdivide the remaining active spinor subset into three subspaces : RAS1, RAS2 and RAS3 consisting of m_{R1}, m_{R2} and m_{R3} spinors respectively. In RAS1 we will usually put the active spinors that belong to the occupied spinors (closed shells) of the reference wave function, in RAS2 we put the spinors that have variable occupation (open shell) in the reference wave function and RAS3 contains the active spinors that are unoccupied in the reference wave function.
We then take the determinantal basis to consist of all determinants which have a maximum of n_{H1} holes in the RAS1 spinor set and a maximum of n_{E3} electrons in RAS3. Appropriate division of the spinors over the three spaces and choice of the parameters n_{H1} and n_{E3} make it possible to perform various types of CI-calculations. In figure 3 the graphical representation of some important types of CI spaces is sketched. The separation in RAS1, RAS2 and RAS3 of the spinor space is indicated by enlarging the vertices which lie at the division.

Figure 3. Graphical representation of CI spaces.

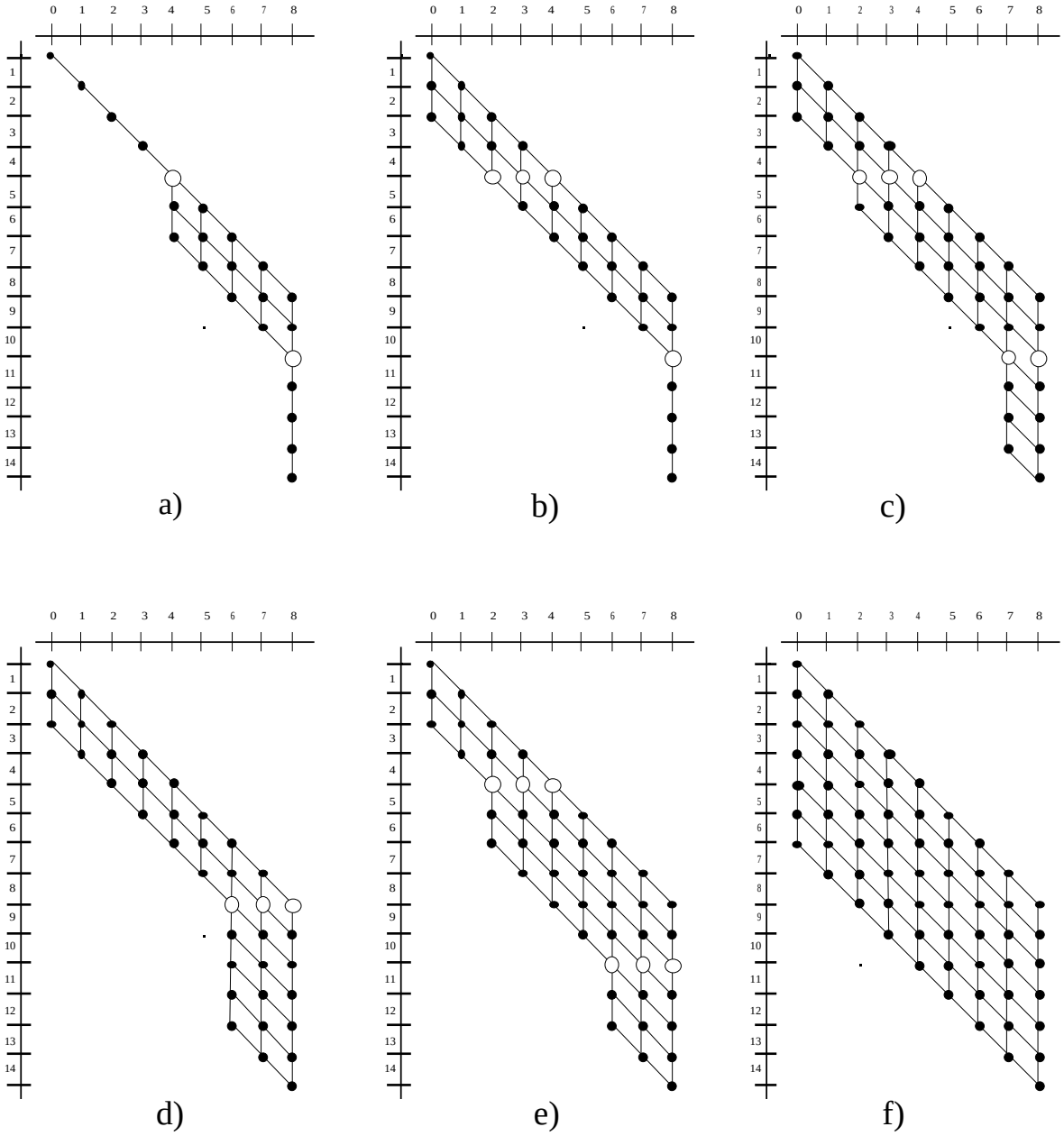

a) Complete Open Shell CI (COSCI).

This method is used as a first step in the description of transition metal d-d like and rare earth f-f like spectra. In this case the active space consists of the open shell spinors in RAS2 only. Formally one may also take non-empty RAS1 and RAS3 spaces and put $n_{H1} = n_{E3} = 0$, as is shown in the figure.

b) Charge Transfer CI (CTCI).

Second step in the description of the d-d like or f-f like spectra. The COSCI space is extended by allowing charge transfer excitations from filled ligand orbitals into the open d or f shell.

c) First Order CI (FOCI).
The CTCI space is extended by allowing single excitations from the active occupied orbital set (RAS1 and RAS2) into the unoccupied (RAS3) set. This allows orbital relaxation of the charge transfer states which were mixed in the LFCI.
d) Single Reference Singles and Doubles CI (SRSDCI).
This type of CI is valuable if a single determinant already gives a good description of the wave functions. Dynamic correlation effects are studied by allowing single and double excitations out of this single determinant.
e) Multi Reference Single and Doubles CI (MRSDCI).
This method is also used to study dynamic correlation effects but allows for a more general reference wave function.
f) CASCI or Full CI (FCI).
The CASCI limit can be reached in various ways in the RASCI formalism, an obvious way is to put all spinors in RAS2, another possibility is to set both $n_{H1} = m_{R1}$ and $n_{E3} = m_{R3}$. If the active space consists of all spinors, then the CASCI is equal to a Full CI calculation.

The relativistic CI program DIRRCI that is designed to calculate wave functions within such CI spaces is described in chapter 3. Spaces of the types a-c were used in the calculations that are described in chapter 6, while the calculations of chapter 5 were done in a space of the form e.

2.7. Use of abelian point group symmetry.

Applications of relativistic theory usually lie in the realm of 5d transition metals and rare earth complexes. Description of the compounds is often done in a cluster model in which a small number of atoms is taken out of the bulk. These clusters are frequently highly symmetric, a symmetry that one can use to label the states of interest and facilitate the computational effort involved in calculations.
If the system under study is invariant under the symmetry operations of a double group D^1, then the eigenvectors of the Dirac-Fock equation will transform as the irreducible representations Γ^1_λ of this double group. Since the Dirac-Fock equation describes spin 1/2 particles the spinors will span the "extra" representations of the double group. The many-electron wave functions span also the extra representations if the number of electrons is odd and span the "normal" representations if the number of electrons is even.
If the double group is abelian then all its representations are one-dimensional and the labelling $\psi_\varepsilon^{\Gamma^1_\lambda}$ of Dirac-Fock spinors with their eigenvalue and representation is unique. In this case the symmetry character of a determinantal wave function is also easily and

uniquely determined by taking the direct product of all the representations of the constituent one-electron functions.

In general the Dirac double group is, however, non-abelian and has multi-dimensional representations. Now the labelling of one-electron functions is no longer unique and degenerate spinor sets, spanning equivalent representations, can be arbitrarily mixed. Another consequence is that the direct product representation that is spanned by determinantal wave functions formed from these spinors will be reducible. This reduction can in principle be done by forming the appropriate linear combinations of determinants but leads to much more complicated expressions for the CI equations.

An elegant way that provides an additional label for the one-electron spinors and allows one to keep the simplicity of the determinantal expansion basis is to make use of a group chain. A group chain is defined as a number of groups D^1, D^2, .., D^n where each group D^{k+1} is a subgroup of the group D^k. We can now choose our one-electron spinors such that they transform according to the representations of all subgroups in a chain, thus making the labelling $\psi_\varepsilon^{\Gamma^1_\lambda,\Gamma^2_\mu,..,\Gamma^n_\nu}$ of the spinor unique. In such a chain the last group will be abelian and consequently the determinants will also transform as irreps of this group. This makes it possible to solve the Dirac-Fock equations using the full symmetry of the problem and the CI equations using only the abelian symmetry operations without having to transform the spinor basis.

The use of abelian symmetry is easily incorporated in the graphical representation of the CI-space. The vertices of the graphs are now split to indicate the symmetry character of the paths (determinants) that pass through it. In figure 4 an example is given for the abelian group C_3^*, the multiplication table of which is given in table 1.

Table 1. Multiplication table of C_3^*. The dotted lines represent the separation between the ordinary (Γ_1, Γ_2, Γ_3) and the "extra" (Γ_4, Γ_5, Γ_6) representations of this group.

C_3^*	Γ_1	Γ_2	Γ_3	Γ_4	Γ_5	Γ_6
Γ_1	Γ_1	Γ_2	Γ_3	Γ_4	Γ_5	Γ_6
Γ_2	Γ_2	Γ_3	Γ_2	Γ_5	Γ_6	Γ_4
Γ_3	Γ_3	Γ_1	Γ_2	Γ_6	Γ_4	Γ_5
Γ_4	Γ_4	Γ_5	Γ_6	Γ_1	Γ_2	Γ_3
Γ_5	Γ_5	Γ_6	Γ_4	Γ_2	Γ_3	Γ_1
Γ_6	Γ_6	Γ_4	Γ_5	Γ_3	Γ_1	Γ_2

Figure 4. Symmetry adapted graphical representation of a (6 spinor, 3 electron) space. Number and kind of the six spinor representations are arbitrarily chosen.

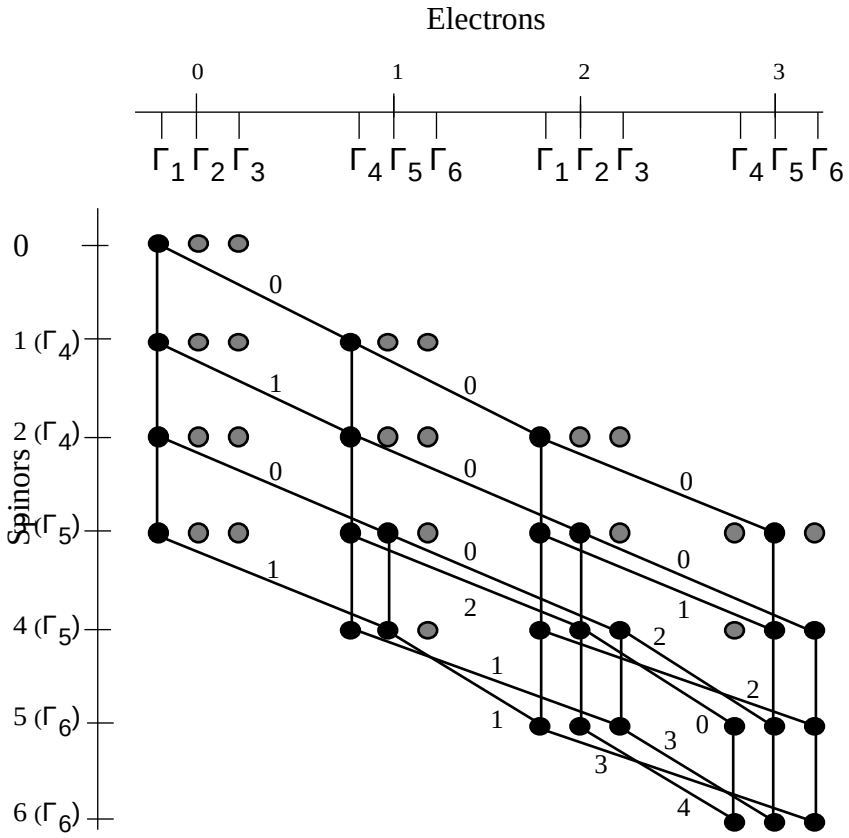

We can use this symmetry adapted graph to define a consecutive labelling of determinants within the same representation. The vertex weights are defined as before as the number of paths that lead from the top of the graph to this vertex. The recursive formula 16 is modified to

$$W(m_1, n_1, \Gamma_i) = W(m_1\text{-}1, n_1\text{-}1, \Gamma_j) + W(m_1\text{-}1, n_1, \Gamma_i) \qquad (18)$$

with $\Gamma_i = \Gamma_j \quad \Gamma(m_1)$. We now redefine the arc weights in the following way

- All vertical arcs (connecting vertices with the same number of electrons) have zero weight.
- The weight $Y(m_1, n_1, \Gamma_i)$ of the arc which connects the vertices $(m_1\text{-}1, n_1\text{-}1, \Gamma_j)$ and (m_1, n_1, Γ_i) is equal to $W(m_1\text{-}1, n_1, \Gamma_i)$.
- If vertex $(m_1\text{-}1, n_1, \Gamma_i)$ lies outside the graph its weight and the weight of $Y(m_1, n_1, \Gamma_i)$ is zero.

One can now easily verify that the determinant |246| that was given index 15 = (1+3+10)+1 in the diagram of figure 1, is now listed as the 8th determinant of representation Γ_4. The sizes of the subspaces are of course easily obtained as the weights of the bottom vertices. In this example we find 8 determinants in representation Γ_4 and 6 determinants in both Γ_5 and Γ_6.

The symmetry adapted graphical representation of the CI-space is used in the direct CI program DIRRCI that will be treated in the next chapter. In the appendix more details are given about the evaluation of CI matrix elements with the aid of graphical methods.

2.8. Kramers' symmetry

An operator that is not contained in the Dirac double point groups, but does commute with the Dirac hamiltonian, is the Kramers'[15] or Time Reversal operator $\hat{K}_4$

$$\hat{K}_4 = -i \begin{pmatrix} \sigma_y & 0_2 \\ 0_2 & \sigma_y \end{pmatrix} \hat{K} \qquad (19)$$

in which $\hat{K}$ is the complex conjugation operator. It can be shown that this antiunitary operator commutes with the one-electron Dirac hamiltonian (formula 7). Since the Coulomb part of the two-electron operator is diagonal and real it is easy to see that the N-electron generalisation of the operator

$$\hat{K}_4^{(N)} = \prod_{i=1}^{N} \hat{K}_4^i \qquad (20)$$

will commute with $g_{ij}^{Coulomb}$. To demonstrate that the magnetic, Gaunt interaction, part of the two-electron operator (9), also commutes with $\hat{K}_4$ we will give the derivation for a system with two electrons :

$$\hat{K}_4^{(2)} = \hat{K}_4^1 \hat{K}_4^2 \qquad (21)$$

$$\left[\hat{K}_4^{(2)}, g_{12}^{Gaunt}\right] = \frac{\left(\hat{K}_4^1 \alpha_1 \,.\, \hat{K}_4^2 \alpha_2\right) - \left(\alpha_1 \hat{K}_4^1 \,.\, \alpha_2 \hat{K}_4^2\right)}{r_{12}} \qquad (22)$$

since $\hat{K}_4^i$ anticommutes with α_i:

$$\left[\hat{K}_4^i, \alpha_i\right]_+ = 0 \qquad (23)$$

one can interchange both $\hat{K}_4^1$ and α_1 and $\hat{K}_4^2$ and α_2 which proves the proposition

$$\left[\hat{K}_4^{(2)},\, g_{12}^{Gaunt}\right] = \frac{\left(\left\{-\alpha_1 \hat{K}_4^1\right\}.\left\{-\alpha_2 \hat{K}_4^2\right\}\right) - \left(\alpha_1 \hat{K}_4^1 \,.\, \alpha_2 \hat{K}_4^2\right)}{r_{12}} = 0 \qquad (24)$$

The time-reversal symmetry is, contrary to the point-group symmetry which depends on the nuclear framework of the system under study, always present in calculationsthat use the Dirac-Coulomb-(Gaunt) hamiltonian. It is therefore tempting to adapt the formalism such that it fully exploits this symmetry. Two points of thought before building a method which is firmly rooted in this symmetry are in place here. First, if one wants to calculate properties of molecules in external magnetic fields one needs to include a magnetic interaction operator that is not invariant under the time-reversal operator. Secondly, if one fully exploits the point group symmetry in high symmetry point groups like O_h, the relations between one-electron spinors that are invoked by the time-reversal operator are already contained in the relations given by the point group symmetry operators. However, full exploitation of point group symmetry is hard to combine with computational efficiency. In many cases one is furthermore not interested in the influence of a magnetic field on the form of the molecular spinors. In that case one may evaluate the magnetic field matrix elements by perturbation theory instead of calculating them variationally.

The inclusion of the Kramers' symmetry in a graphical formalism like it was done with the abelian point group symmetry is non-trivial. A problem is the labelling of the spinors by their behaviour under the Kramers' operator. It is always possible to define two subsets of spinors $\{\psi\}$ and $\{\bar{\psi}\}$, for which each spinor ψ_i is related to $\bar{\psi}_i$ by $\bar{\psi}_i = \hat{K}_4\psi_i$ and $\psi_i = -\hat{K}_4\bar{\psi}_i$. Since ψ_i and $\bar{\psi}_i$ have the same eigenvalue this separation is, however, rather arbitrary since they may be rotated among each other and still be eigenfunctions of the hamiltonian. If the system under consideration possesses point group symmetry then this choice may be done such that the functions also transform according to the representations of this double group[16]. This procedure has no advantages relative to a procedure in which one uses only point group symmetry, however.

Nevertheless the use of the Kramers' symmetry to reduce the expansion spaces in relativistic calculations seems very promising and should be investigated further. In the next chapter use of the relations between the spinors to reduce the number of non-zero matrix-elements in SCF and CI type of calculations is discussed[17,18]. A further step may be the use of these relations to redefine the E_{ij} operators of equation 16 in a way that is analogous to the non-relativistic unitary group method. In this method one integrates over the spin variables by using $E'_{ij} = E_{ij}^{\alpha\alpha} + E_{ij}^{\beta\beta}$ to obtain a formalism in which the integrals are defined over orbitals instead of spinorbitals. Similar redefinitions like $E'_{ij} = E_{ij} + E_{ji}^{-}$ may be very useful in the relativistic formalism. At

present this matter has not yet been investigated in enough detail, however, to give a definite opinion on the way to proceed.

References

1) P.A.M Dirac, Proc. Roy. Soc. A **117**, 610 (1928);

P.A.M Dirac, Proc. Roy. Soc. A **118**, 351 (1928).

2) A. Messiah, Quantum Mechanics, (John Wiley and Sons Inc. (1968).

3) R. E. Moss, Advanced Molecular Quantum Mechanics, (Chapman and Hall: London 1973).

4) M. E. Rose, Elementary Theory of Angular Momentum, (John Wiley and Sons Inc. 1937).

5) Many of the early papers can be found in The Physical Review volumes 74-76. See for instance R. P. Feynman, Phys. Rev. **74**, 939 (1948); **76**, 749 (1949); **76**, 769 (1949) and J. Schwinger Phys. Rev. **74**, 1439 (1948); **75**, 651 (1949); **76**, 790 (1949).

6) M. Born, J.R. Oppenheimer, Ann. der Phys. **84**, 457 (1927).

7) M. Born, K. Huang, in: Dynamical Theory of Crystal Lattices, Appendix 8, (Oxford University Press: Oxford 1955).

8) I. P. Grant, H.M. Quiney, Advances in Atomic and Molecular Physics **23**, 37 (1988).

9) G. Breit, Phys. Rev. **34**, 553 (1929).

10) J. A. Gaunt, Proc. Roy. Soc. A **122**, 513 (1929).

11) J. Sucher, Phys. Rev. A **22**, 348 (1980).

12) W. Duch, GRMS or Graphical Representation of Model Spaces, Lecture Notes in Chemistry **42**, (Springer: Berlin 1986).

13) The MCSCF theory, B. O. Roos, European Summer School in Quantum Chemistry, Lecture Notes (1989).

14) J. Olsen, B. O. Roos, P. Jørgensen, H. J. Aa. Jensen, J. Chem. Phys. **89**, 2185 (1988).

15) H. A. Kramers, Proc. Acad. Amsterdam **33**, 959 (1930).

16) J. G. Snijders, Ph. D. Thesis, Free University of Amsterdam (1979).

17) K. G. Dyall, in "Relativistic and Electron Correlation Effects in Molecules and Solids", ed. by G. L. Malli, (Plenum 1993).

18) O. Visser, Ph. D. Thesis, University of Groningen (1992).

3. Relativistic Quantum Chemistry
The MOLFDIR program package

3.1. Introduction

A relativistic description of electrons in molecules that contain one or more heavy atoms is essential for accurate calculations of the electronic structure of such molecules. One of the best examples is the well known yellow absorption band of gold which, when calculated by non-relativistic methods, is predicted to lay in the ultraviolet. Relativistic calculations give the correct position in the visible part of the spectrum. An extensive review of the consequences of relativity on chemical properties is given by Pyykkö in 1988[1].

Most computational quantum chemical methods are based on the non-relativistic Schrödinger equation and treat relativity, if at all, by introducing correction operators in the hamiltonian. These correction operators may be derived from the Dirac-Coulomb-(Breit) equation and the validity of these approaches can be tested by the calculation of the solutions of the Dirac-Coulomb-(Breit) equation itself. We have developed a set of computer codes called the "MOLFDIR package" that can perform such calculations for molecules of general shape.

In this article the basic concepts of the underlying theory are summarised, followed by a more extensive description of the method chosen to solve the Dirac-Coulomb equation. The technical aspects of the method are discussed in the description of the modules of the MOLFDIR package. The computer resources necessary for calculations of this type are discussed in section 5 while we conclude by considering the possibilities for further methodological and technical extensions and improvements.

3.2. Basic Theory

The many-electron equation that we use in our relativistic calculations is the Dirac-Coulomb-(Gaunt) equation for N electrons

$$H \Psi = E \Psi \tag{1}$$

$$H = \sum_{i}^{N} h_i + \frac{1}{2} \sum_{i \neq j}^{N} g_{ij} \tag{2}$$

Where h_i is the one-electron Dirac hamiltonian for electron i

$$h = \begin{pmatrix} - e\varphi.1_2 & c\, \sigma\ \mathbf{p} \\ c\, \sigma\ \mathbf{p} & (- e\varphi - 2mc^2).1_2 \end{pmatrix} \tag{3}$$

The inner product $\sigma.\mathbf{p}$ is taken between the vector of the three Pauli spin matrices σ (σ_x, σ_y, σ_z) and the momentum operator $\mathbf{p}$ (p_x, p_y, p_z). We will work in atomic units in which m, the mass of the electron, e, the elementary charge and $\hbar$ are 1. The speed of light, c, is taken to be 137.036 in these units. In our notation we use 1_2 for the 2x2 unit matrix.

The scalar potential, φ, arises from the nuclear framework in which the electrons move. The nuclei are considered to be fixed in space and may have either a finite or a point charge distribution. Properties of this relativistic one-electron hamiltonian are well known and can be found in standard textbooks[2,3].

To define our many-electron hamiltonian (2) we need to specify the two-electron operator g_{ij}. The problem here is that a correct relativistic two-electron operator can not be written down in closed form. From the theory of Quantum Electro Dynamics (QED) one can however derive a series expansion of the complete interaction[4] in which the first term is the Coulomb interaction

$$g_{ij}^{\text{Coulomb}} = \frac{1}{r_{ij}} \tag{4}$$

The next term is the Breit interaction[5], represented in our program package by its magnetic part, an operator that was first derived by Gaunt in 1929[6]

$$g_{ij}^{\text{Gaunt}} = - \frac{(\alpha_i.\alpha_j)}{r_{ij}} \tag{5}$$

α is the vector of the 4-component matrices that are formed from the Pauli matrices in the following way

$$\alpha_x = \begin{pmatrix} 0_2 & \sigma_x \\ \sigma_x & 0_2 \end{pmatrix} \quad \alpha_y = \begin{pmatrix} 0_2 & \sigma_y \\ \sigma_y & 0_2 \end{pmatrix} \quad \alpha_z = \begin{pmatrix} 0_2 & \sigma_z \\ \sigma_z & 0_2 \end{pmatrix} \tag{6}$$

With $g_{ij} = g_{ij}^{Coulomb} + g_{ij}^{Gaunt}$ equations (1) and (2) define our basic physical starting point and level of approximation to QED. The next sections will deal with the methods that we have developed to find approximations to the many-electron energy E and the wave function Ψ of equation (1).

3.3. Methodology

The exact wave functions for molecular many-electron problems cannot be obtained in closed form. Approximation by means of direct integration of the equation would be attractive but is in general not feasible due to the large dimensionality and lack of symmetry of the problem.

The usual approach in quantum chemistry is to break down the molecular problem in terms of the constituent atoms and build molecular wave functions from (anti-symmetrised) products of atomic centred one-electron functions. We will apply this method to the Dirac-Coulomb-(Gaunt) equation and start with a discussion of the influence of the form of the nuclear potential on the choice of the one-electron basis functions. In section 3.3.2 the one-electron basis functions are defined, while sections 3.3.3 and 3.3.4 describe in detail the methods employed to solve the many-electron problem. This part is concluded by considering the use of symmetry to simplify the computations.

3.3.1. Nuclear model

The basis functions are chosen to resemble the solutions of the one-electron (hydrogen-like) atomic problem. These solutions are dependent on the nuclear potential that is used. This presents a problem since the exact charge distribution of nuclei is not known in analytical form, but at best as measured data sets.

If one is interested in core electron properties one has to consider the structure of the nuclear charge distribution. Especially in the case of heavy atoms, in which the nuclei are large and the inner spinors are strongly contracted, use of a nuclear model that resembles the measured structure is desirable. In molecular calculations, however, the primary interest is the correct description of chemical bonding and low-energy (valence) electron spectroscopy. In this case the bonding region of the molecule has to be calculated accurately. The structure of the wave function in that region does not

depend strongly on the detailed structure of the nuclei, so we may choose a simple and convenient nuclear model in the calculations.

In non-relativistic theory a commonly used nuclear model is that of a point-charge. An advantage of this model is that it has the same form for all nuclei, independent of their nuclear charge and mass. The radial solutions of the Schrödinger equation for the point-charge potential can be exactly represented by Slater type functions ($r^n e^{-\lambda r}$). This makes the Slater type functions a natural expansion set for atomic orbitals. In molecular calculations direct use of Slater functions is in general not feasible because they give rise to complicated integrals. In these calculations sets of Gaussian type ($r^n e^{-\alpha r2}$) functions are used, because multi-centre integrals over this type of functions are relatively easy to evaluate[7].

In relativistic theory one can also find exact solutions of the Dirac equation for the point-nucleus potential. The radial part of the $1s_{1/2}$ solution for this choice of nucleus is given by equation (7).

$$R(r) = r^{\gamma-1} e^{-\lambda r}, \qquad \gamma = \sqrt{1 - \frac{Z^2}{c^2}} \tag{7}$$

Z is the charge of the nucleus. We see that the finite speed of light gives rise to radial solutions with a non-integer power of r. The resulting weak singularity at the origin for the $1s_{1/2}$ (and also the $2p_{1/2}$) solution is hard to describe with the conventional Slater functions and even harder to describe with Gaussian functions. This means that we need much larger sized basis sets to get the same convergence to the exact solutions as in the non-relativistic case.

Use of the point-charge model is therefore, especially in relativistic calculations, not recommendable, because the appearance of such a singularity is just an artefact of the crude point-charge model. If a more physical, finite, model of the nucleus is used, the singularity disappears and the form of R(r) at the origin becomes Gaussian-like[8]. The choice of a finite nuclear model combined with the use of Gaussian type basis functions is computationally favourable and physically more sound than the point-nucleus model. A slight disadvantage is that there is no agreement in literature yet on a standard finite nuclear model, so that different models and parametrisations are in use. This makes it difficult to compare total electronic energies obtained with different codes. With our code one may use the crude but unambiguous point-charge model for test calculations in which comparison of results with other codes is necessary. Our standard model is based on a Gaussian distribution function of the nuclear charge. In this model[9] φ is given by

$$\varphi(\mathbf{r}) = \sum_{K=1}^{\#\,\text{Nuclei}} N_K \int \frac{Z_K\, e^{-\xi_K (\mathbf{r} - \mathbf{R}_K)^2}}{(\mathbf{r} - \mathbf{R}_K)}\, d\mathbf{R}_K \qquad (8)$$

$$\xi_K = 3.88 * 10^{-9} (M_K)^{-2/3} \qquad N_K = \left(\frac{\xi_K}{\pi}\right)^{\frac{3}{2}} \qquad (9)$$

Z_K is the charge of nucleus K and M_K is its mass. In this formula ξ is related to the homogeneously charged sphere model by the formula $\sigma = R/2$, with R the radius of the sphere and σ the standard deviation of the radial Gaussian distribution. The formula[10] $R = 2.27*10^{-5}\, M_k^{1/3}$ is used to relate the radii and mass of the nuclei.

3.3.2. Basis set approach

In this section we will describe the basis sets that are used to expand the one-electron spinors in. Since our one-electron hamiltonian (3) is defined in 4-spinor space we have to use basis sets that consist of 4-component functions. We shall start with the definition of two scalar (1-component) basis sets and then define our 4-component basis sets using these scalar functions.

The first scalar basis set is formed by primitive cartesian Gaussian basis functions. The primitive basis set is subdivided in a large (L) and small (S) component set, that will be used to describe the upper and lower two components of the 4-spinors respectively.

$$g_u^L = N_u^L\, x^{\kappa_u^L}\, y^{\lambda_u^L} z^{\mu_u^L}\, e^{-\alpha_u^L r^2}, \quad g_v^S = N_v^S\, x^{\kappa_v^S}\, y^{\lambda_v^S} z^{\mu_v^S}\, e^{-\alpha_v^S r^2} \qquad (10)$$

We now make a second (contracted) scalar basis set consisting of linear combinations of functions with different exponential parameters. These functions will also be denoted by g but bear different indices (p, q). In the contraction process we use the general contraction scheme that was introduced by Raffenetti[11].

$$g_p^L = \sum_u c_{up}^L\, g_u^L\,, \quad g_q^S = \sum_v c_{vq}^S\, g_v^S \qquad (11)$$

The primitive functions g_u^L and g_v^S may contribute to all g_p^L and g_q^S, provided that no functions with different values of κ, λ or μ are combined. This scheme makes it possible to use (parts of) atomic solutions as basis functions for molecular calculations and allows significant reductions of the basis set size without loosing much accuracy.

From these real scalar functions a set of 4-component functions is constructed in the following way

$$\vartheta_p^{L\alpha} = \begin{pmatrix} g_p^L \\ 0 \\ 0 \\ 0 \end{pmatrix}, \vartheta_p^{L\beta} = \begin{pmatrix} 0 \\ g_p^L \\ 0 \\ 0 \end{pmatrix}, \vartheta_q^{S\alpha} = \begin{pmatrix} 0 \\ 0 \\ g_q^S \\ 0 \end{pmatrix}, \vartheta_q^{S\beta} = \begin{pmatrix} 0 \\ 0 \\ 0 \\ g_q^S \end{pmatrix} \qquad (12)$$

This basis set is used to expand the atomic or molecular spinors and defines a matrix representation of the one-electron Dirac or pseudo one-electron Dirac-Fock hamiltonian. Since it does not utilise the (point group) symmetry that often is present in the nuclear framework, an additional transformation of the basis to a double group symmetry adapted basis may be preferable. This is done by the following unitary transformation

$$\chi_l^L = \sum_p d_{pl}^{L\alpha}\vartheta_p^{L\alpha} + d_{pl}^{L\beta}\vartheta_p^{L\beta}, \; \chi_s^S = \sum_q d_{qs}^{S\alpha}\vartheta_q^{S\alpha} + d_{qs}^{S\beta}\vartheta_q^{S\beta} \qquad (13)$$

Double group characters can be complex, hence we define the transformation coefficients, $d_{pl}^{L\alpha}$ and $d_{qs}^{S\alpha}$, as complex numbers. Note that with this transformation the separation of spin and space coordinates disappears by the combination of functions of different spin.

The functions χ may also be expressed directly in terms of the contracted scalar functions in the following way

$$\chi_l^L = \begin{pmatrix} \chi_l^{L\alpha} \\ \chi_l^{L\beta} \\ 0 \\ 0 \end{pmatrix} \quad \text{and} \quad \chi_s^S = \begin{pmatrix} 0 \\ 0 \\ \chi_s^{S\alpha} \\ \chi_s^{S\beta} \end{pmatrix} \qquad (14)$$

$$\chi_l^{L\alpha} = \sum_p g_p^L d_{pl}^{L\alpha}, \; \chi_l^{L\beta} = \sum_p g_p^L d_{pl}^{L\beta}, \; \chi_s^{S\alpha} = \sum_q g_q^S d_{qs}^{S\alpha} \text{ and } \chi_s^{S\beta} = \sum_q g_q^S d_{qs}^{S\beta} \qquad (15)$$

The different basis sets are summarised in table 1.

Table 1 : Basis sets used in the MOLFDIR program package.

Symbol	Labels	# of comp.	Description	Use
g	L, u; S, v	1 component	Primitive cartesian Gaussians.	Low level integral evaluation routines.
g	L, p; S, q	1 component	General contracted cartesian Gaussians.	Two electron integral evaluation and storage.
ϑ	L, p, σ; S, q, σ	4 component	Non-symmetry adapted basis.	Building of the Fock-matrix. Storage of SCF vectors.
χ	L, l; S, s	4 component	Symmetry adapted basis.	Storage of one-electron matrix elements. Storage of density matrices.

3.3.2.1. Kinetic and Atomic Balance

Since all basis sets contain a large component (L) and a small component (S) set it is possible to establish the relation between the large and small component parts of the 4-component spinors at Dirac-Fock level. This variational freedom will give a better description of the electron and positron space than would be obtained if this relation was fixed on forehand, because one now considers the effect of both the nuclear potential and of the average potential of the electrons on the separation of the two spaces. The positron solutions that explicitly occur are identified easily by their eigenvalues below $-2mc^2$ and are kept unoccupied. The remaining electron solutions are used to set up the many-electron wave function. Before discussing the optimisation of these electron spinors with the Dirac-Fock method in more detail, we need to consider some restrictions that must be applied with regard to the definition of the large and small component basis.

If we look at a one-electron equation with a hamiltonian as given in equation (3) we see that we can express the small component of the solution as a function of its large component

$$\begin{pmatrix} -e\varphi\, 1_2 & c\,\boldsymbol{\sigma}\cdot\mathbf{p} \\ c\,\boldsymbol{\sigma}\cdot\mathbf{p} & (-e\varphi - 2mc^2).1_2 \end{pmatrix} \begin{pmatrix} \psi^L \\ \psi^S \end{pmatrix} = \varepsilon \begin{pmatrix} \psi^L \\ \psi^S \end{pmatrix} \qquad (16)$$

$$\psi^S = \frac{-1}{e\varphi + \varepsilon + 2mc^2}\, c\,\boldsymbol{\sigma}\cdot\mathbf{p}\ \psi^L \qquad (17)$$

In the case of a one-electron atom both φ and ε are known exactly for a given solution $\begin{pmatrix}\psi_L\\ \psi_S\end{pmatrix}$, hence the operator on the right hand side of (17) is known. In many-electron Dirac-Fock calculations the form of the average electron potential and the value of ε are not known on forehand, so an approximated operator has to be used to find an initial ψ^S for a given ψ^L. The simplest approximation, which neglects both φ and ε in (17) because these are assumed to be small relative to $2mc^2$, is the kinetic balance[12] relation

$$\psi^S = \frac{-1}{2mc}\,\sigma\ \mathbf{p}\ \psi^L \qquad (18)$$

This relation becomes exact only in the non-relativistic limit. If a basis set is chosen in which this relation between the large and small component part of the spinors cannot be fulfilled, convergence to the non-relativistic limit upon enlarging the value of c is not possible. Such lack of balance between the large and small component bases manifests itself by giving too small values for the kinetic energy in this limit. Basis sets that can fulfil relation (18) are hence called kinetically balanced.

To see how such basis sets can be constructed we need to consider the action of the operator on the right-hand side of (18) on the large component functions. It's effect on the spatial part of the function is determined by the differential operators $\partial/\partial x$, $\partial/\partial y$ and $\partial/\partial z$ in $\sigma\mathbf{.p}$. The action of $\partial/\partial x$ on a primitive scalar Gaussian function is

$$\frac{\partial}{\partial x}\, x^\lambda\, e^{-\alpha r^2} = \left(\lambda x^{(\lambda-1)} - 2\alpha x^{(\lambda+1)}\right) e^{-\alpha r^2} \qquad (19)$$

We see that a linear combination of two functions with the same value of α, but with different values of λ arises. To fulfil the kinetic balance condition, these functions have to be contained in the small component basis $\{g_v^S\}$.

The connection of a large component function to a small component function with the same exponential parameter, but with its l-value shifted up or down by one, is typical for the kinetic balance operator and is retained if the relations are further worked out for the 4-component functions. In our case we construct a kinetically balanced basis by including all scalar primitive functions that arise from the operation of $\partial/\partial x$, $\partial/\partial y$ or $\partial/\partial z$ on all g_u^L in the basis set $\{g_v^S\}$.

For primitive basis sets, this concept of kinetic balance is widely accepted as a prerequisite for the choice of the small component basis functions. In contracted basis sets the situation is less clear-cut. In particular the determination of contraction coefficients for the small component basis functions g_p^S has been a matter of

discussion[13,14] in recent years. Straightforward application of the kinetic balance operator in highly contracted basis sets gives erroneous results for contracted functions that describe the core region of a heavy atom. In this region φ is not small compared to $2mc^2$ and (18) becomes a poor approximation to the exact relation. In this case an operator that resembles more closely the exact operator has to be used. These considerations lead to the development of the atomic balance procedure[15].

In the atomic balance procedure one first performs calculations on the constituent atoms (or ions) of the molecule (cluster) using kinetically balanced, uncontracted, basis sets ($\{ g^L_p \} = \{ g^L_u \}$, $\{ g^S_q \} = \{ g^S_v \}$). New large component bases $\{ g'^L_p \}$ and new small component bases $\{ g'^S_q \}$ are then formed by contracting the primitive basis functions with the spinor coefficients from these calculations. A good description of relation (17) will be obtained since the atomic and molecular potential are much alike in the core region while the differences that occur in the valence region will be small compared to $2mc^2$.

With this technique highly contracted basis sets can be made and used in much the same way as in non-relativistic calculations. An important difference, that makes the contraction less favourable compared to the non-relativistic case, is caused by the spin-orbit splitting. The difference in radial character of the l - 1/2 and l + 1/2 spinors makes it important to use a contraction scheme that treats both on equal footing. This in principle doubles the number of contracted Gaussian functions relative to a comparable non-relativistic contraction scheme.

3.3.3. Closed and Open Shell Dirac-Fock

In this section the Dirac-Fock SCF scheme is derived that is used to tackle the many-electron problem. A closed shell molecular Dirac-Fock formalism in which 4-component atomic spinors were used as basis functions was first proposed by Malli in 1975[16]. With the improvement of computer architectures in the eighties it became feasible to use more flexible basis sets. Codes that use separate large and small component basis sets, coupled by kinetic or atomic balance, are now in development at several places[17,18,19,20,21]. We have implemented a scheme, analogous to the non-relativistic Hartree-Fock-Roothaan method, that can handle arbitrary open and closed shell molecules.

In order to describe open shell systems in an average field formalism Roothaan in 1960[22] derived the open shell Hartree-Fock equations. The relativistic analogue of his energy expression becomes for an average of configurations[23]

$$E = \sum_k^C h_k + \frac{1}{2}\sum_{kl}^C Q_{kl} + f\left[\sum_m^O h_m + \frac{1}{2}af\sum_{mn}^O Q_{mn} + \sum_{k,m}^{C,O} Q_{km}\right] \qquad (20)$$

In this formula k and l label closed shell spinors which have occupation one, while m and n label open shell spinors which have a fractional occupation. $Q_{ij} \equiv J_{ij} - K_{ij}$ in which J_{ij} and K_{ij} are the Coulomb and exchange integrals. For the average of configuration energy the coupling constant, a, and the fractional occupation number, f, are given as a function of the number of open shell spinors, m, and the number of open shell electrons, n

$$f = \frac{n}{m} \tag{21}$$

$$a = \frac{m\,(n - 1)}{n\,(m - 1)} \tag{22}$$

Optimising this average of configuration energy will give us a set of spinors which can be used to describe all open shell states arising from a given configuration. The Fock equations are derived in the usual way by putting

$$\frac{\partial E}{\partial \psi_i} = 0, \qquad \delta \langle \psi_i \mid \psi_j \rangle = 0, \qquad i, j \tag{23}$$

i and j label the occupied positive energy spinors. Note that the stationary E will only be a local minimum since there will be lower energies possible by occupying negative energy spinors. Such solutions are not particle conserving and will not be considered in our approach.

In the following lines we present the equations which are obtained by expanding the Fock equations in the non-symmetry adapted basis set $\{\vartheta\}$. In formulas (26-30) the labels X and σ that explicitly refer to the large/small and spin character of the basis function will be omitted for clarity. A defined matrix element A_{pq} represents the block of elements $A_{pq}^{XY\sigma\tau}$ (X,Y $\in$ {L, S}; σ, τ $\in$ {α, β}).

$$\alpha = \frac{1-a}{1-f} \tag{24}$$

$$\psi_i = \sum_{p,\,X,\,\sigma} \vartheta_p^{X\sigma} b_{pi}^{X\sigma} \tag{25}$$

$$S_{pq} = \langle p \mid q \rangle \tag{26}$$

$$D^C_{pq} = \sum_k^C b^*_{qk} b_{pk} \qquad D^O_{pq} = f \sum_m^O b^*_{qm} b_{pm} \tag{27}$$

$$Q^C_{pq} = \sum_{rs} (pq||rs) D^C_{sr} \quad Q^O_{pq} = \sum_{rs} (pq||rs) D^O_{sr} \tag{28}$$

$$L^C_{pq} = \sum_{rs} \left[S_{pr} D^C_{rs} Q^O_{sq} + Q^O_{pr} D^C_{rs} S_{sq} \right] \qquad L^O_{pq} = \sum_{rs} \left[S_{pr} D^O_{rs} Q^O_{sq} + Q^O_{pr} D^O_{rs} S_{sq} \right] \tag{29}$$

$$F^C = h + Q^C + Q^O + \alpha L^C \qquad F^O = h + Q^C + aQ^O + \alpha L^C \tag{30}$$

For the closed shell orbitals the Fock equation is

$$F^C|k\rangle = \varepsilon_k |k\rangle \tag{31}$$

and for the open shell orbitals we get the equation

$$F^O|m\rangle = \varepsilon_m |m\rangle \tag{32}$$

Equations (31) and (32) are solved iteratively. The coupling operators L^C and L^O take care of the orthogonality between the closed shell and open shell solutions. In this formalism Koopman's theorem is valid and the open and closed shell spinor energies ε_i can be interpreted as estimates of ionisation energies.
We get the following expression for the total energy

$$\begin{aligned} E = {} & \mathrm{Tr}\left[H^D D^C\right] + \frac{1}{2}\mathrm{Tr}\left[Q^C D^C\right] + \\ & \mathrm{Tr}\left[H^D D^O\right] + \frac{1}{2} a \mathrm{Tr}\left[Q^O D^O\right] + \\ & \mathrm{Tr}\left[Q^O D^C\right] \end{aligned} \tag{33}$$

Since the separation between positive and negative energy spinors is not established until the Fock equations are solved, one might expect that the search for this local minimum with an iterative Self Consistent Field (SCF) procedure could cause convergence problems. In practise the energy eigenvalues of the two types of solutions are so far apart that their mixing is weak and does not critically depend on the initial density. Convergence of the SCF process is usually smooth with the energy expectation value approaching the stationary value from above. After convergence of the SCF process the energy of the configurational average is known together with a set of Dirac-Fock spinors. To get the energy of the individual many-electron states that are present in the average we use the Complete Open Shell Configuration

Interaction (COSCI)[24] method. In this method we construct the CI matrix equations in the basis of all determinants which can be formed by distributing the n open shell electrons over the m open shell spinors. The basis consists of $\binom{m}{n}$ determinants which gives a matrix that is usually small enough to fit in computer central memory and can be diagonalised completely. The resulting wave functions can be used as a starting point for Configuration Interaction methods.

3.3.4. Relativistic Multi Reference Configuration Interaction

The Dirac-Fock-COSCI approach gives intermediately coupled wave functions that include some correlation between the open shell electrons. In many applications, however, correlation between the open and closed shell electrons is important and also a more extensive description of the correlation between the open shell electrons is desirable. We have developed a relativistic variant of the Restricted Active Space Configuration Interaction (RASCI)[25] method which can be used to improve the wave functions and energy differences found in the COSCI step.

To describe the method it is convenient to write the Dirac-Coulomb-(Gaunt) hamiltonian in second quantised form. Using the generators of the unitary group E_{ij} ($E_{ij} = a_i^\dagger a_j$) the hamiltonian can be written as

$$H = \sum_{i,j} \langle i | h | j \rangle E_{ij} + \sum_{i,j,k,l} (ij | g | kl) \left(E_{ij} E_{kl} - E_{il} \delta_{jk} \right) \qquad (34)$$

In this equation molecular spinors are labelled by i and j. The summation is restricted to the electron solutions, we do not consider the process of (virtual) positron-electron pair creation.

We expand the many-electron wave functions in a basis of determinants $\{\Phi_I\}$.

$$\Psi_R \quad \sum_{I}^{N} \Phi_I C_{IR} \qquad (35)$$

$$\Phi_I (r_1, r_2, \ldots, r_n) = (n!)^{-1/2} \det | \psi_{I1}(r_1) \psi_{I2}(r_2) \ldots \psi_{In}(r_n) \qquad (36)$$

The result is a matrix representation of the hamiltonian that can be expressed as a sum of 1- and 2-electron integrals multiplied by coupling constants γ_{ij}^{IJ} and Γ_{ijkl}^{IJ} respectively.

$$\mathbf{H}_{IJ} = \sum_{i,j} h_{ij} \gamma_{ij}^{IJ} + \sum_{i,j,k,l} (ij | kl) \Gamma_{ijkl}^{IJ} \qquad (37)$$

with $h_{ij} = < i \mid h \mid j >$, $(ij \mid kl) = (ij \mid g \mid kl)$, $\gamma_{ij}^{IJ} = \langle I \mid E_{ij} \mid J \rangle$ and $\Gamma_{ijkl}^{IJ} = \langle I \mid E_{ij}\, E_{kl} \mid J \rangle$.

Since the size of the matrix will in general be in too large to be able to store all matrix elements, we use the direct diagonalisation technique of Davidson[26] to find the desired eigensolutions Ψ_R. In this iterative method a small subspace is constructed that spans the space of the desired eigensolutions. As zeroth order approximation the subspace is spanned by M (usually of the order 1-10) trial functions T_P

$$T_P = \sum_I^N \Phi_I \, \mathbf{D}_{IP} \qquad\qquad P = 1, M \qquad\qquad (38)$$

This gives an MxM matrix representation $\mathbf{H}^0_{PQ}$ of the hamiltonian.

$$\mathbf{H}^0_{PQ} = \langle T_P \mid H \mid T_Q \rangle = \sum_{I,\,J}^N \mathbf{D}^*_{IP}\, \mathbf{D}_{JQ}\, \mathbf{H}_{IJ} \qquad\qquad (39)$$

The eigenvectors, **B**, of this small matrix give the zeroth order wave functions Ψ^0_R in terms of the expansion functions T_P.

$$\Psi^0_R = \sum_P^M T_P \, \mathbf{B}^0_{PR} = \sum_P^M \sum_I^N \Phi_I \, \mathbf{D}_{IP} \mathbf{B}^0_{PR} = \sum_I^N \Phi_I \, \mathbf{C}^0_{IR} \qquad\qquad (40)$$

This space is then (repeatedly) extended with M new expansion functions to reduce the error in the wave functions and eigenvalues. Given the n^{th} order energy E^n_R and wave functions Ψ^n_R

$$\Psi^n_R = \sum_I^N \Phi_I \, \mathbf{C}^n_{IR} = \sum_P^{(n+1)M} \sum_I^N \Phi_I \, \mathbf{D}_{IP} \, \mathbf{B}^n_{PR} \qquad\qquad (41)$$

$$\mathbf{C}^n_{IR} = \sum_P^{(n+1)M} \mathbf{D}_{IP} \, \mathbf{B}^n_{PR} \qquad\qquad (42)$$

the coefficients, **F**, for the $(n+1)^{th}$ order corrections can be calculated as

$$\mathbf{F}_{IR} = \frac{\left(\sum_P^{(n+1)M} \Sigma_{IP} \, \mathbf{B}^n_{PR} \right) - \mathbf{C}^n_{IR} \, E^n_R}{\left(\mathbf{H}_{II} - E^n_R \right)} \qquad\qquad (43)$$

$$\text{with} \quad \Sigma_{IP} = \sum_{J}^{N} \mathbf{H}_{IJ}\, \mathbf{D}_{JP} \tag{44}$$

The M functions defined by **F** are normalised and form the $((n+1)M+R)^{th}$ expansion functions. In this procedure the critical step is the evaluation of Σ_{IP} (equation 44). The evaluation is done directly from the files of 1- and 2-electron integrals. This direct CI approach resembles the methods developed by Knowles and Handy[27] and by Jensen et al[28] but is more difficult to optimise. The main problem is that spin integration of the generators E_{ij} is not possible due to the implicit spin-orbit coupling present in the one-electron spinors. We will sketch our algorithm after a short description of the RAS choice of the determinantal space.

In the Restricted Active Space method the active spinor space is divided into 3 groups. The first group, RAS1, contains spinors that are occupied in the reference space. The second group, RAS2, contains the spinors that are variably occupied in the reference space. The spinors that were unoccupied in the reference space form RAS3. The CI space is now defined by specifying a maximum excitation level n_{H1} from RAS1 and a maximum excitation level n_{E3} to RAS3. The determinants that have n_{H1}, or less, holes in RAS1 and n_{E3}, or less, electrons in RAS3 form the CI space. This definition allows most of the conventional types of CI to be done as a special case.

To evaluate Σ_{IP} we use equation (37) to arrive at an expression in terms of the integrals and coupling coefficients :

$$\Sigma_{IP} = \sum_{J}^{N} \left(\sum_{i,j} h_{ij}\, \gamma_{ij}^{IJ} + \sum_{i,j,k,l} (ij \mid kl) \left(\Gamma_{ijkl}^{IJ} - \gamma_{il}^{IJ} \delta_{jk} \right) \right) \mathbf{D}_{JP} \tag{45}$$

The two-electron coupling coefficients Γ_{ijkl}^{IJ} can be replaced by a product of one-electron coupling coefficients γ_{ij}^{IJ} if we substitute the resolution of the identity.

$$\Sigma_{IP} = \sum_{J}^{N} \left(\sum_{i,j} h_{ij}\, \gamma_{ij}^{IJ} + \sum_{i,j,k,l} \sum_{K}^{N} \left((ij \mid kl)\, \gamma_{ij}^{IK} \gamma_{kl}^{KJ} - \gamma_{il}^{IJ} \delta_{jk} \right) \right) \mathbf{D}_{JP} \tag{46}$$

The summation over K, which on first sight would extend over all single excitations from the CI-space, can be restricted to a summation over the N determinants within the CI space. This restriction is a special feature of the RAS type of determinantal spaces. The procedure was given by Olsen and Roos[23] for real integrals (ij|kl) but works for complex integrals as well. It uses the permutation symmetry

(ij | kl) = (kl | ij) to exclude all integrals which are multiplied by coupling coefficients that couple to determinants that are not present in the CI space itself.
The final formula which is to be calculated is

$$\Sigma_{IP} = \sum_{J}^{N} \sum_{ij} g_{ij} \gamma_{ij}^{IJ} \mathbf{D}_{JP} + \sum_{J,K}^{N} \sum_{ij} \sum_{kl<ij} \frac{(ij \mid kl)}{1+\delta_{ij,kl}} \gamma_{ij}^{IK} \gamma_{kl}^{KJ} \mathbf{D}_{JP} \quad (47)$$

$$i \geq j : g_{ij} = h_{ij} + \frac{(ii \mid ij)}{1+\delta_{ij}} - \sum_{k<i} (ik \mid kj)$$

$$i < j : g_{ij} = h_{ij} - \sum_{k<i} (ik \mid kj)$$

3.3.5. Symmetry

Relativistic effects are most important in 5d transition metal complexes and actinide complexes. Many of these systems possess high symmetry. An efficient use of these symmetries can be helpful to keep the calculations feasible while point group representations may be used to label the different states and to clarify the interpretation. The MOLFDIR package is capable of handling all double groups that are subgroups of the O_h double group.
The full point group symmetry is used up to the Dirac-Fock level. At the relativistic CI level the highest abelian subgroup of the point group under consideration is used. In order to get an easy correspondence between the two point groups our symmetry adapted functions $\chi_l^{X\gamma}$ of equation (13) are constructed in such a way that they transform according to the irreducible representations of both groups.
In the calculation of the necessary one-electron integrals over $\chi_l^{X\gamma}$ only the integrals that are non-zero by symmetry need to be evaluated and stored.
The two-electron integrals are not calculated in the symmetry adapted 4-component basis but in the basis formed by the scalar functions g_p^X . The two-electron part of the Fock-matrix is constructed in the non-symmetry adapted basis $\{\vartheta\}$ and later transformed to the symmetry adapted basis $\{\chi\}$ and added to the one-electron part.
The reason for the use of such a two-step procedure lies in the sizes of the different basis sets, that were defined in equations 10-13. Since the same set of scalar cartesian Gaussian functions $\{g_i^X\}$ is used for both $\{\vartheta_i^{X\alpha}\}$ and $\{\vartheta_i^{X\beta}\}$, the size of the 4-component basis $\{\vartheta\}$ is twice the size of the scalar basis. The basis $\{\chi\}$ has essentially the same size as $\{\vartheta\}$ but is generally complex. Calculating and storing the integrals in the scalar basis thus gives a factor of 2^5 reduction in both disk storage and I/O processing, relative to the storage in the 4-component symmetry adapted basis. The treatment of point group symmetry in the scalar basis is done by means of a 4-

component generalisation[29] of the formalism of Dacre[30] and Elder[31]. In this formalism a "skeleton" Fock-matrix is formed from a symmetry unique list of two-electron integrals. The contributions of the missing integrals are included by averaging over degenerate representations of the Fock-matrix.

The CI calculations are done in the molecular spinor basis $\{\psi\}$. This set is, like $\{\chi\}$, by construction adapted to both the double group and the highest abelian subgroup. This blocks the CI matrix of the COSCI step and reduces the lengths of the CI vectors in the direct CI step. It also reduces the number of two-electron molecular spinor integrals that have to be handled. These integrals over the molecular 4-spinors are formed by a 4-index transformation of the symmetry unique list of scalar integrals. The contributions of the missing integrals are included by a generalisation of the method of Häser et al.[32]

Another symmetry which can be used is the Kramers' or Time-Reversal symmetry[33]. This symmetry causes the twofold degeneracy of all spinor eigenvalues of systems in the absence of external magnetic fields. The time-reversal operator, that commutes with the hamiltonian, is defined as

$$\hat{K}_4 = -i\begin{pmatrix}\sigma_y & 0_2\\ 0_2 & \sigma_y\end{pmatrix}\hat{K} \qquad (48)$$

in which $\hat{K}$ is the complex conjugation operator.

Operating with this operator on a given spinor $|\, i >$ gives another spinor, $|\, \bar{i} >$ which has the same eigenvalue. Substituting expression (25) gives the relation between spinor $|i>$ and spinor $|\, \bar{i} >$ in the basis $\{\vartheta\}$

$$|\bar{i}\ = \hat{K}_4\,|i\ = \ \hat{K}_4\left(\vartheta_p^{X\alpha} b_{pi}^{X\alpha} + \vartheta_p^{X\beta} b_{pi}^{X\beta}\right) = \vartheta_p^{X\beta}\left(b_{pi}^{X\alpha}\right)^* - \vartheta_p^{X\alpha}\left(b_{pi}^{X\beta}\right)^* \qquad (49)$$

Since both $|\, i >$ and $|\, \bar{i} >$ have the same (fractional) occupation, their contribution to the density-matrix, as given by equation (27) is the same, but occurs at a different place. This gives the following relations for the density, Fock and coupling matrices

$$A_{pq}^{XY\alpha\alpha} = \left(A_{pq}^{XY\beta\beta}\right)^*,\ A_{pq}^{XY\alpha\beta} = -\left(A_{pq}^{XY\beta\alpha}\right)^* \qquad (50)$$

The relations give a reduction of a factor of two in CPU time and memory requirements in the construction and storage of the Fock and the other matrices.

Using relation (49), one can furthermore derive the following relations for the 4-component molecular spinor integrals

$$(ij \mid kl) = (\bar{j}\bar{i} \mid kl) = (ij \mid \bar{l}\bar{k}) = (\bar{j}\bar{i} \mid \bar{l}\bar{k}) \quad (51)$$

$$(\bar{i}j \mid \bar{k}l) = -(\bar{j}i \mid \bar{k}l) = -(\bar{i}j \mid \bar{l}k) = (\bar{j}i \mid \bar{l}k) \quad (52)$$

$$(\bar{i}j \mid k\bar{l}) = -(\bar{j}i \mid k\bar{l}) = -(\bar{i}j \mid l\bar{k}) = (\bar{j}i \mid l\bar{k}) \quad (53)$$

These relations are exploited in the 4-index transformation program but are at present not used in the CI codes.

3.4. Structure of the MOLFDIR program package

The MOLFDIR program package consists of 11 separate FORTRAN programs that communicate by means of data files. The input data may be grouped on one file because NAMELIST type input is required for all modules. The input is usually specific for a (group of) modules with the exception of the general option TWOC. This option makes it possible to perform two-component (non-relativistic) calculations in double group symmetry. The feature facilitates comparison with non-relativistic results and may also be used to generate starting vectors for the Dirac-Fock SCF step. Figure 1 gives a flow diagram that shows the organisation of the package.

Figure 1. Flow diagram of the MOLFDIR program package.

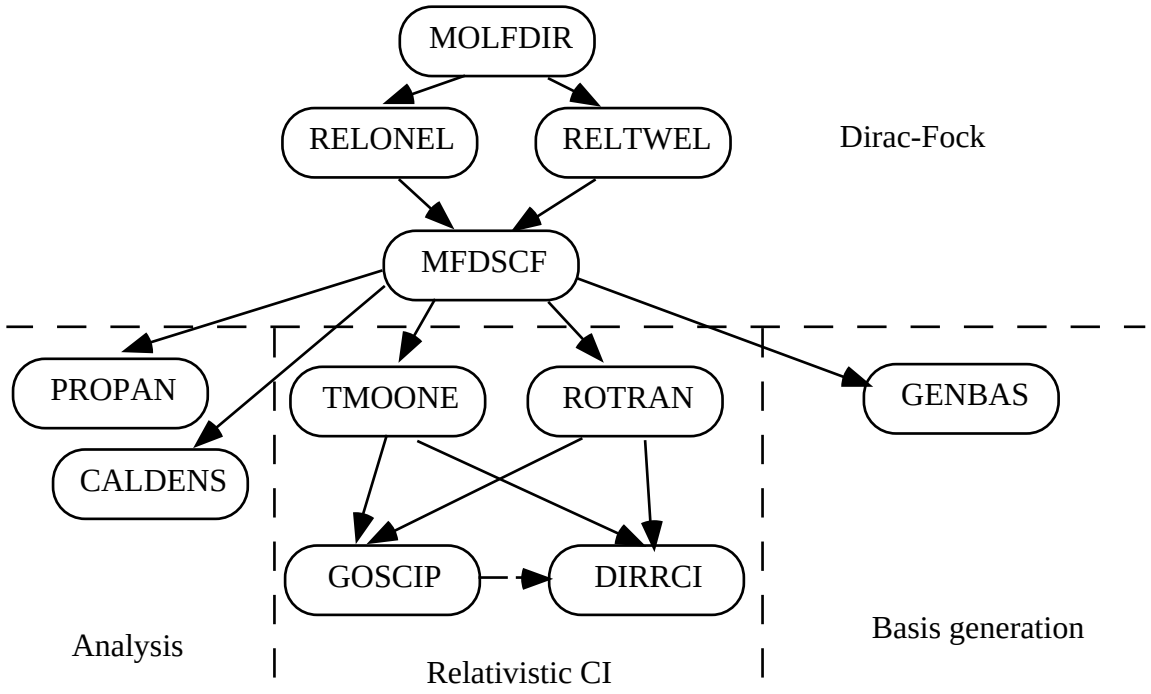

The programs are divided in four types. The first set of programs is necessary for the evaluation of the Dirac-Fock equations. Given the results of these calculations, three types of additional calculations are possible.

First one usually wants to analyse the spinors and the density. This can be done by means of Mulliken population analysis (PROPAN) or by calculating the electron density on a 3 or less dimensional grid (CALDENS).

If electron correlation is important or if an open shell calculation was done, additional CI calculations are necessary to obtain accurate energies. This can be done by the third set of programs. TMOONE and ROTRAN transform the integrals in the atomic basis to the 4-component molecular spinor basis, while GOSCIP and DIRRCI do the actual CI calculation. GOSCIP diagonalises a complete CI matrix and is to be used for the small COSCI calculations. DIRRCI optimises a few roots and can be used for larger RASCI calculations.

Finally GENBAS can be used to generate the general contracted (atomically balanced) basis sets that are used in calculations on large molecular systems.

3.4.1. MOLFDIR

The main function of the MOLFDIR program is to generate the double group symmetry adapted functions.

The cartesian Gaussian scalar functions g_p^X are grouped such that contaminant combinations, like $(x^2 + y^2 + z^2)e^{-\alpha r^2}$, that arise from the d-functions, and similar combinations that arise from f- and g-functions, may be removed in the transformation to the basis $\{\chi\}$. The groups are furthermore constructed such that all functions which transform among each other under the symmetry operations of the (single) point group are in the same group.

Symmetry functions that transform as the irreducible representations of the double group are then constructed from these groups. The number of symmetry functions is in principle equal to the number of cartesian Gaussian functions but may optionally be decreased if contaminant combinations are to be excluded. MOLFDIR excludes by default only the contaminant combinations that are formed in the large component basis. The reason for keeping the small component contaminants is the occurrence of the $r^{\lambda+1}$ term in the kinetic balance relation (19) that can not be described accurately without these small component 3s, 4p, etc. combinations. When looking at relation (19) one can conclude that an l-type contaminant may instead be combined with an (l-2)-type function to one small component function. Since the two-electron integrals are calculated in the primitive scalar cartesian basis, this contraction has no computational advantage in our method and we prefer to leave them uncontracted. This procedure is usually referred to as unrestricted kinetic balance.

The symmetry adapted functions χ are constructed by operating with a character projection operator $P^{\Gamma^1_\lambda,\Gamma^2_\mu,\Gamma^3_\nu}$ on the functions ϑ. The projection operator is the product of (maximally) 3 projection operators for representations of the highest molecular double group D_1 and two of its subgroups D_2 and D_3 (D_3 D_2 D_1). The functions χ generated in this way are orthogonal and span a basis for the irreducible representations Γ^1_λ, Γ^2_μ and Γ^3_ν of the three double groups. A matrix representation of these irrep's is now determined except for an arbitrary phase factor, in the case of multidimensional irrep's. The phases of the functions χ are chosen such that the matrix representations for multidimensional irreps that are spanned more than once by the basis are equal.

3.4.2. RELONEL

This module generates one-electron integrals over the symmetry adapted functions χ. It calculates the overlap, potential energy, "σ.p" and kinetic energy integrals. The kinetic energy integrals are only stored in non-relativistic (TWOC) calculations, in the relativistic calculations they are used to calculate the difference

$$d_l = [p^2]_{ll} - \sum_{s,\,t} [\sigma\ \mathbf{p}]_{ls}\,[S^{-1}]_{st}\,[\sigma\ \mathbf{p}]_{tl} \qquad (54)$$

d_l measures the deviation from the kinetic balance relation for a large component function l. If the small component basis functions (labelled by s,t) are formed by kinetic balance on the large component these differences will vanish. When using uncontracted, kinetically balanced, basis sets this relation gives a useful check on input errors. When using atomically balanced basis sets d_l will not be zero.

The potential energy matrix integrals are calculated using either a point charge nuclear model or the Gaussian model defined in equations (8) and (9). The nuclear masses, taken to be those of the most abundant isotopes, that were used in formula (9) are tabulated in the MOLFDIR program.

3.4.3. RELTWEL

This program generates two-electron integrals over the scalar cartesian Gaussian functions g^X_p. The integrals are calculated in four groups (LL|LL), (SS|LL), (SS|SS) and (SL|SL) in which charge cloud notation is used and the label p is omitted. Other groups of integrals do not contribute to the two-electron interaction or are related to these groups by permutation symmetry. The first three groups appear in the calculation of the Coulomb part of the two-electron operator, while the (SL|SL) integrals contribute to the Gaunt operator. For each of these sets a separate threshold

may be specified, which makes it possible to neglect small (SS|SS) integrals that contribute little to the Fock-matrix.

The calculation is done over the groups of primitive functions that have the same values of κ, λ and μ. This gives efficient vectorisation with vector lengths of the order n_u^4, with n_u being the number of primitives of the same type. The calculated integrals over the primitive functions are transformed to integrals over the general contracted functions by a limited 4-index transformation.

Symmetry is used by calculating only one representative of a group of integrals that are related by a symmetry operation of the point group or by permutational symmetry. Since only integrals which are above the specified threshold are stored, additional storage of a label is necessary. Packing the four indices makes it possible to store the label in an 8-byte word, just like the integrals that are calculated and stored in double (8-byte) precision. The integrals are sorted into 14 groups, depending on the relations between the 4 indices, before they are written. This sorting will allow efficient processing in the SCF process.

3.4.4. MFDSCF

MFDSCF performs the SCF procedure necessary to solve the Dirac-Fock equations (formulas 31and 32). To define the average of configuration energy expression, only the fractional occupation number, f, of the open shell spinors has to be specified. A technical restriction, resulting from the use of a single open-shell Fock-matrix, is that all open shell spinors need to have the same fractional occupation number. This limits the number of possible configurational averages that can be treated.

The initial electron density is usually that of a bare nucleus hamiltonian. Another possibility is the use of non-relativistic two-component starting vectors that are calculated using the two-component option of the program.

The work done in one SCF iteration can be divided into different steps :

1) Construction of the closed and open shell density matrices in the non-symmetry adapted basis {θ}.

2) Building the two-electron part of the Fock-matrix in this basis.

The two-electron integrals come in batches that have been sorted on their relations between the indices p, q, r and s. Of the 14 types, the integrals with all indices different are most abundant. These integrals contribute at 18 places in the Fock-matrix which makes it possible to form a short vector-loop for the addition.

3) Optional addition of the Gaunt interaction.

If the Gaunt interaction is to be included in the two-electron interaction, the batches of (SL |SL) integrals are read and handled in much the same way as the Coulomb

integrals. Differences are introduced by the off-diagonal character of the σ matrices which for instance makes integrals of the type (Sα Lβ | g^G | Sβ Lα) non-zero.
4) Transformation to the symmetry-adapted basis {χ}.
5) Completion of the skeleton Fock-matrix.
We here include contributions from the omitted two-electron integrals by averaging the Fock-matrix over degenerate representations. The validity of this procedure has been shown by Pitzer[34] and is more efficient than the original procedure of applying all symmetry operations to the matrix and adding the results.
6) Adding the one-electron matrix.
7) Transformation to the orthogonal basis and diagonalisation.
8) Selection of the closed and open shell vectors.
9) Construction of the new density-matrix in the symmetry adapted basis and extrapolation of the density.
10) Check on convergence and other stopping criteria.

The most time consuming parts of this process are steps 2 and 3. The CPU time involved is linear in the number of two-electron integrals that have to be processed. This number is dominated by the (SS | SS) and (SL | SL) type of integrals. In the discussion (section 6) some attention will be paid to attempts that may decrease this number without loosing accuracy. A number of such approximate methods have already been coded but more systematic research is necessary to give a sound judgement of their validity.
The SCF process is slowly convergent due to the large size of the basis set and may give oscillatory behaviour due to wrong ordering of closed and open shell spinors in the initial stage of the process. To cope with these problems various convergence accelerating and damping techniques have been implemented and tested. The best procedure turned out to be the use of a fixed damping on the density-matrix followed by Pulay's DIIS method[35], with the error vector taken to be the commutator of the Fock and density matrices. Other methods available are overlap selection with the previous vectors, selection of open shell spinors by their population and a three- or four-point extrapolation method on the density[36]. An implementation of the quadratically convergent SCF method[37] is in development.

3.4.5. CALDENS

CALDENS calculates the electron density on a grid that can be specified by the user. These data can be used to visualise the electron density with the aid of the visualisation package AVS[38], or with similar packages. To analyse contributions of

the individual spinors a partial density may be defined by considering contributions from one, or a limited number of spinors only.
The program first transforms the MS vectors to the non-symmetry adapted basis $\{\vartheta\}$ in which the total density function $\Delta(x, y, z)$ is defined as

$$\Delta = \Delta^L + \Delta^S \tag{55}$$

$$\Delta^X(x, y, z) = \sum_{p, q, \sigma} \left(D_{pq}^{XX\sigma\sigma, C} + D_{pq}^{XX\sigma\sigma, O} \right) \vartheta_p^{X\sigma}(x, y, z)\, \vartheta_q^{X\sigma}(x, y, z)$$

Note that cross terms in X or σ do not contribute to the value of Δ, because of the orthogonality of the ϑ's.
The program gives by default the value of Δ ,but can also be used to calculate the values of Δ^L or Δ^S separately.

3.4.6. PROPAN

Another analysis is possible by splitting contributions to the molecular spinors by their atomic contributions. PROPAN uses the well-known Mulliken[39] scheme to do this analysis. The following quantities are defined

$$Q_{pq}^i = \sum_{X, \sigma} (2 - \delta_{pq}) \left(d_{pi}^{X\sigma} \right)^* d_{qi}^{X\sigma}\, s_{pq}^{XX, \sigma\sigma} \tag{56}$$

with $$s_{pq}^{XY, \sigma\tau} = \int g_p^X(r)\, g_q^Y(r)\, dr\, \delta_{XY}\, \delta_{\sigma\tau}$$

The diagonal element of Q, Q_{pp}^i, is the net population of basis function p in spinor $|i\rangle$, off-diagonal elements are called overlap populations. Since the molecular spinor coefficients d are complex numbers, the off-diagonal elements may be complex as well. The diagonal elements and the trace will be real, however. An additional quantity P_p^i is sometimes useful to distribute the charge found in the off-diagonal elements. This gross population of the basis function p is defined as

$$P_p^i = Q_{pp}^i + \frac{1}{2} \sum_{q \neq p} Q_{pq}^i \tag{57}$$

The total electron charge can now be written as :

$$Q = \sum_{i,\,p,\,q} f_i\, Q^i_{pq} = \sum_{i,\,p} f_i\, Q^i_{pp} = \sum_{i,\,p} f_i\, P^i_p \qquad (58)$$

with f_i the fractional occupation of spinor $|i>$.
PROPAN calculates P^i_p and Q^i_{pq} for a specified set of spinors.

3.4.7. TMOONE

This program generates effective one-electron integrals that represent the Coulomb and exchange interaction of the valence electrons with the frozen cores and the interaction with the nuclei. The integrals are obtained by constructing a density-matrix D^C_{pq}, like the one given in equation (27), but with the sum over spinors being restricted to the frozen core spinors. The desired effective one-electron matrix elements are then obtained by transforming the closed shell Fock-matrix to the active spinor space.

3.4.8. ROTRAN

This program generates two-electron integrals over the active molecular spinors. A detailed description of the basic algorithm has been given by Visser[40]. The algorithm has recently been improved by the use of time-reversal symmetry. This gave a storage and CPU reduction with a factor of 2 in the half-transformed integrals. The relations introduced for the half transformed integrals are given in formulas (59-62). Note that the relations for the Gaunt and Coulomb interaction differ by a sign factor. This difference disappears for the fully transformed integrals (relations 51-53).

$$(ij \mid g^C \mid pq) = (\bar{j}\bar{i} \mid g^C \mid pq) \qquad (59)$$

$$(ij \mid g^G \mid pq) = -\,(\bar{j}\bar{i} \mid g^G \mid pq) \qquad (60)$$

$$(i\bar{j} \mid g^C \mid pq) = -\,(j\bar{i} \mid g^C \mid pq) \qquad (61)$$

$$(i\bar{j} \mid g^G \mid pq) = (j\bar{i} \mid g^G \mid pq) \qquad (62)$$

A second difference with the algorithm as described by Visser is the breakdown of the final step into two parts. In this step the contributions to the MO-integrals, that come from omitted non symmetry unique integrals, were included by the transformation

$$(ij \mid kl) = \sum_{\hat{R}} \sum_{abcd} (ab \mid cd)\, \Gamma^{*}_{ai}(R)\, \Gamma_{bj}(R)\, \Gamma^{*}_{ck}(R)\, \Gamma_{dl}(R) \qquad (63)$$

in which the sum over R is the sum over all operations in the point group. Häser et al.[20] developed a method to reduce the large memory requirements ($2m^4$, m being the number of active molecular spinors) that straightforward implementation of this formula would ask. If we define A as the compound label (abcd) and I as the compound label (ijkl) we can write the transformation (63) as

$$(I) = \sum_{A} (A)\, P_{AI} \qquad (64)$$

with

$$P_{AI} = \sum_{\hat{R}} \Gamma^{*}_{ai}(R)\, \Gamma_{bj}(R)\, \Gamma^{*}_{ck}(R)\, \Gamma_{dl}(R) \qquad (65)$$

Diagonalisation of P yields mostly zero eigenvalues and a small number of eigenvalues g, with g being the dimension of the group

$$P_{AI} = \sum_{\nu} U_{A\nu}\, \lambda_\nu\, U_{\nu I} \quad , \lambda_\nu = 0, g \qquad (66)$$

The transformation is thus broken down in two steps :

$$(\nu) = \sum_{A} (A)\, U_{A\nu} \qquad (67)$$

$$(I) = \sum_{\nu} (\nu)\, \lambda_\nu\, U_{\nu I} \qquad (68)$$

in which at each stage only the small number of non-zero reduced matrix elements (ν) has to reside in core. Use of this new algorithm makes transformations to a large number of active spinors possible.

3.4.9. GOSCIP

Given a set of m active spinors $\{\psi\}$ and a number of electrons n, GOSCIP generates bit representations of the $\binom{m}{n}$ determinants that can be formed within this space. By construction, as a product of symmetry adapted spinors, these determinants will transform according to a representation of the highest abelian double group of the problem. The appropriate representation of the determinant in this abelian double group is easily obtained by table lookups. Using the bit representations the CI matrix

elements in the non-zero blocks are calculated. The resulting blocked matrix is fed to a standard complex diagonalisation routine that gives the complete set of eigenvalues and eigenvectors. The eigenvectors are written to file and may be used as starting vectors for direct CI calculations.

3.4.10. DIRRCI

This program performs the direct RASCI type of calculations that were described in section 3.3.4. In one run a number of wave functions (n_{roots}) that belong to the same irreps of the (abelian) double group are calculated. The wave functions that are to be optimised are usually the multi-determinantal wave functions that were obtained in a preliminary COSCI calculation.

In the case of a closed shell or another reference wave function that can be written as a single determinant, the COSCI step can be skipped. DIRRCI then takes the determinants in the CI space that have the lowest expectation values as the reference wave functions.

The program starts by producing a sorted two-electron MS integral file. For a given (kl) all non-zero integrals (ij|kl) with (ij) ≥ (kl) are stored consecutively. Subsequently the effective one-electron integrals are read and the g_{ij} matrix elements that are defined in equation (47) are formed.

The next step is the generation of the one-electron coupling coefficients γ_{ij}^{IJ}. Since the many-electron basis is defined to consist of simple determinants these coupling coefficients will be either -1, 0 or 1. Their number scales like Nm^2, with N the number of determinants and m the number of spinors. Although only non-zero elements are calculated it is still impossible to store all elements in core memory. The calculated elements are stored on a direct access file with for each (ij) combination a list of addresses of pairs I and J, combined with the sign of the coupling coefficient. In the calculation use of a graphical representation of the CI space[41] has been very useful. More details about this method can be found in chapter 2 and the appendix of this thesis.

Since for each two-electron integral (ij|kl) this list has to be read back into memory, the performance of the program is largely determined by the I/O overhead. An alternative procedure, that reduces this overhead at the expense of extra CPU time, is to regenerate the list of addresses whenever needed. Depending on the computer used and the size of the CI-space, the user may choose the most efficient of both strategies.

In non-relativistic singles and doubles CI calculations the coupling coefficients are often factorised into an internal and an external part[42]. Such a factorisation is also possible in our case, if no more than two electrons are excited to the RAS3 space. The

implementation of this factorisation made it possible to keep all γ_{ij}^{IJ}, for which i or j belong to RAS3, in core memory and reduced the I/O problems.
As a final step before the iterative diagonalisation process is started, the diagonal matrix elements H_{II} that are needed in the evaluation of equation (43) are generated.
In the iterative diagonalisation process all CI vectors **D** and Σ are kept in memory. The evaluation of formula (47) is done by the following algorithm

```
zero the array  Σ (N, nroots)
loop over (kl)
        zero the array F (N, nroots)
        read all integrals (ij|kl), ij) ≥ (kl)
        read or generate all γ_kl^KJ
        loop over iroot
                loop over J
                        add Σ (K, iroot) = Σ (K, iroot) + γ_kl^KJ * D (J, iroot) * g_ij
                        calculate F (K, iroot) = γ_kl^KJ * D (J, iroot)
                endloop over J
        endloop over iroot
        loop over (ij)
                read or generate all γ_ij^IK
                loop over iroot
                        loop over K
                                add Σ (I, iroot) = Σ (I, iroot) + γ_ij^IK * F (K, iroot) * (ij|kl)
                        endloop over K
                endloop over iroot
        endloop over (ij)
endloop over (kl)
```

In the loop over J, a loop over K is implied because only one γ_{kl}^{KJ} will be non-zero for a given (kl) and J. The same holds for the loop over K, where a loop over I is implied. The algorithm is vectorised in these inner loops (J, K) and may be parallelised in the loops (iroot) over the roots.
After the calculation of the sigma vectors, new expansion vectors **D** are obtained following the normal Davidson procedure. The calculation is converged if all residual vectors **R** (**R** = **HC** - E**C**) have norms beneath the specified threshold. This stopping criterium is the most rigorous, other criteria that may be specified are a convergence threshold on the energy or a maximum number of iterations.

The final wave functions that are given by the vectors **C** are written to file for further analysis and restart purposes. The default analysis is to calculate the diagonal matrix elements of the CI density-matrix

3.4.11. GENBAS

This program generates the contraction coefficients c^L_{up} and c^S_{vq}, that were defined in equation (11). It assumes that an atomic calculation was done in a given uncontracted basis $\{\vartheta^L_u,\ \vartheta^S_v\}$ which yielded a set of molecular spinor coefficients $b^{L\sigma}_{ui}$ and $b^{S\sigma}_{vi}$. In the atomic case these complex coefficients can be multiplied by a phase factor that makes the large component part completely real and the small component part completely imaginary. This means that they can be mapped on a set of real coefficients c.

As an example we take a look at the generation of contraction coefficients for a large component p basis function from the atomic $2p_{1/2}$ and $2p_{3/2}$ spinors. We number the $p_{1/2}$ as spinor 1 and the $p_{3/2}$ as spinor 2. After multiplying with the appropriate phase factor we get 4 different scalar functions

$$g^L_I = \sum_u b^{L\alpha}_{u1}\ g^L_u, \qquad g^L_{II} = \sum_u b^{L\beta}_{u1}\ g^L_u,$$
$$g^L_{III} = \sum_u b^{L\alpha}_{u2}\ g^L_u, \qquad g^L_{IV} = \sum_u b^{L\beta}_{u2}\ g^L_u \tag{69}$$

Non-zero contributions in this sum will only come from functions of the type p_x, p_y and p_z. Since the relation between these three functions for a given spinor is fixed by the spherical symmetry, we have to consider only the radial character : the relation between functions of the same type, but with a different exponent α . We thus further restrict the sum over u (u') to functions of one of these types (for instance only p_x functions).

$$g'^L_I = \sum_{u'} b^{L\alpha}_{u'1}\ g^L_{u'}, \quad g'^L_{II} = \sum_{u'} b^{L\beta}_{u'1}\ g^L_{u'}$$
$$g'^L_{III} = \sum_{u'} b^{L\alpha}_{u'2}\ g^L_{u'}, \quad g'^L_{IV} = \sum_{u'} b^{L\beta}_{u'2}\ g^L_{u'} \tag{70}$$

The resulting set of functions is representative for the radial character of the $p_{1/2}$ and the $p_{3/2}$ spinor that was used. Since we use an average of configuration formalism in which no spin-polarisation will occur, $g'^L_I \equiv g'^L_{II}$ and $g'^L_{III} \equiv g'^L_{IV}$. GENBAS normalises the functions and then projects out the part of g'^L_{III} that is orthogonal to g'^L_I. Inclusion of this differential function in the basis is important if the spin-orbit splitting of the

shell is large. An appropriate measure for this splitting is the norm of the differential function. GENBAS enables the user to specify a threshold (default 1.E-5), above which the differential function is included in the basis set.

If more than one p-shell is present in the atom the orthogonalisation procedure is continued and functions that have a non-orthogonal part with a norm above the threshold are added to the basis. To get flexibility in the valence region the procedure is usually ended by orthonormalising and adding some diffuse primitive functions.

To generate functions for the small component essentially the same scheme is used. The main difference here is that apart from these fuctions that arise form the atomic calculation (the atomically balanced functions) an additional set of functions may be defined by kinetic balance (equations 18 and 19) on the newly formed large component basis. This set can also be orthogonalised to, and included in the basis if it is significantly different from the set already obtained. The threshold for inclusion in the small component basis is by default set to 1.E-7.

Following this procedure general contracted basis sets can be obtained that give exactly the same atomic energies as the uncontracted bases and have sufficient variational freedom to describe the changes that occur in the molecule. Due to the doubling of contracted functions in the core, where the l±1/2 spinors differ most, the reduction of the number of basis functions is, however, not as large as can be obtained in non-relativistic calculations.

3.5. Timings for some sample calculations

The first (closed shell Dirac-Fock) part of the package was completed in 1985. The open shell part including GOSCIP was finished in 1991, while the direct CI code DIRRCI has become operable in 1992. During this period many of the older modules were optimised and changed which makes it difficult to compare timings of the older calculations with newer calculations. We will give two examples of recent calculations to give an impression of the resources that are needed.

3.5.1. Methane

A small calculation, that we use for testing purposes, is a calculation on the carbon atom and methane molecule. Results of these calculations and of other calculations on the whole series XH_4 (X=C, Si, Ge, Sn, Pb) have been published by Visser et al.[43]

The performance in these small computations is dominated by the SCF part. The disk space necessary is almost solely determined by the number of (SS|SS) and (SL|SL) integrals.

Table 2. Timings C and CH4. Calculations performed on a Convex C240.

	Carbon atom		Methane	
Module	Diskspace	CPU time	Diskspace	CPU time
MOLFDIR	0.1 Mb	2.1 s	0.3 Mb	3.7 s
RELONEL	0.2 Mb	2.9 s	0.7 Mb	17. s
RELTWEL	1.8 Mb	4.7 s	37. Mb	101. s
MFDSCF	2.6 Mb	67.0 s	39. Mb	443. s
TMOONE	2.6 Mb	3.5 s	--	--
ROTRAN	2.6 Mb	3.8 s	--	--
GOSCIP	7.0 Kb	0.3 s	--	--

3.5.2. Platinumhydride

One of the recent large calculations that was done involved the PtH molecule (chapter 5). This molecule serves as the simplest model for the bonding of hydrogen on platinum surfaces.

The basis set employed for Pt is (22s18p14d11f | 18s22p18d14f11g), generally contracted to [8s10p9d3f | 6s13p12d11f4g]. The Dirac-Fock calculations were followed by CI-SD calculations. In the latter calculations 11 valence electrons were correlated, using a RAS space of (10, 2, 70) with $N_{H1} = N_{E3} = 2$.

Table 3. Timings Pt and PtH. Calculations performed on a Cray Y-MP 464.

	Platinum atom		PtH molecule	
Module	Diskspace	CPU time	Diskspace	CPU time
MOLFDIR	0.9 Mb	6.8 s	0.4 Mb	3.6 s
RELONEL	3.0 Mb	54. s	3.5 Mb	313. s
RELTWEL	2.2 Gb	0.4 h	1.8 Gb	3.5 h
MFDSCF*	2.3 Gb	3.2 h	1.9 Gb	0.4 h
TMOONE	--	--	1.9 Gb	280. s
ROTRAN	--	--	3.0 Gb	0.8 h
DIRRCI	--	--	0.6 Gb	0.4 h
GENBAS	5.1 Mb	23. s		

* Different versions of MFDSCF were used in the Pt and PtH calculations.

When comparing the atomic and the molecular disk usage one finds that for the atom one needs more space to run the SCF part than for the molecule. This is caused by the general contraction that was applied in the molecular basis set, making the integral

files shorter even though the symmetry that could be used is lowered (O_h -> C_{4v}). The large CPU time for the atomic SCF part was caused by the large number of iterations that was necessary to converge. The reason for this was that at that time the DIIS extrapolation procedure was not yet implemented. This procedure usually reduces the number of iterations by a factor of 2 to 3 and has significantly speeded up the molecular calculation.

3.6. Discussion and future developments

The program package presented here is applicable to various types of molecules and has proven to give reliable results. It's development has not stopped yet however, because further optimisations of the present modules are still possible to reduce the rather formidable computational resources that are needed for large-scale calculations. Also additional features and modules, like MCSCF or Coupled Cluster, may be implemented to increase the level of theory available. We will discuss some of the ongoing research and give an outlook on what developments are likely to come in the near future.

3.6.1. Reduction of the number of scalar two-electron integrals

The time spent in one SCF-iteration and the time necessary for the 4-index transformation scales almost linearly with the number of two-electron integrals that are calculated in the scalar basis. The amount of diskspace that is to be used is also solely dependent on this number.

The problem of the large two-electron integral files is of course familiar from experiences with non-relativistic quantum chemical calculations. Some of the remedies that have been developed in that field may be well suitable in our case and additional techniques may be used that take the different importance of the four sets (LL | LL), (SS | LL), (SS | SS) and (SL | SL) into account.

A technique that seems to work fairly well is to discard small-valued (SS | SS) integrals. The justification for this procedure is given by the estimate of the coefficients for $b_{vi}^{S\sigma}$ that can be obtained from equation (18)

$$b_{qi}^{S\sigma} \sim \frac{1}{2c} b_{pi}^{L\sigma} \qquad (71)$$

This means that an (SS | SS) integral will give a contribution to the Fock-matrix that is of the order $\left(\frac{1}{2c}\right)^4$ = 2E-10 times smaller as the contributions from the (LL | LL) integrals. Relation (71) is, however, only applicable for free electrons with low energies. In the inner shell $1s_{1/2}$ spinor in Pt the ratio between $b_{ui}^{L\sigma}$ and $b_{vi}^{S\sigma}$ is about 3.3

giving an (SS | SS) contribution that is only of the order 1.E-2 times smaller than the (LL | LL) contribution. This makes it more difficult to leave out integrals.
Our experience is that a threshold of 1.E-6 on the (SS | SS) integrals, and a threshold of 1.E-9 for the (SL | SL) and (SS | LL) type of integrals may be used without loss of accuracy.
Another related technique is to calculate only a specific type of (SS | SS) integrals, for example only those that involve small component core functions. This may however lead to imbalances in the SS and SL part of the Fock-matrix that give rise to so-called intruder states : positron states that have energies (far) above $-2mc^2$. Dyall has shown that these problems may be overcome by defining radially localised functions after which valence integrals that involve the outer shells may be skipped[44].
We are at present experimenting with a somewhat different scheme in which only one-centre (SS | SS) integrals are calculated. Preliminary results indicate that this practical scheme may work, but more research needs to be done.
All these schemes use the fact that the (SS | SS) contributions to the Fock-matrix will be small and will not change much going from the atom to the molecule. This makes the method suitable for the direct SCF scheme[45] or a hybrid scheme of partly storing and partly regenerating integrals[46]. The direct schemes recalculate the integrals whenever they are needed (if the differences in the density-matrix are above a given threshold) and thus reduce the disk and I/O requirements at the expense of CPU effort. This scheme is attractive for the relativistic method for two reasons. The first is that the differences for most SS density matrix elements between subsequent iterations will not be large, so that recalculation of the (SS | SS) contribution and integrals will be required only a few times. Another, but somewhat conflicting, reason is that use of kinetic balance leads to shells of functions that differ by their values of (κ, λ and μ), but share the same exponent. This allows very efficient generation of batches of integrals[47] which reduces the additional CPU requirements. The conflict with the first reason is in the fact that some of the recalculated integrals will be important while others don't give rise to important changes in the Fock-matrix. This implies a fast generation of unnecessary integrals.

3.6.2. Contraction and the use of symmetry

A different approach that may also reduce the number of integrals and hence improve the performance is to use strongly contracted basis sets. In our scheme contraction is hampered by the fact that it must be specified in the scalar basis. If we would build our functions χ (equation 13) directly from the primitive functions g (equation 10), then we would be able to specify different contractions for different j-values. The

orthogonalisation that was described in the GENBAS module is then unnecessary since the 4-component functions χ will be orthogonal by their spin character.

The problem with this scheme is that the two-electron integrals should be calculated either in the uncontracted scalar basis, or in the 4-component symmetry adapted basis. Both basis sets contain more functions than the scalar contracted basis set. However, if we limit ourselves to the SCF stage we find that of all integrals over {χ} only integrals of the type $(\Gamma_i\Gamma_i \mid \bar{\Gamma}_j\Gamma_j)$ and $(\Gamma_i\Gamma_j \mid \bar{\Gamma}_i\Gamma_j)$ do contribute. This restriction to integrals that contain only two irreps can be exploited in a supermatrix formalism[22]. For highly symmetric molecules these supermatrices will be much smaller than the complete two-electron integrals files, which combined with the more flexible contraction possibilities probably give smaller files than can be obtained with the present scheme.

A problem is that the non-SCF type of integrals are necessary in the CI calculations and therefore also in the 4-index transformation. This problem may be overcome by recalculating the integrals for this step, thus making the 4-index transformation "direct".

We expect to have a working version of this supermatrix based scheme in the beginning of 1994, after which experience must learn which scheme (scalar integrals or 4-component symmetry integrals) is preferable.

3.7. Conclusions

We have presented a method and a FORTRAN program package that can be used for reliable and accurate relativistic electron structure calculations for heavy atom containing systems. The structure of the package is flexible so that optimisations and additions can be made within the existing structure.

Given the research stage of relativistic quantum chemistry methods in general this program is not yet to be considered a "black-box" tool. The present stage of development does however allow the general use of the package provided that sufficient computational resources are available. Interested quantum chemists can thus use it as a benchmark code for methods that treat relativity in a more approximate way.

References

1) P. Pyykkö, Chemical Reviews **88**, 563 (1988).

2) R. E. Moss, Advanced Molecular Quantum Mechanics, (W. A. Benjamin, Inc.: London 1968).

3) M. E. Rose, Relativistic Electron Theory, (Wiley & Sons: New York 1961).

4) I. P. Grant and H. M. Quiney, Adv. At. Mol. Phys. **23**, 37 (1988).

5) G. Breit, Phys. Rev. **34**, 553 (1929).

6) J. A. Gaunt, Proc. R. Soc. A **122**, 513 (1929).

7) S. F. Boys, Proc. Roy. Soc. A, **200**, 542 (1950).

8) F.G. Werner and J.A. Wheeler, Phys. Rev. **104** , 126 (1958).

9) O. Visser, P. J. C. Aerts, D. Hegarty and W. C. Nieuwpoort, Chem. Phys. Letters **134** , 34 (1987).

10) R. Hofstadter, Rev. Mod. Phys. **28**, 214 (1956);

D. G. Ravenhall, Rev. Mod. Phys. **30**, 430 (1958);

J. P. Desclaux, Computer Phys. Comm. **9**, 31 (1975).

11) R. C. Raffenetti, J. Chem. Phys. **58**, 4452 (1973).

12) A. D. McLean and Y. S. Lee, in: "Current Aspects Of Quantum Chemistry 1981", ed. R. Carbó, (Elsevier: Amsterdam 1982).

13) Y. Ishikawa, H. Sekino and R.C. Binning, Jr., Chem. Phys. Lett. **165**, 237 (1990).

14) O. Matsuoka, Chem. Phys. Lett. **195**, 184 (1992).

15) L. Visscher, P.J.C. Aerts, O. Visser and W.C. Nieuwpoort, Int. J. Quant. Chem.: Quant. Chem. Symp. **25**, 131 (1991).

16) G. Malli and J. Oreg, J. Chem. Phys. **63**, 830 (1975).

17) P. J. C. Aerts and W. C. Nieuwpoort, proceedings of the 6th Seminar on Computational Methods in Quantum Chemistry, Schloss Ringberg (Tegernsee), September 4-7, (1984).

18) S. Okada and O. Matsuoka, J. Chem. Phys. **91**, 4193 (1989).

19) K. G. Dyall, K. Fægri, Jr. and P.R. Taylor, in : The effects of relativity in atoms, molecules and the solid state, ed. I. P. Grant, B. Gyorffy and S. Wilson, (Plenum: New York 1991).

20) A. K. Mohanty and E. Clementi, Int. J. Quantum Chem. **39**, 487 (1990).

21) T. Saue, Thesis, University of Oslo (1991).

22) C. C. J. Roothaan, Rev. Mod. Phys. **32**, 179 (1960).

23) O. Visser, L. Visscher and P. J. C. Aerts, in : The effects of relativity in atoms, molecules and the solid state, ed. I. P. Grant, B. Gyorffy and S. Wilson, (Plenum: New York 1991).

24) O. Visser, L. Visscher, P. J. C. Aerts and W. C. Nieuwpoort, J. Chem. Phys. **96**, 2910 (1992).

25) J. Olsen, B. O. Roos, P. Jørgensen and H. J. Aa. Jensen, J. Chem. Phys. **89**, 2185 (1988).

26) E. R. Davidson, J. Comput. Phys. **17**, 87 (1975).

27) P. J. Knowles and N. C. Handy, Chem. Phys. Lett. **111**, 315 (1984).

28) H. J. Aa Jensen, H. Ågren and J. Olsen, in Motecc 1990 : chapter 8, (Escom Science Publishers B.V.: Leiden 1990).

29) P. J. C. Aerts, Ph. D. Thesis, Rijks Universiteit Groningen (1986).

30) P. D. Dacre, Chem. Phys. Lett. **7**, 47 (1970).

31) M. Elder, Int. J. Quantum Chem. **7**, 75 (1973).

32) M. Häser, J. Almlöf and M. W. Feyereisen, Theoretical Chemistry Acta **79**, 115 (1991).

33) H. A. Kramers, Proc. Acad. Amsterdam **33**, 959 (1930).

34) R. M. Pitzer, J. Chem. Phys. **58**, 3111 (1973).

35) P. Pulay, J. Comp. Chem. **3**, 556 (1982).

36) H. Merenga and J. Andriessen, Stratech 92-06 (internal report TU Delft), Oct. 1992.

37) G. B. Bacskay, Chem. Phys. **61**, 385 (1981);

G. B. Bacskay, Chem. Phys. **65**, 383 (1982).

38) AVS is a trademark of Stardent Computer Inc.

39) R. Mulliken, J. Chem. Phys. **23**, 1833 (1955).

40) O. Visser, Ph. D. Thesis (Appendix A), Rijks Universiteit Groningen (1992).

41) W. Duch, Lecture Notes in Chemistry **42**, (Springer: Berlin 1986).

42) P. E. M. Siegbahn, J. Chem. Phys. **70**, 5391 (1979).

43) O. Visser, L. Visscher, P.J.C. Aerts and W. C. Nieuwpoort, Theoretica Chimica Acta **81**, 405 (1992).

44) K. G. Dyall, Chem. Phys. Lett. **196**, 178 (1992).

45) J. Almlöf, K. Faegri, Jr. and K. Korsell, J. Comp. Chem. **3**, 385 (1982).

46) M. Häser and R. Ahlrichs, J. Comput. Chem. **10**, 104 (1989).

47) S. Obara and A. Saika, J. Chem. Phys. **84**, 3963 (1986).

4. Kinetic balance in contracted basis sets for relativistic calculations

4.1. Abstract

A demonstration of kinetic balance failure in heavily contracted basis sets is given. Other possible methods of constructing small component basis sets for 4-component relativistic calculations are discussed. The position of the additional negative energy levels in extended balance calculations in some recent many-electron calculations is examined.

4.2. Introduction

Relativistic calculations based on the Dirac equation or the effective one-electron Fock-Dirac equation are often performed by means of basis set expansion. The most common way to do this is to define two basis sets, one describing the upper two (large) components of the wave function and one describing the lower two (small) components. As is argued by many authors[1-5] it is important for the small component basis set to be related to the large component by means of the so-called "kinetic balance" condition. This condition assures that the non-relativistic limit (which can be obtained by letting the speed of light, c, grow to infinity) is correctly described even in a finite basis.

However, if one attempts to do relativistic calculations one is not too much interested in the convergence to the non-relativistic limit but rather in a correct description of the solutions for the real finite value of c. In this case straight forward application of the kinetic balance prescription may lead to erroneous results as we show here by examining the $1s_{1/2}$ and $2p_{1/2}$ orbitals of a hydrogen like system.

We furthermore examine the behaviour of extended kinetic balance basis sets in a few recent many-electron calculations in order to give some insight about the position of the extra states introduced in the spectrum by the extension.

4.3. Theory

The Dirac equation is given by

$$\begin{pmatrix} V(\vec{r}) & c\vec{\sigma}.\vec{p} \\ c\vec{\sigma}.\vec{p} & V(\vec{r}) - 2mc^2 \end{pmatrix} \begin{pmatrix} \psi^L(\vec{r}) \\ \psi^S(\vec{r}) \end{pmatrix} = E \begin{pmatrix} \psi^L(\vec{r}) \\ \psi^S(\vec{r}) \end{pmatrix} \tag{1}$$

If we have a spherical symmetric potential V(r) as is the case in atoms, the radial part of the equation can be separated following Grant and Quiney[2]

$$\psi^L(\vec{r}) = \frac{1}{r} P(r) \chi_{\kappa,m}(\theta,\phi) \tag{2a}$$

$$\psi^S(\vec{r}) = \frac{i}{r} Q(r) \chi_{-\kappa,m}(\theta,\phi) \tag{2b}$$

$$\begin{pmatrix} V(r) & c\left(-\frac{d}{dr} + \frac{\kappa}{r}\right) \\ c\left(\frac{d}{dr} + \frac{\kappa}{r}\right) & V(r) - 2mc^2 \end{pmatrix} \begin{pmatrix} P(r) \\ Q(r) \end{pmatrix} = E \begin{pmatrix} P(r) \\ Q(r) \end{pmatrix} \tag{3}$$

This equation can be used to express Q (r) as a function of P (r)

$$Q(r) = (E + 2mc^2 - V(r))^{-1} c\left(\frac{d}{dr} + \frac{\kappa}{r}\right) P(r) \tag{4}$$

If we take the non-relativistic limit by letting the speed of light, c, approach infinity the relation simplifies to

$$Q(r) = \frac{1}{2mc}\left(\frac{d}{dr} + \frac{\kappa}{r}\right) P(r) \tag{5}$$

This gives the (restricted) kinetic balance condition. If P (r) is expanded in the basis set $\{\phi^L\}$, the expansion set $\{\phi^S\}$ is said to be kinetically balanced if it contains all functions $(d/dr + \kappa/r)\phi^L$. If this mapping is 1 to 1 the basis set is of the restricted kinetic balance type. If the small component contains additional functions it is said to be of extended kinetic balance type.

4.4. One electron systems

As an example of the failure of restricted kinetic balance calculations we take the hydrogenlike system Sn^{49+}. We expand P(r) in a basis of n_{prim} normalised uncontracted gaussian functions and construct the basis for Q(r) by kinetic balance. In this basis the Dirac matrix is diagonalised, yielding an energy ε and an approximation of P(r) in terms of gaussian type functions

$$P(r) \quad \sum_{i}^{nprim} c_i N_i r^{l+1} e^{-\alpha_i r^2} \tag{6}$$

We normalise this linear combination and use it as a minimal basis for P (r)

$$P'(r) = N_{P'} \sum_{i}^{nprim} c_i N_i r^{l+1} e^{-\alpha_i r^2} \tag{7}$$

We now generate a minimal basis for Q(r) by operating with the kinetic balance operator as was defined in (5) on the large component basis function P'(r)

$$\frac{1}{N_{Q'}} Q'(r) = \frac{1}{2mc}\left[\frac{d}{dr} + \frac{\kappa}{r}\right] P'(r) = \frac{1}{2mc} \sum_{i}^{nprim} c_i N_i [(1 + \kappa + 1) r^l - 2\alpha_i r^{l+2}] e^{-\alpha_i r^2} \tag{8}$$

Together the functions give a minimal (2x2) matrix representation of the Dirac equation:

$$\begin{pmatrix} V^{LL} & c\Pi \\ c\Pi & V^{SS} - 2mc^2 \end{pmatrix} \begin{pmatrix} P'_{P'} \\ Q'_{Q'} \end{pmatrix} = \varepsilon' \begin{pmatrix} P'_{P'} \\ Q'_{Q'} \end{pmatrix} \tag{9}$$

$$V^{LL} = \int_0^\infty \frac{P'(r) Z e P'(r)}{r} dr \tag{9a}$$

$$V^{SS} = \int_0^\infty \frac{Q'(r) Ze Q'(r)}{r} dr \tag{9b}$$

$$\Pi = \int_0^\infty Q'(r) \left(\frac{d}{dr} + \frac{\kappa}{r}\right) P'(r) dr \tag{9c}$$

Another possible way of forming a contracted basis is to split Q' (r) in two functions in the following way

$$Q''_1(r) = N_{Q''_1} \sum_i^{nprim} c_i N_i (1 + \kappa + 1) r^l e^{-\alpha_i r^2} \tag{10a}$$

$$Q''_2(r) = N_{Q''_2} \sum_i^{nprim} c_i N_i r^{l+2} \alpha_i e^{-\alpha_i r^2} \tag{10b}$$

Now we have an extended kinetic balance (3x3) matrix representation of the Dirac equation with an eigenvalue ε".

We have studied the relation between E, ε, ε' and ε" as a function of the number of primitive basis functions.

4.4.1. The $1s_{1/2}$ orbital

In this case κ = -1 and l = 0. Since the first term in (8) cancels for this value of κ, Q_1" is zero and ε' = ε". Table 1 shows the convergence of ε and ε' with respect to the exact eigenvalue E.

It is clear that constructing a small component basis in this way leads to large errors if the level of contraction increases. In this kind of extremely contracted basis sets it might be informative to look at the individual matrix elements V^{LL}, V^{SS} and cΠ. Since the exact solutions P (r) and Q (r) are known to be the same for the $1s_{1/2}$ orbital, V^{LL} and V^{SS} should converge to the same value.

From table 2 it can be seen that while V^{LL} and cΠ are convergent, V^{SS} is diverging as the number of basis functions increases.

Table 1. The approximated energy eigenvalues for the $1s_{1/2}$ orbital with respect to the exact value in the kinetic balance approximation as a function of the number of primitive basis functions.

$n_{prim.}$	ε	ε - E	ε'	ε' - E
1	-1071.5184	223.1077	-1071.5184	223.1077
2	-1244.1555	50.4706	-1245.2324	49.3937
3	-1281.3753	13.2508	-1284.3684	10.2577
4	-1290.6821	3.9440	-1295.6702	-1.0441
5	-1293.3270	1.2991	-1300.1402	-5.5141
6	-1294.1621	0.4640	-1302.6253	-7.9992
7	-1294.4492	0.1769	-1304.4402	-9.8141
8	-1294.5549	0.0712	-1306.0006	-11.3745
9	-1294.5961	0.0300	-1307.4582	-12.8321
10	-1294.6130	0.0131	-1308.8771	-14.2510
11	-1294.6202	0.0059	-1310.2858	-15.6597
12	-1294.6233	0.0028	-1311.7004	-17.0743
E	-1294.6261			

Table 2. The approximated Dirac matrix elements for the $1s_{1/2}$ orbital in the kinetic balance approximation as a function of the number of primitive basis functions.

$n_{prim.}$	V^{LL}	V^{SS}	cΠ
1	-2185.832	-1457.222	-6502.377
2	-2563.276	-2253.057	-7129.592
3	-2650.936	-2667.018	-7294.838
4	-2674.380	-2885.604	-7346.651
5	-2681.424	-3013.749	-7365.113
6	-2683.749	-3099.353	-7372.476
7	-2684.578	-3164.085	-7375.733
8	-2684.893	-3218.150	-7377.311
9	-2685.018	-3266.644	-7378.139
10	-2685.071	-3312.285	-7378.605
11	-2685.094	-3356.533	-7378.880
12	-2685.104	-3400.277	-7379.051

4.4.2. The $2p_{1/2}$ orbital

Now we take $\kappa = 1$ and $l = 1$. In this case operating with the kinetic balance operator on P' (r) gives both the term with r^l and the one with r^{l+2} so Q_1" (r) and Q_2" (r) are both different from zero and $\varepsilon' \neq \varepsilon''$. Table 3 shows the convergence of ε, ε' and ε'' with respect to the exact eigenvalue E.

Again ε' falls below the uncontracted energy ε and below the exact eigenvalue as the basis set increases. Using an extended kinetically balanced basis as defined in (10) does not significantly alter the result (ε'').

The matrix elements leading to ε' are given in table 4.

V^{SS} is divergent as we saw before in the $1s_{1/2}$ case.

Table 3. The approximated energy eigenvalues for the $2p_{1/2}$ orbital with respect to the exact value in the restricted and unrestricted kinetic balance approximation as a function of the number of primitive basis functions.

n_{prim}	ε	ε - E	ε'	ε' - E	ε''	ε'' - E
1	-289.5540	36.9408	-289.5547	36.9401	-289.5540	36.9408
2	-319.5654	6.9294	-319.6855	6.8093	-319.6692	6.8256
3	-324.9465	1.5483	-325.2949	1.1999	-325.2541	1.2407
4	-326.0916	0.4032	-326.6797	-0.1849	-326.6295	-0.1347
5	-326.3763	0.1185	-327.1777	-0.6829	-327.1241	-0.6293
6	-326.4563	0.0385	-327.4375	-0.9427	-327.3847	-0.8899
7	-326.4811	0.0137	-327.6230	-1.1282	-327.5671	-1.0723
8	-326.4895	0.0053	-327.7715	-1.2767	-327.7177	-1.2229
9	-326.4926	0.0022	-327.9043	-1.4095	-327.8536	-1.3588
10	-326.4939	0.0009	-328.0371	-1.5423	-327.9823	-1.4875
11	-326.4944	0.0004	-328.1602	-1.6654	-328.1071	-1.6123
12	-326.4946	0.0002	-328.2871	-1.7923	-328.2338	-1.7390
E	-326.4948					

Table 4. The approximated Dirac matrix elements for the $2p_{1/2}$ orbital in the restricted kinetic balance approximation as a function of the number of primitive basis functions.

$n_{prim.}$	V^{LL}	V^{SS}	$c\Pi$
1	-588.2487	-1176.497	3388.691
2	-653.9547	-1756.138	3610.331
3	-666.8790	-2025.902	3661.971
4	-669.8956	-2153.181	3676.588
5	-670.7026	-2220.834	3681.382
6	-670.9429	-2262.467	3683.200
7	-671.0215	-2291.720	3684.000
8	-671.0494	-2314.542	3684.400
9	-671.0603	-2333.850	3684.622
10	-671.0646	-2351.146	3684.755
11	-671.0664	-2367.249	3684.838
12	-671.0674	-2383.123	3684.894

4.4.3. Discussion of the one electron results

The failure of kinetic balance in the above presented examples is of course not surprising. For one electron atomic-like systems the exact results are known and enlarging the size of basis sets should lead to an increasingly better description of those solutions.

A simple explanation of the divergences of V^{SS} can be found as was shown by Aerts[3]. Operating with the kinetic balance operator on the exact solution P (r) for a $1s_{1/2}$ orbital gives

$$Q'(r) \equiv \left(\frac{d}{dr} + \frac{-1}{r}\right) r^{\gamma} e^{-\lambda r} = (\gamma - 1)\, r^{\gamma-1} e^{-\lambda r} - \lambda r^{\gamma} e^{-\lambda r} \qquad (11)$$

The first part of Q' (r) gives rise to the integral

$$\int_0^{\infty} Z r^{2\gamma-3} e^{-2\lambda r}\, dr \qquad (12)$$

when evaluating V^{SS} which is divergent for

$$\gamma = \sqrt{1 - \frac{Z^2}{c^2}} < 1 \qquad (13)$$

The sample calculations show that applying kinetic balance as defined by (5) to heavily contracted basis functions will lead to wrong results and numerical problems in the evaluation of the nuclear attraction integrals for the small component basis.
Ishikawa et al. , however, reported[4] practical calculations in which they did not observe any problems of this kind (contrary to earlier findings of Aerts and Nieuwpoort[5]). The reason why the problem does not always show up is in our opinion that in practice Q(r) has additional variational freedom consisting of contributions from other kinetically balancing functions. If the large and therefore the matched small component bases are large, the variational space might be large enough to account for the error made by applying (5).
We think it is better to start with a more accurate relation in the first place and take the atomic balance condition (4) as a generator for small component basis functions. A possible problem with this balance relation is the dependence on ε and V. If we use the generated contracted basis to describe a different system we get another potential V and another eigenvalue ε. This means that the contracted small component functions no longer match the newly formed combinations of large component functions and the possibility of variational collapse appears again. Since in many-electron Fock-Dirac calculations V is depending on the form of the solutions it seems impossible to give an always working prescription for the generation of the small component basis. A save way to proceed as we described previously[6] is to add additional functions to the small component in order to get enough variational freedom. The additional functions have no matching large component function and thus might give rise to so-called spurious solutions as Grant and Quiney[2] anticipated.

4.5. Many electron systems

In this section we will discuss the position of the additional negative energy solutions in the spectrum in some recent Fock-Dirac calculations. In all the calculations extended balanced basis sets, fulfilling both atomic (4) and extended kinetic balance as defined by (10), were used. This kind of basis sets, with n_l large component basis functions and n_s small component basis functions, lead to a spectrum with n_l orbital energies on the positive energy side and n_s orbital energies on the negative energy side of the spectrum. A typical spectrum of those calculations is shown in figure 1.

Figure 1. Orbital energies in a calculation on a neutral Lead atom.

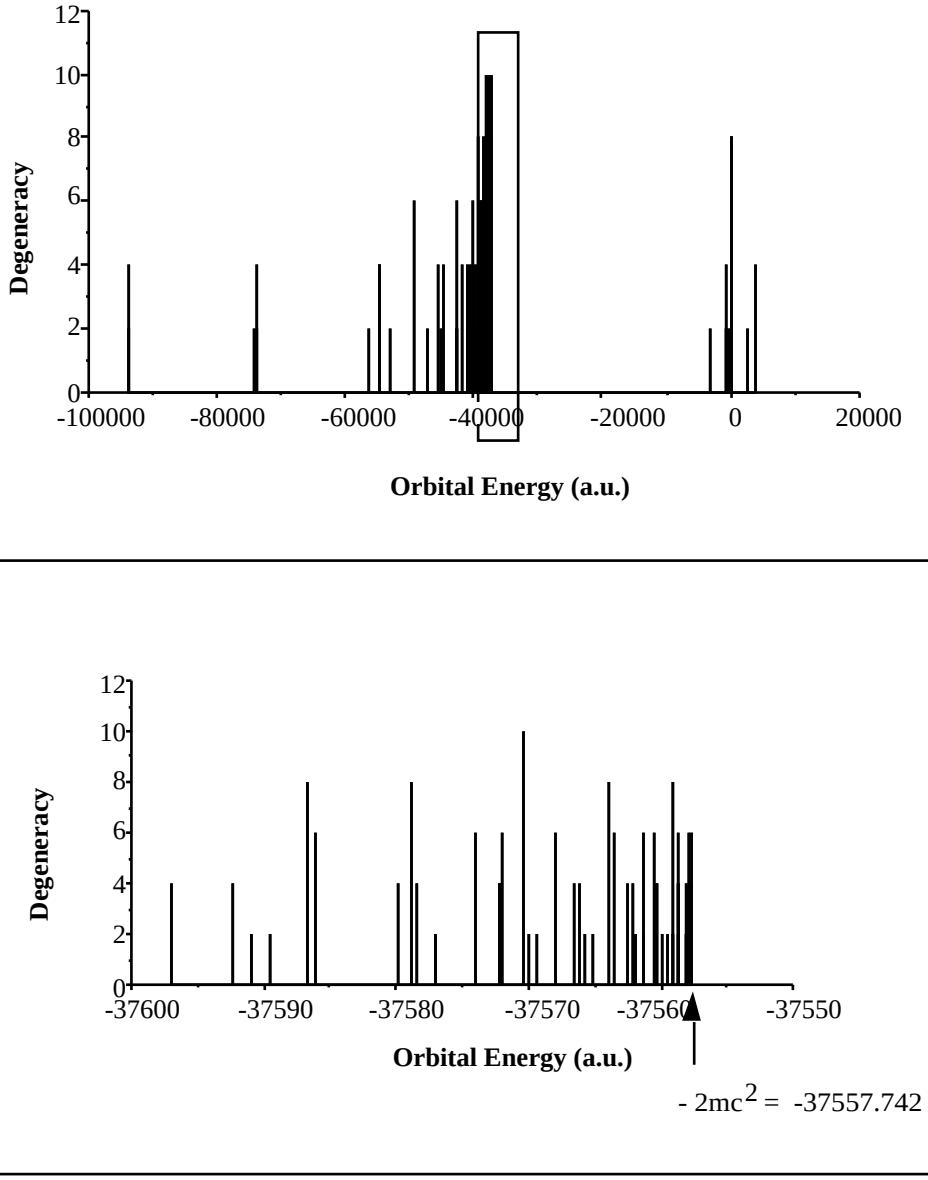

In this calculation on neutral Pb all the negative energy levels remain below $-2mc^2$, the gap which separates the negative continuum states from the bound positive energy states. The same kind of spectrum appears in a calculation on Eu^{3+}, but now the upper bound of the negative levels is shifted 0.78 a.u. downwards. This is consistent with the interpretation of those states as positronlike: a positively charged particle will feel an increasing repulsion and is pushed further into the continuum.

The picture changes if we take a negatively charged atom or molecule or apply a Madelung potential. Now the negative energy levels are shifted upwards and get an energy a little above $-2mc^2$. The gap between those levels and the electron like positive

energy levels remains however much larger than this shift and a clear identification of the positive energy levels can still be given.

Orbital energies above $-2mc^2$ also appear in the following cases:

1) Performing a calculation in which the Gaunt interaction[7] is treated variationally.
This operator is the first and most important part of the more accurate Breit operator[8]:

$$B_{ij} = -\frac{1}{2}\left[\frac{(\alpha_i.\alpha_j)}{r_{ij}} + \frac{(\alpha_i.r_{ij})(\alpha_j.r_{ij})}{r_{ij}^{3}}\right] \qquad (14)$$

The Gaunt operator probably overestimates the electron repulsion and creates thus a (slightly) more negative potential which leads to the same kind of results as we saw in calculations on negatively charged systems.

2) Using approximations or extrapolations during the SCF iterations.
We have observed levels going far into the gap after constructing the Fock matrix using Aitken extrapolated orbitals. The levels disappear at convergence indicating that this is purely a technical defect of this kind of extrapolation.
Furthermore levels just in the gap are observed when electron repulsion integrals (SS/SS) over the small component part are ignored if they are smaller than a threshold value of 0.000001. This indicates one has to take some care with (completely) neglecting those small contributions, as was done by Dyall et al.[9], but no serious problems seem to arise.

3) Linear dependencies.
During a test calculation on Pb some very serious problems with negative energy states were encountered with levels going up to an order of a 1000 a.u. in to the gap. Analysing the basis sets showed linear dependencies leading to small component overlap matrix eigenvalues of $\sim 10^{-12}$. Removing the dependency immediately solved the problems.

The results mentioned are summarised in table 5.

Table 5. The position of the highest negative energy levels (a.u.) in calculations on many electron systems.

System	Approximation	n_{large}	n_{small}	# in gap	Highest orbital energy + $2mc^2$
Pb	None	162	596	0	-0.0083
Eu^{3+}	None	158	566	0	-0.7797
Eu^{3+}	Madelung potential	158	566	22	0.7076
Eu^{3+}	Aitken extrapolation	296	658	4	1099.8176
Ar	Gaunt interaction	90	150	12	1.3736
PbH_4	Partial neglect of SS/SS electron repulsion integrals	178	644	4	0.0026

4.6. Conclusions

Solution of the Dirac or the Dirac-Fock equation by means of basis set expansion can lead to accurate and meaningful results if the small component basis set is constructed with care and fulfils the atomic balance condition.

Strict kinetic balance can lead to failure, especially if the level of contraction increases. Giving the small component part of the orbitals more flexibility does not produce variational collapse since the introduced extra states are clearly separated from the desired positive energy solutions. Using approximations in extended balance calculations is also possible without running into variational collapse problems.

The biggest pitfall in extended balance calculations is probably the occurrence of linear dependence problems leading to numerical inaccuracy and unpredictable results. This can be remedied by checking these dependency in advance and adapting the contraction coefficients to produce an orthogonal basis.

References

1) Y. S. Lee and A. D. McLean, J. Chem. Phys. **76**, 735 (1982).

2) I. P. Grant, H. M. Quiney, Adv. At. Mol. Phys. **23**, 37 (1988).

3) P. J. C. Aerts, Towards Relativistic Quantum Chemistry, Ph. D. Thesis, Rijks Universiteit Groningen (1986).

4) Y. Ishikawa, H. Sekino, R. C. Binning Jr., Chem. Phys. Lett. **165**, 237 (1990).

5) P. J. C. Aerts and W. C. Nieuwpoort, Chem. Phys. Lett. **113**, 165 (1985).

6) L. Visscher, P. J. C. Aerts and O. Visser, in "The effects of relativity in atoms, molecules and the solid state", edited by I. P. Grant, B. Gyorffy and S. Wilson, (Plenum: New York 1991).

7) J. A. Gaunt, Proc. R. Soc. A **122**, 513 (1929).

8) G. Breit, Phys Rev. A **34**, 553 (1929).

9) K.G. Dyall, K. Fægri Jr., P. R. Taylor and H. Partridge, J. Chem. Phys. **95**, 2583 (1991).

5. The electronic structure of the PtH molecule

Fully Relativistic CI calculations of the ground and excited states

5.1. Abstract

Fully relativistic all-electron SCF calculations based on the Dirac-Coulomb hamiltonian have been performed on the 3 lowest lying states of the PtH molecule. The resulting 4-component Dirac-Hartree-Fock (DHF) molecular spinors are subsequently used in relativistic Configuration Interaction (CI) calculations on the 5 lower states of PtH. Spectroscopic properties are obtained by fitting the potential curve to a Morse function and show good agreement with experimental data. The effect of relativistic corrections to the Coulomb electron-electron interaction is investigated at the DHF level and is found to be insignificant for the molecular spectroscopic properties investigated by us. The CI wave functions are found to have only one dominant configuration, indicating a lack of static correlation. Dynamic correlation in the d-shell is however important for the spectroscopic properties of PtH. The results conform with a bonding scheme in which the three lower and two upper states of PtH are assigned $5d^4_{3/2}\ 5d^5_{5/2}\ \sigma^2_{1/2}$ and $5d^3_{3/2}\ 5d^6_{5/2}\ \sigma^2_{1/2}$ electronic configurations respectively. The configurations are only approximate and are perturbed by 5d-participation in bonding. The stability of the Pt-H bond is explained in terms of the relativistic stabilisation of the 6s orbital in analogy with the electron affinity of the platinum atom.

5.2. Introduction

The catalytic versatility of platinum makes it one of the most widely applied metal catalysts[1]. A number of the reactions for which platinum is active involves hydrogen. This has motivated extensive research on the nature of the platinum-hydrogen bonding. Platinum hydride offers the simplest example of the platinum-hydrogen bond and this open-shell molecule has therefore been the subject of several studies, most of them *ab initio* calculations[2,3,4,5,6,7,8].

Platinum being a third row transition metal, both correlation and relativistic effects are expected to be of importance in its chemistry[9]. Transition metal atoms in general are characterised by the close proximity of nd, (n+1)s and (n+1)p orbitals which gives rise to an abundance of low-lying atomic states with strong configurational mixing. Proper handling of static correlation is therefore a prerequisite for the correct description of the atomic spectra. With an increasing number of d-electrons dynamic correlation becomes more and more significant. At the molecular level these features give rise to a number of possible bonding mechanisms and may lead to complicated molecular spectra. An additional complicating factor for third row transition metals in particular is that relativistic effects may significantly influence bonding and spectroscopic properties[10]. Spin-orbit effects in the platinum atom give a splitting of the order of 10,000 cm^{-1} for the $^3D(5d^96s^1)$ state whereas the singlet-triplet splitting for this configuration is only 3,800 cm^{-1}. The relativistic contraction of the 6s orbital and the expansion of the 5d shell will influence the bonding and change the character of the bonding orbitals.

In the majority of *ab initio* calculations on PtH relativistic effects are introduced through the use of relativistic effective core potentials (RECPs)[11], an approach which also yields significant reduction of computational effort relative to all-electron calculations. Effective core potentials replace the core electrons under the assumption that the core remains frozen during bond formation. RECPs may be obtained by fitting the potential to a fully relativistic atomic calculation or alternatively a semirelativistic calculation such as the Cowan Griffin method[12] or the second order Douglas-Kroll ("no-pair") approximation[13]. In general some averaging procedure is employed to generate spin-free RECPs. The RECP approach has the advantage of staying within the non-relativistic theoretical framework so that most computational methods and computer codes for non-relativistic calculations may be used with little or no modification. Spin-orbit effects may be introduced by adding spin-orbit matrix elements to the hamiltonian matrix of LS-coupled states connected through the spin-orbit operator. The disadvantage of the RECP method is that the fitting and averaging procedure introduces uncertainties and that the quality of the RECP may be difficult to

assess without performing all-electron atomic and molecular calibration calculations at the same level of approximation.

An alternative approach is to solve the relativistic Dirac-Hartree-Fock (DHF) equations[14]. This will generate 4-component spinors which provide a natural description of the relativistic effects. The disadvantage of this approach is mainly the large computer resources necessary to carry out 4-component relativistic calculations. Over the past few years, however, a number of DHF molecular codes and results[15,16,17,18,19] have been reported. Recently Dyall[8] presented results from DHF calculations on platinum hydrides, including PtH. The next step towards a quantitatively correct description of heavy atoms like platinum is to include electron correlation in the formalism and go beyond the mean field approach. The molecular spinor basis generated by the DHF method may be used to generate many-electron (determinantal) wave functions with which one can expand the Configuration Interaction (CI) equations in a completely relativistic framework.

In this work we present the results of fully relativistic CI calculations on the 5 lowest states of the PtH molecule and compare the result with other methods and with experiment. Below we give a brief introduction to the computational methods used by us. We then discuss the atomic aspects of calculations on PtH before presenting results from molecular DHF and CI calculations.

5.3. Computational methods

We have performed CI calculations using references obtained from DHF calculations. Below a short resumé of the DHF method is given followed by a description of the CI method recently developed by one of us [LV]. Unless otherwise stated all calculations have been performed using the MOLFDIR program package[20].

5.3.1. The DHF method

The starting point of our calculations is the Dirac-Coulomb equation

$$H \Psi = E \Psi \qquad (1)$$

$$H = \sum_{i}^{N} h_i + \sum_{i<j} g_{ij} \qquad (2)$$

where h is the one-electron Dirac hamiltonian

$$h = \begin{bmatrix} V.\,I_2 & c(\sigma\,\mathbf{p}) \\ c(\sigma\,\mathbf{p}) & (V - 2c^2)\;\; I_2 \end{bmatrix} \qquad (3)$$

I_2 and σ are the 2 x 2 identity and Pauli matrices respectively, while the potential V describes the interaction of the electrons with the fixed nuclear framework. A detailed description of this hamiltonian may be found in standard textbooks[21,22]. The electron-electron interaction, g_{ij}, is given by the Coulomb operator

$$g_{ij} = \frac{1}{r_{ij}} \qquad (4)$$

and represents in this context the 0th order approximation to the full relativistic electron-electron interaction. A first order correction is provided by the Breit operator[23], which may be split[24] into a magnetic part, usually termed the Gaunt interaction[25], and a retardation part.

$$g_{ij}^{Breit} = -\frac{(\alpha_i \quad \alpha_j)}{r_{ij}} - \frac{(\alpha_i \quad _i)(\alpha_j \quad _j)\, r_{ij}}{2} = g_{ij}^{Gaunt} + g_{ij}^{retardation} \qquad (5)$$

Our computer program allows for the inclusion of the Gaunt interaction either in a variational or in a perturbative scheme.

From the Dirac-Coulomb equation open-shell DHF equations can be derived in the same way as the non-relativistic Hartree-Fock equations[26]. By minimising the (averaged) energy expression of a system with one open shell, we get the following set of equations

$$F^C = h + Q^C + Q^O + \alpha L^O \qquad F^O = h + Q^C + aQ^O + \alpha L^C \qquad (6)$$

$$Q^C = \sum_k J_k - K_k \qquad Q^O = f\sum_m J_m - K_m \qquad (7)$$

$$L^C = \sum_k L_k \qquad L^O = f\sum_m L_m \qquad (8)$$

$$J_i \mid j > = < i \mid g_{12} \mid i > \mid j > \qquad K_i \mid j > = < i \mid g_{12} \mid j > \mid i > \qquad (9)$$

$$L_i \mid j > = < i \mid Q^O \mid j > \mid i > + < i \mid j > Q^O \mid i > \qquad (10)$$

In these equations k and m are used to label closed and open shell molecular 4-spinors respectively. The fractional occupation number (f) of the open shell spinors and the coupling coefficients (a and α) are defined by the number of open shell electrons (n) and the number of open shell spinors (m)

$$f = \frac{n}{m} \qquad a = \frac{m\,(n-1)}{n\,(m-1)} \qquad \alpha = \frac{1-a}{1-f} \tag{11}$$

The DHF equations are expanded in a Gaussian type basis set. This basis set is made up of two subsets describing the upper (large) components and the lower (small) components of the spinors. In order to get a correct representation of all operators these bases are chosen to be related by the kinetic or atomic balance relation[27]. For open shell systems the average of configuration energy is minimised after which the energies of individual states can be obtained by Complete Open Shell Configuration Interaction[28] (COSCI) — diagonalisation of the CI-matrix of all possible configurations in the open shell manifold.

5.3.2. The Relativistic CI method

We have developed a relativistic version of the Restricted Active Space Configuration Interaction (RASCI)[29] method which can be used to improve the wave functions and energy differences found in the DHF (-COSCI) step.

In the Restricted Active Space method the active spinor space is divided in 3 groups. The first group (RAS1) contains the highest occupied closed shell spinors of the reference determinant(s). The second group (RAS2) contains the open shell spinors of the reference determinant(s). The spinors that were unoccupied in the reference determinant(s) are in the third group (RAS3). The CI space is now defined by specifying a maximum excitation level (n_{H1}) from RAS1 and a maximum excitation level (n_{E3}) to RAS3. Determinants that fulfil the constraint of having n_{H1}, or less, holes in RAS1 and n_{E3}, or less, electrons in RAS3 form the CI space. This definition allows most of the conventional types of CI to be done as a special case.

To describe the method it is convenient to write the Dirac-Coulomb-(Gaunt) hamiltonian in second quantised form. Using the generators of the unitary group $E_{ij} = a_i^+ a_j$ the hamiltonian can be written as

$$H = \sum_{i,j} \langle i|\, h\,|j\rangle\, E_{ij} + \sum_{i,j,k,l} (ij|\, g\,|kl)\left(E_{ij}\, E_{kl} - E_{il}\, \delta_{jk}\right) \tag{12}$$

In this equation molecular spinors are labelled by i, j, k and l. The summation is restricted to the electron solutions, since we neglect any (virtual) positron-electron pair creation. We expand the many-electron wave functions in the determinantal basis $\{\Phi_I\}$ defined above. The result is a matrix representation of the hamiltonian which can be expressed as a sum of 1- and 2-electron integrals multiplied by coupling constants γ_{ij}^{IJ} and Γ_{ijkl}^{IJ} respectively.

$$\mathbf{H}_{IJ} = \sum_{i,j} h_{ij}\, \gamma_{ij}^{IJ} + \sum_{i,j,k,l} (ij \mid kl)\ \Gamma_{ijkl}^{IJKL} \qquad (13)$$

with $h_{ij} = \langle i \mid h \mid j \rangle$, $(ij \mid kl) = (ij \mid g \mid kl)$, $\gamma_{ij}^{IJ} = \langle I \mid E_{ij} \mid J \rangle$ and $\Gamma_{ijkl}^{IJ} = \langle I \mid E_{ij}\, E_{kl} \mid J \rangle$.

Since the matrix in general will be too large to hold in memory, we use the direct diagonalisation technique of Davidson[30] to find the desired roots. The main difference with non-relativistic direct CI methods is that the number of relativistic integrals is about 2^4 times as large since each molecular orbital corresponds to two molecular spinors. Another complication is that the integrals in general will be complex since the hamiltonian contains complex operators. Thus the number of virtual spinors and the number of determinants that can be used is smaller than what is presently possible with efficient non-relativistic CI methods. Our direct RASCI code can at present handle expansions up to about 200,000 determinants using an active spinor space of about 100 spinors. In the present application a number of high-lying virtual spinors were deleted to make the calculations feasible.

5.4. Atomic calculations

The classification of some of the observed lines in the platinum atomic optical spectrum was done already in 1927 and a review of the assigned lines can be found in Moore's tables[31]. The ground state of the platinum atom is a J=3 state designated $^3D_3$.The first two states arise mainly from the $5d^9(^2D_{5/2})6s^1$ configuration and the 7th and 8th states from the $5d^9(^2D_{3/2})6s^1$ configuration. The atomic spectrum is complicated because the configurations d^9s^1 and d^8s^2 are close in energy and the individual states mix strongly with each other due to the strong spin-orbit coupling[8]. This makes the assignment of LS-coupling term symbols rather arbitrary and we shall use instead the J value and parity to designate the states. Below we describe the basis set used in the molecular calculations and compare finite basis DHF results with corresponding numerical results for an estimate of the sensitivity to basis set errors. We then discuss results obtained at different levels of theory and compare them with the experimental (spectroscopic) data

of the Pt atom. The relativistic optimisation of single exponents and all the numerical calculations were done using the GRASP atomic structure code[32] .

5.4.1. Basis Sets

The platinum basis was derived from a non-relativistically optimised 22s16p13d8f Gaussian basis[33] (basis I). Due to the relativistic contraction of s-and p-orbitals a relativistic reoptimisation of the basis would be expected to give a shift towards higher exponents in the basis . We have not done this explicitly, but found that inclusion of a relativistically optimised p-function with exponent 7.9E5 gave an improvement of 827 mH in the total energy (see also reference 34) . No tight s-exponent was needed, due to our use of a finite nucleus model[35] (a Gaussian charge distribution with exponent 0.12E9). This large (L) component primitive basis was subjected to general contraction using the coefficients from an atomic DHF calculation and augmented with diffuse correlation and polarisation functions. Due to the relativistic contraction of p-orbitals the outer p-exponent in the primitive basis mainly describes the 6p-orbital and it was thus sufficient to add only one diffuse relativistically optimised p-function to obtain a double zeta description of this orbital. The basis was furthermore supplemented with one d-function and one f-function, the latter contracted from three primitives[36]. The small (S) component contracted basis was generated using the atomic balance relation[37]. For both basis subsets different contraction coefficients were used for spinors that differ by their j-value, but an overlap criterion was used to reduce the resulting number of contracted functions. The final [8s10p9d3f(L)|6s13p12d11f4g(S)] basis (basis II) was used in the subsequent atomic and molecular calculations. The two different basis sets are compared in table 1.

For hydrogen a primitive 6s1p Gaussian basis was relativistically contracted to 3s1p. The hydrogen basis set is given in appendix A. The atomic energy is -0.499952 H, differing from the numerical energy by 55 μH. The size of all basis sets is summarised in table 2.

Table 1. Total and orbital energies (in Hartrees) from numerical and finite basis DHF calculations on the $5d^4_{3/2}(5d_{5/2}, 6s_{1/2})^6$ *configurational average of the platinum atom.*

	Numerical DF	Basis I	Basis II
Total Energy	-18434.181187	-18433.181171	-18434.007850
ε ($1s_{1/2}$)	-2899.6195	-2899.6450	-2899.6270
ε ($2s_{1/2}$)	-514.7000	-514.7116	-514.7124
ε ($2p_{1/2}$)	-492.3144	-492.0991	-492.2879
ε ($2p_{3/2}$)	-428.6614	-428.6741	-428.6756
ε ($3s_{1/2}$)	-123.3795	-123.3897	-123.3926
ε ($3p_{1/2}$)	-113.3776	-113.3291	-113.3805
ε ($3p_{3/2}$)	-99.1889	-99.2001	-99.2024
ε ($3d_{3/2}$)	-82.7461	-82.7547	-82.7560
ε ($3d_{5/2}$)	-79.7133	-79.7237	-79.7262
ε ($4s_{1/2}$)	-27.8662	-27.8868	-27.8774
ε ($4p_{1/2}$)	-23.5882	-23.5944	-23.5968
ε ($4p_{3/2}$)	-20.1647	-20.1877	-20.1754
ε ($4d_{3/2}$)	-13.1548	-13.1556	-13.1642
ε ($4d_{5/2}$)	-12.5010	-12.4992	-12.5110
ε ($4f_{5/2}$)	-3.4763	-3.4963	-3.4855
ε ($4f_{7/2}$)	-3.3387	-3.3596	-3.3475
ε ($5s_{1/2}$)	-4.4622	-4.4793	-4.4667
ε ($5p_{1/2}$)	-3.0409	-3.0527	-3.0445
ε ($5p_{3/2}$)	-2.4255	-2.4410	-2.4292
ε ($5d_{3/2}$)	-0.4970	-0.4902	-0.4997
ε ($5d_{5/2}$)	-0.4191	-0.4178	-0.4216
ε ($6s_{1/2}$)	-0.3080	-0.3062	-0.3084
DHF+Breit:	-18413.910101	DHF+Gaunt:	-18410.843679

Table 2. Basis set sizes.

	Large component		Small component	
	primitive	contracted	primitive	contracted
Pt Basis I	22s16p13d8f		16s22p16d13f8g	
Pt Basis II	22s18p14d11f	8s10p9d3f	18s22p21d14f11g	6s13p12d11f4g
H Basis	6s1p	3s1p	1s6p1d	1s3p1d

5.4.2. The atomic spectrum

The first 12 lines in the platinum atomic spectrum arise from the $5d^86s^2$, $5d^96s^1$ and $5d^{10}$ configurations. In principle the excitation energies can be calculated by performing a full CI within this configurational space. However, it is difficult to find a one-particle basis which describes all configurations in a balanced way. It has been pointed out by Hay[38] that orbitals of first-row transition metal atoms vary appreciably from one valence state to another. This also holds true for the platinum atom. Radial expectation values of the lower J = 0,2,3,4 atomic states from numerical DHF calculations are presented in table 3. We see that they may differ by as much as 0.5 bohrs. As a further complication the $5d^86s^2$ configuration will be biased in an optimisation of spinors for the total energy average of all states arising from the three configurations, since this configuration gives rise to the majority of these states. A numerical calculation based on this spinor set therefore gives a J=4 ($5d^86s^2$) ground state which is not in agreement with experiment. A better choice for one spinor set to describe all configurations is the relativistic configurational average of the $5d^4_{3/2}5d^4_{5/2}6s^2_{1/2}$, $5d^4_{3/2}5d^5_{5/2}6s^1_{1/2}$ and $5d^4_{3/2}5d^6_{5/2}6s^0_{1/2}$ configurations. This average yields spinors that are most suitable for the low-lying states and will describe d^8s^2 and d^9s^1 states about equally well, but with the d^{10} state somewhat high.

Table 3. Radial expectancies (Bohrs) of the lower J = 0,2,3,4 states of platinum. Non-relativistic results have been obtained by scaling the speed of light by a factor of 1000.

Relativistic	J = 0	J = 2	J = 3	J= 4
$5d_{3/2}$	1.665	1.608	1.611	1.561
$5d_{5/2}$	1.778	1.693	1.703	1.629
6s	2.469	3.094	3.098	3.004
Nonrelativistic	"d^{10}"	"d^9s^1"		"d^8s^2"
5d	1.694	1.615		1.549
6s	2.366	3.708		3.546

We have performed both numerical and finite basis DHF atomic calculations using the latter relativistic average. The resulting spinors were used in COSCI calculations to obtain the energy of individual atomic states. The finite basis calculations were performed in O_h double group symmetry. The results of the DHF and COSCI calculations are presented in table 1 and 4 respectively. The total DHF energy obtained with the finite basis is 173 mH above the numerical limit while the differences in the COSCI spectrum indicate that the basis set is accurate to about 0.02 eV in the description of atomic splittings.

Table 4. Spectrum of the platinum atom. Figures in electronvolts, relative to the J=3 ground state.

	J, Parity	Experiment.[9]		Num. DHF	Basis set DHF	Num. DHF+B	Basis set DHF+G	Basis set CI
1	3+	"$^2D_{5/2}$ ^2S"	0.000	0.000	0.000	0.000	0.000	0.000
2	2+	"$^2D_{5/2}$ ^2S"	0.096	0.159	0.163	0.145	0.146	0.145
3	4+	"$^3F_4$"	0.102	0.095	0.116	0.039	0.045	0.262
4	0+	"$^1S_0$"	0.761	2.173	2.186	2.151	2.160	1.822
5	2+	"$^3P_2$"	0.814	0.846	0.856	0.803	0.805	0.926
6	3+	"$^3F_3$"	1.254	1.280	1.302	1.190	1.195	1.378
7	1+	"$^2D_{3/2}$ ^2S"	1.256	1.146	1.146	1.109	1.107	1.206
8	2+	"$^2D_{3/2}$ ^2S"	1.673	1.868	1.874	1.814	1.812	
9	2+	"$^3F_2$"	1.922	2.170	2.192	2.082	2.087	
10	0+			3.037	3.039	3.034	3.037	
11	1+	"$^3P_1$"	2.302	2.786	2.808	2.697	2.702	2.691
12	4+	"$^1G_4$"	2.724	3.110	3.132	3.022	3.027	3.180
13	2+	"$^1D_2$"	3.303	3.649	3.668	3.542	3.545	3.562
14	0+			6.813	6.832	6.716	6.719	

The finite basis results as well as the numerical results in table 4 show rather poor agreement with experiment. There are a number of possible reasons for these discrepancies. One of these is the neglect of correlation effects which are expected to be important. We therefore performed a somewhat larger CI calculation with the finite basis method. The number of high lying virtuals neglected in the atomic CI was the same as in the subsequent molecular calculations (70) in order to facilitate the evaluation of molecular dissociation energies. We included the $5d_{3/2}$, $5d_{5/2}$ and $6s_{1/2}$ spinors in the RAS2 space and 60 virtual spinors in the RAS3 space. The CI was then set up to allow all single and double excitations from 10 electrons in the ($5d_{3/2}$,$5d_{5/2}$,$6s_{1/2}$) manifold giving an expansion of 889,416 determinants, which is reduced by symmetry to 111,646. The results should have approximately the same precision as the molecular results. These CI calculations (table 4) give the right order of the three lowest states, although the magnitude of the splittings is still not correct. The correlation energy for the ground state was found to be 233 mH.

Another possible cause of disagreement with experiment is the neglect of relativistic corrections to the Coulomb electron-electron interaction. We have estimated the Gaunt and Breit corrections from perturbation theory. The results are not strictly

commensurate since the first (Gaunt only) calculation was done in the finite basis set approach and the other (Breit) was done with the numerical GRASP code. The corrected DHF energies in table 1 indicate, however, that the Gaunt correction forms the major contribution to the Breit correction. As seen from table 4, at the COSCI level the trends in the Breit corrected splitting are very well represented with the Gaunt only calculation and we therefore conclude that the Gaunt only approach is accurate enough for our purposes. The effect of the Gaunt interaction on the atomic spectrum of platinum is of the same order as the CI corrections and the influence of both on molecular properties should therefore be considered.

From our atomic calculations we draw the conclusion that it is difficult to obtain a quantitatively correct description of the platinum atomic spectrum. The Breit (or Gaunt) interaction as well as correlation effects should be accounted for. In our atomic calculations basis set deficiencies appear to be small compared to the other sources of errors.

5.5. Molecular calculations

In a simple approach to PtH within a non-relativistic framework (Hunds case a) the Pt-H bond may be regarded as a σ(s - s) bond arising from the platinum d^9s^1 configuration. According to Mulliken[39] the electronic structure of most diatomic hydrides may be accounted for by assuming that the electrons of the heavier atom retain their n,l, quantum numbers in the molecule and furthermore have a definite $\lambda = |m_l|$ value imposed by the strong axial electric field of the hydrogen nucleus. The electronic configuration of PtH may then be given as $5d^9\sigma^2$ and will give rise to three states, characterised by $\Lambda = |M_L|$ and $\Sigma = |M_S|$, in the order $^2\Delta < {}^2\Pi < {}^2\Sigma$ with $^2\Delta$ as the ground state, provided that the bonding orbital has the same character in all three states. The splitting between the three states will depend chiefly on the splitting of the non-bonding d-orbitals in the axial field of the hydrogen atom.

The analogous approach within the fully relativistic framework (Hunds case c) first considers the spin-orbit splitting on the platinum atom, that splits the 5d shell into a $5d_{3/2}$ and a $5d_{5/2}$ shell. The configurations $5d^4_{3/2}\ 5d^5_{5/2}\ \sigma^2_{1/2}$ and $5d^3_{3/2}\ 5d^6_{5/2}\ \sigma^2_{1/2}$ give two groups of states that can be characterised by their $\Omega = |M_J|$ value. The lower group (1) of three states arises from the $5d^4_{3/2}\ 5d^5_{5/2}\ \sigma^2_{1/2}$ configuration and will be in the order 5/2(1) < 3/2(1) < 1/2(1) with $\Omega = 5/2$ as the ground state. The upper group (2) has the two states arising from the $5d^3_{3/2}\ 5d^6_{5/2}\ \sigma^2_{1/2}$ configuration in the order 3/2(2) < 1/2(2).

With the platinum 5d-orbitals so close in energy to the hydrogen s-orbital this simple bonding picture may be perturbed by d-participation in the bond, a feature that will mainly change the relative position of $\Omega = 1/2$ states in the spectrum.

Figure 1. Spectrum of PtH based on a s-s platinum-hydrogen bond arising from the Pt (d^9s^1) configuration. The figures in brackets are the excitation energies T_e obtained from the relativistic CI. Note the reordering of 3/2(1) and 1/2(1) states.

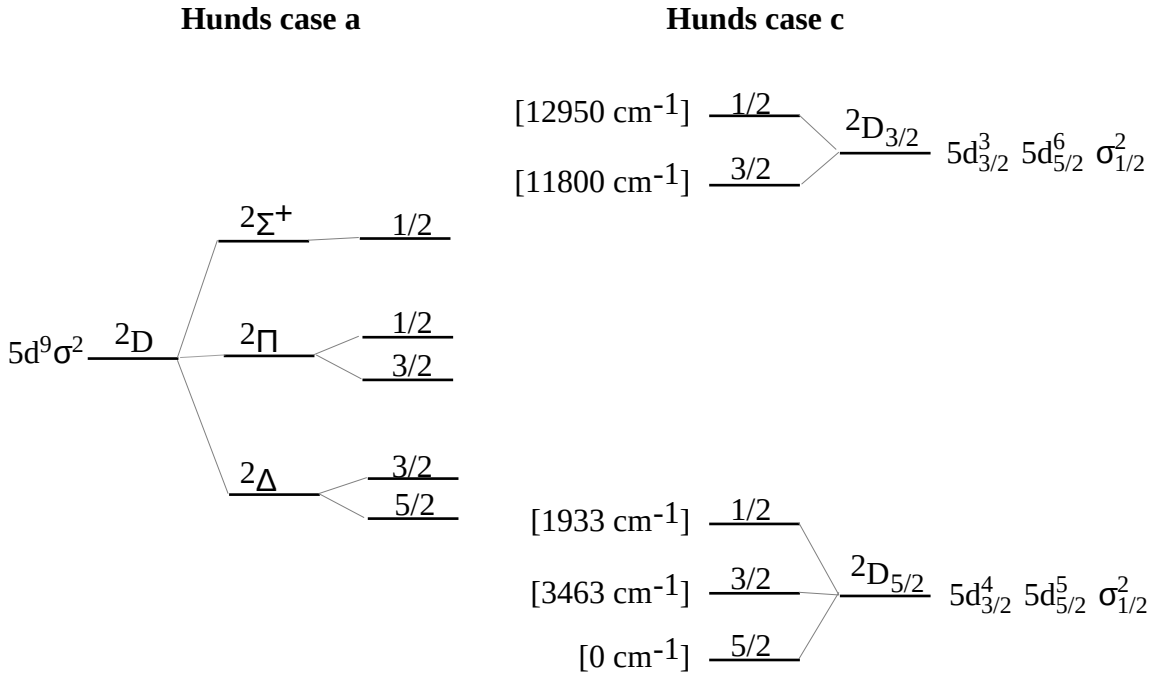

The two bonding schemes and their predicted spectra (sketched in figure 1) are connected by the spin-orbit interaction which splits the three $\Lambda\Sigma$ - states into $^2\Sigma_{1/2}$, $^2\Pi_{1/2}$, $^2\Pi_{3/2}$, $^2\Delta_{3/2}$ and $^2\Delta_{5/2}$ states. The strong spin-orbit coupling observed in platinum gives reason to expect considerable mixing between $^2\Sigma_{1/2}$ and $^2\Pi_{1/2}$ as well as between $^2\Pi_{3/2}$ and $^2\Delta_{3/2}$, thus making a Λ Σ - assignment to the resulting states meaningless. We will therefore in general label the spinors with $\omega = |m_j|$ and the many-electron states with Ω (Hunds case c) and discuss bonding in PtH in terms of the latter bonding scheme.

5.5.1. Computational details

The molecular calculations were performed using C_{4v} double group symmetry as our program package cannot exploit the full $C_{\infty v}$ double group symmetry. In this symmetry $\omega = 3/2, 5/2$ spinors transform as the E2 representation, while the $\omega = 1/2, 7/2$ spinors transform as the E1 representation. At the DHF level the lowest three states (1/2(1), 3/2(1) and 5/2(1)) are described by one-determinantal wave functions with a hole in the highest E1 spinors, a hole in the second highest E2 spinors, or a hole in the highest E2 spinors, respectively. We have calculated the energies of the molecule at six distances

from 1.5 Å to 1.6 Å. The energy of the separated atoms was calculated by taking the sum of the DHF platinum J=3 COSCI energy and the hydrogen energy calculated with our hydrogen basis. At three points the Gaunt interaction was calculated for the $\Omega = 5/2$ and 1/2 states as a perturbation after the SCF process.

Using the spinor set generated by the DHF calculations three separate CI calculations were performed at each Pt-H distance. One CI calculation was performed for E1 states using the Ω=1/2 DHF wave function as reference, while the Ω=3/2 and 5/2 DHF wave functions were separate references in two CI calculations for E2 states. We put the ten occupied valence spinors into the RAS1 space, the two open valence spinors in RAS2 and 70 virtual spinors in RAS3. Virtual spinors with energies above 3.4 a.u. are deleted. All excitations from RAS1 to RAS2 are allowed, and single and double excitations from these spaces to RAS3 are allowed. This procedure is roughly equivalent to a multi-reference singles and doubles CI in which the reference consists of the six lowest two-fold degenerate states. The resulting CI space consists of 535,932 determinants which is reduced by symmetry to 133,983 determinants for each component of the E1 and E2 representations. Only the Coulomb interaction was included in the two-electron integrals. Spectroscopic constants for PtH at the CI as well as the DHF level were obtained by fitting the potential curve to a Morse function. In accordance with the bonding scheme outlined above we used the platinum J = 3 ($5d^9(^2D_{5/2})6s^1$) atomic asymptote for the lower three states and correspondingly the J = 1 ($5d^9(^2D_{3/2})6s^1$) asymptote for the upper two states.

5.5.2. DHF results

The results from our DHF calculations are presented in table 5. The D_e values will be somewhat high since the atomic energies were based on an average spinor set while the molecular results were obtained by optimisation of the separate states. The splitting between the lowest states is hardly affected by the Gaunt interaction. Hence, differential effects which are of importance for the atomic spectrum are of little significance for the molecular spectroscopic constants calculated. In our atomic calculations we found that the size of the Breit and Gaunt corrections is strongly dependent on the electronic configuration. As several configurations contribute to the lower states of the platinum atom one may expect differential effects of the Breit and Gaunt corrections on the atomic spectrum. The lack of corresponding differential effects on the three lower states of the PtH spectrum is then consistent with our assumption that all these states have a $5d^4_{3/2}\ 5d^5_{5/2}\ \sigma^2_{1/2}$ configuration. Our molecular calculations further show insignificant differential effects of the Gaunt interaction on bond lengths and vibrational constants. This is consistent with previous calculations on hydride molecules[40] which showed that

the differential effect of the Gaunt term is quite small and may be neglected for most molecular properties.

Table 5. Molecular properties of PtH calculated by the DHF method. DHF+G refers to results obtained by the DHF method with the Gaunt correction added as a perturbation.

Method	State	r_e (Å)	D_e (eV)	ω_e (cm^{-1})	$\omega_e x_e$ (cm^{-1})	T_e (eV)
DHF	5/2 (1)	1.548	2.28	2251	69	0.00
	1/2 (1)	1.568	1.96	2095	70	0.32
	3/2 (1)	1.581	1.86	2044	69	0.41
DHF+G	5/2 (1)	1.549	2.32	2246	68	0.00
	1/2 (1)	1.568	2.00	2095	68	0.31

The spinors obtained from the DHF calculation can be analysed by Mulliken population analysis[41] in much the same way as non-relativistic orbitals. Table 6 shows the valence populations of the DHF wave functions in terms of the atomic basis functions. Conclusions based on a Mulliken population analysis should be viewed with caution as the analysis is basis dependent and the total energy is invariant to rotations among occupied spinors. An exception to this is the open shell spinor that can not be rotated into other spinors. Due to this property, the significant platinum s-contribution (0.348) to the open shell-spinor for the 1/2(1) state is a clear indication of considerable d-participation in the Pt-H bond. The total valence populations confirm that the dominant configuration of the platinum atom contributing to the molecule is d^9s^1. The d valence population is 9.0 for the 1/2(1) state, but somewhat smaller – about 8.7 – for the 3/2(1) and 5/2(1) states. This may be taken as an indication of some contribution from the platinum d^8s^2 atomic configuration to the bonding in the latter two states. The platinum atom is found to have a small positive charge of about 0.13, which is in agreement with the other ab initio calculations. The density contribution of the small component basis functions (0.002 electron) is hardly noticeable at this scale.

Table 6. Valence density Mulliken population analysis of the DHF wave functions for the 3 lower states of PtH. Net charges are derived from total density.

$\Omega = 5/2$. Pt net charge: 0.124

ω	Occ.	Pt(s)	Pt(p)	Pt(d)	H(s)	H(p)	σ	π	δ
1/2	6.0	1.161	0.068	3.655	1.097	0.013	4.005	1.994	0.000
3/2	4.0	0.000	0.000	3.994	0.000	0.000	0.000	2.000	2.000
5/2	hole	0.000	0.000	1.000	0.000	0.000	0.000	0.000	0.999
Sum	11.0	1.161	0.068	8.648	1.097	0.018	4.005	3.994	2.999

$\Omega = 1/2$. Pt net charge: 0.143

ω	Occ.	Pt(s)	Pt(p)	Pt(d)	H(s)	H(p)	σ	π	δ
1/2	4.0	0.412	0.071	2.421	1.080	0.012	2.301	1.698	0.000
	+hole	0.348	0.000	0.614	0.037	0.001	0.855	0.145	0.000
3/2	4.0	0.000	0.000	3.993	0.000	0.000	0.000	2.000	2.000
5/2	2.0	0.000	0.000	1.999	0.000	0.000	0.000	0.000	2.000
Sum	11.0	0.759	0.072	9.027	1.117	0.018	3.156	3.844	3.999

$\Omega = 3/2$. Pt net charge: 0.148

ω	Occ.	Pt(s)	Pt(p)	Pt(d)	H(s)	H(p)	σ	π	δ
1/2	6.0	1.102	0.071	1.842	1.123	0.015	4.008	1.991	0.000
3/2	2.0	0.000	0.000	1.997	0.000	0.001	0.000	0.856	1.144
	+ hole	0.000	0.000	0.998	0.000	0.001	0.000	0.572	0.428
5/2	2.0	0.000	0.000	1.999	0.000	0.000	0.000	0.000	2.000
Sum	11.0	1.102	0.716	8.679	1.123	0.018	4.008	3.419	3.571

The population analysis may also be set up in terms of the single group functions σ, π and δ. These figures are also shown in table 6 and illustrate clearly the failure of the ΛΣ coupling scheme. The Ω=5/2 ground state may be described by the single $1\sigma^2 2\sigma^2 1\pi^4 1\delta^3$ configuration, but the Ω=1/2 state is clearly not a pure $1\sigma^2 2\sigma^1 1\pi^4 1\delta^4$ configuration. In the Ω=3/2 states the mixture of the $1\sigma^2 2\sigma^2 1\pi^3 1\delta^4$ and $1\sigma^2 2\sigma^2 1\pi^4 1\delta^3$ configurations is so strong (58% vs. 42%) that the assignment to one of them is difficult. This strong mixing was also observed by Balasubramanian and Feng[6] and by Dyall[8].

Another way of looking at the PtH electron distribution is by plotting the electron density. A plot of the total density will be dominated by the contribution of the platinum core electrons, and we have therefore plotted the density of open shell spinors only for the three lower states (figures 2 a-c). The plots clearly show that the hole is located in a platinum d spinor.

Figure 2. Electron density plots of the open shell spinors. Coordinates of the Pt atom are (0, 0), coordinates of the H atom are (0, 2.93). Figures in atomic units.
a) ω=5/2 open shell spinor ; b) ω=1/2 open shell spinor; c) ω=3/2 open shell spinor.

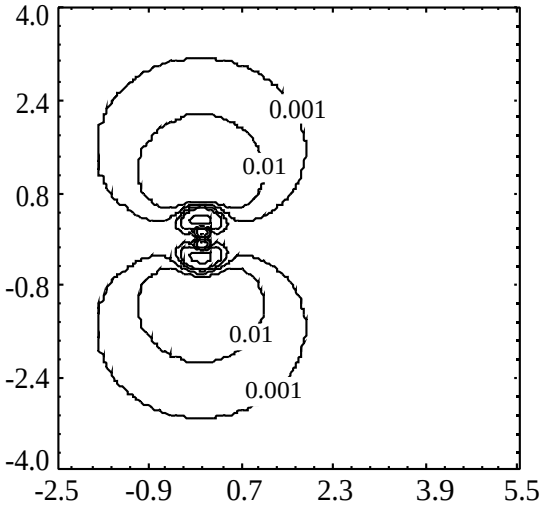

a)

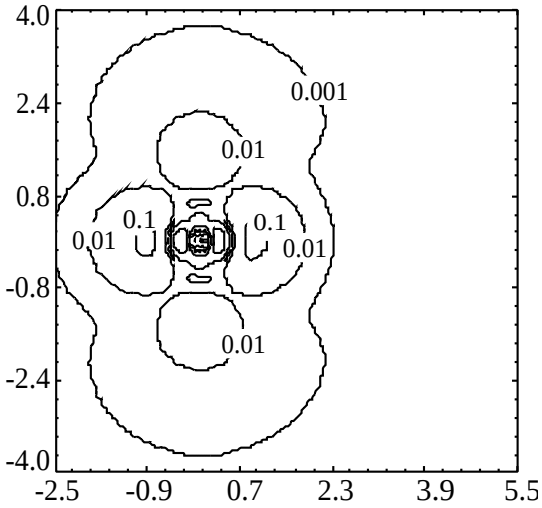

b)

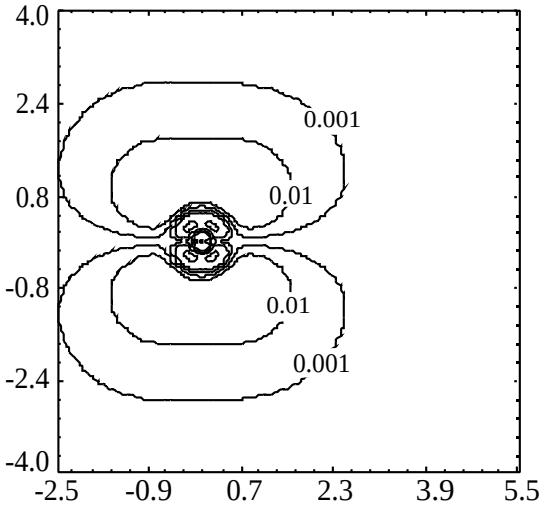

c)

5.5.3. CI results

The CI results are presented in table 7. In the lower three states the weights of the DHF references are approximately 90 % while other configurations contribute at most 0.4 %. Static correlation is therefore not very important in the PtH molecule, as opposed to the platinum atom. The correlation energy is 258 mH for the 5/2(1) and 3/2(1) states and 261 mH for the 1/2(1). The somewhat larger correlation energy for the 1/2(1) state may be attributed to the larger valence d population of the corresponding reference. The effect on the electronic excitation spectrum is a small but significant reduction of the splitting between the 5/2(1) and 1/2(1) state. Correlation further shortens the bond lengths by 3-4 pm. Correlating f-functions in the basis appears to be of importance, as was demonstrated by performing a small CI calculation on the 5/2(1) state in which 32 more virtual spinors, including the 14 non-bonding 5f spinors, were deleted from the active space. A three-point fit then gave a bond length of 1.544 Å as compared with 1.518 Å obtained with the larger CI. From the bond shortening and the enlargement of D_e and ω_e one can conclude that the bond is stronger than would be expected on basis of the DHF results. The gap between the lower three and the upper two states is about the same magnitude as the spin-orbit splitting in the platinum d-shell (Table 4).

Table 7. Molecular properties of PtH calculated by the relativistic CI method.

State	r_e (Å)	D_e (eV)	ω_e (cm^{-1})	$\omega_e x_e$ (cm^{-1})	T_e (eV)
5/2 (1)	1.518	2.98	2458	63	0.00
1/2 (1)	1.526	2.74	2419	66	0.24
3/2 (1)	1.542	2.54	2313	65	0.44
3/2 (2)	1.540	2.73	2365	62	1.46
1/2 (2)	1.562	2.58	2277	64	1.61

5.6. Discussion

Our CI as well as DHF results fit within the relativistic bonding scheme outlined above in which the electronic configuration of the three lower and two upper states of PtH may be written as $5d^4_{3/2}\ 5d^5_{5/2}\ \sigma^2_{1/2}$ and $5d^3_{3/2}\ 5d^6_{5/2}\ \sigma^2_{1/2}$ respectively. The assigned configurations are only approximate and are perturbed by 5d-participation in bonding that changes the order of the three lower states from the expected 5/2(1) < 3/2(1) < 1/2(1) sequence to 5/2(1) < 1/2(1) < 3/2(1). Further confirmation of the bonding scheme stems from the DHF results of Dyall[8]. Dyall performed DHF calculations on the five lower states of PtH using a 9s8p7d3f contracted Gaussian large component basis for platinum derived from the same primitive Gaussian basis (basis I) as our con-

tracted Pt basis(basis II). The lowest three PtH states were analysed by Dyall to be mainly $d_{5/2}$ hole states while the upper two are essentially $d_{3/2}$ hole states.

Most *ab initio* calculations on PtH, however, employ spin-free RECPs and optimise the $\Lambda\Sigma^-$states ($^2\Delta$,$^2\Pi$ and $^2\Sigma$) as a first stage. In table 8 we list some results obtained for the $\Lambda\Sigma^-$states. Rohlfing et al[4] used a RECP obtained from the Cowan-Griffin method[12] and a 5s5p3d1f uncontracted Gaussian valence basis. They did unrestricted Hartree-Fock (UHF) calculations and then introduced electron correlation through fourth order Møller-Plesset perturbation theory [MP4(SDTQ)]. Balasubramanian and Feng[6], using a j-averaged RECP fitted to numerical atomic DHF calculations and a 3s2p3d contracted Gaussian valence basis, performed a small Complete Active Space SCF (CASSCF) calculation with 11 electrons in an active space of 14 spin-orbitals. They then did multireference singles CI (MRSCI) to determine potential surfaces and multireference singles plus doubles CI (MRSDCI) to determine dissociation and excitation energies at the optimised geometries. At the singles level the $^2\Delta$ state is 0.12 eV above the $^2\Sigma$ state, while the order is reversed at the MRSDCI level with $^2\Delta$ as the ground state. Gropen et al.[7] obtained their RECP from an atomic calculation using the second order Douglas-Kroll approximation[13] and employed a 3s3p4d2f contracted Gaussian valence basis. They did a CASSCF-calculation with 11 electrons in an active space of 14 spin-orbitals followed by MRSDCI. Their article contains an error as the $^2\Sigma$ state at the CASSCF level is 0.04 eV above and not 0.34 eV below the $^2\Delta$ state, the latter being the MRSDCI result.

Table 8. Excitation energies T_e (eV) for $\Lambda\Sigma$ - states calculated by different methods.

	RECP			All - electron	
State	MP4[a]	MRSDCI[b]	MRSDCI[c]	CASSCF[d]	MRSDCI[e]
$^2\Sigma$	0.00	0.00	0.00	0.00	0.00
$^2\Delta$	- 0.16	- 0.05	0.34	- 0.09	0.09
$^2\Pi$	0.52	0.69	0.69	0.50	0.73

a) Rohlfing et al.[4]: RECP-UHF-MP4

b) Balasubramanian and Feng[6]: RECP-CASSCF-MRSDCI

c) Gropen et al.[7]: RECP-CASSCF-MRSDCI

d) Gropen[43]: All-electron CASSCF using the second order Douglas-Kroll approximation

e) Gropen[43]: All-electron CASSCF-MRSDCI using the second order Douglas-Kroll approximation

The results obtained for the $\Lambda\Sigma^-$states and listed in table 8 vary considerably and it is difficult to assess to what extent this spread may be related to the correlation treatment

or to the quality of basis sets or the RECPs. The RECP used by Wang and Pitzer[3] was fitted to a j-averaged atomic DHF calculation and appears to be too repulsive as the resulting bond lengths and spectrum deviate markedly from all other results. Clearly there is a need for an all-electron molecular calibration calculation at this level of approximation. Gropen[42] has recently performed an all-electron CASSCF-MRSDCI using the second order Douglas-Kroll approximation[13] and a 8s7p5d3f contracted Gaussian basis. Preliminary results from CASSCF as well as MRSDCI calculations at 1.55 Å are included in table 8. The results indicate that the $^2\Delta$ and $^2\Sigma$ states are near degenerate, but that correlation tends to favour $^2\Sigma$ as ground state.

Spin-orbit interaction is introduced in the RECP calculations through various perturbational schemes. Balasubramanian and Feng[6] add spin-orbit matrix elements to their CI matrix. The spin-orbit matrix elements were derived from the RECP[43] and thus depend on the quality of the potential. Rohlfing et al.[4] introduce spin-orbit splitting semi-empirically. To the diagonal matrix of electronic energies of the $\Lambda\Sigma$ - states they add a spin-orbit matrix for the separated atoms using an atomic spin-orbit parameter derived from experiment. They do not state exactly what parameter value they used, but it appears to be the parameter A = 0.418 eV derived from the splitting of the platinum positive ion d^9 state[44]. The approach of Gropen et al.[7] is quite similar, but neglects off-diagonal matrix elements.

Experimental data on the PtH molecule are scarce and restricted to the 3/2 and 5/2 states. Most experimental work has been done by the group of Scullman[45], but one may also mention the early study by Loginov[46] . Recently McCarthy et al.[47] reported laser excitation and Fourier transform spectroscopic results which give more precise estimates of $5/2(1) \rightarrow 3/2(1)$and $3/2(1)\text{-}5/2(1) \rightarrow 3/2(2)$ excitation energies. They also note a reversal of parity in the Ω-doubling for vibronic states at the 3/2(2) level and attribute this to the 1/2(2) state being above and pushing down on 3/2(2) vibronic states. This is the only experimental indication so far of the position of Ω = 1/2 states in the PtH spectrum. The possible 1/2 - 1/2 transition reported by Scullman was later shown to be caused by a gold impurity[48]. The experimental studies indicate an unusual stability of the Pt-H bond. The experimental value of 3.6±0.4 eV obtained by Birge-Sponer extrapolation is the largest measured bond energy of any transition metal hydride[49].

Table 9 lists excitation energies T_e and table 10 bondlengths r_e and harmonic frequencies ω_e obtained from a number of studies of PtH. Experimental excitation energies T_e were deduced from the corresponding T_0 values using the formula $T_e = T_0^0 + \frac{1}{2}\Delta\omega_e - \frac{1}{4}\Delta\omega_e x_e$. The relativistic CI gives the best overall agreement with

experiment for these properties. Since our relativistic CI results should be better than our DHF results, agreement on the DHF level with the 5/2(1)-3/2(1) splitting is probably somewhat coincidental. The good agreement between our DHF results and those of Dyall[8] should also be noted. The differences in r_e are smaller than 0.005 Å while the excitation energies differs by at most 0.02 eV. This indicates that basis set errors in the two calculations are of equal size.

Table 9. Comparison of excitation energies T_e (in eV) for states of PtH obtained by different methods.

	RECP			All - electron				
State	MP4[a]	SDCI[b]	SDCI[c]	SDCI[d]	DHF[e]	DHF[f]	Rel. CI[f]	Exp[g]
5/2 (1)	0.00	0.00	0.00	0.00	0.00	0.00	0.00	0.00
1/2 (1)	0.31	0.19	0.19	0.11	0.34	0.32	0.24	--
3/2 (1)	0.45	0.52	0.45	0.44	0.42	0.41	0.44	0.41
3/2 (2)	1.28	1.35	1.29	1.37	1.43	--	1.46	1.45
1/2 (2)	1.57	1.35	1.55	1.61	1.55	--	1.61	--

a) Rohlfing et al.[4]: RECP-UHF-MP4+spin-orbit(semi-empirically) [A = 0.418 eV]

b) Balasubramanian and Feng[6]: RECP-CASSCF-MRSDCI + spin-orbit(RECP)

c) Gropen et al.[7]: RECP-CASSCF-MRSDCI + spin-orbit(semi-empirically) [A = 0.418 eV]

d) Gropen[43]: All-electron CASSCF-MRSDCI using the second order Douglas-Kroll approximation + spin-orbit [A = 0.467 eV]

e) Dyall[8]: DHF

f) Present work

g) McCarthy et al.[47].

Table 10. Bondlengths r_e (in Å) of PtH calculated by different methods. Corresponding harmonic frequencies ω_e (in cm^{-1}) are given in parenthesis.

State	MRSCI[a]	DHF[b]	DHF[c]	Rel. CI[c]	Experiment[d]
5/2 (1)	1.55 (2177)	1.551 (2234)	1.548 (2251)	1.518 (2458)	1.528 (2378)
1/2 (1)	1.54 (2188)	1.573 (2094)	1.568 (2095)	1.526 (2419)	--
3/2 (1)	1.58 (2155)	1.584 (2080)	1.581 (2044)	1.542 (2313)	1.520 (2265)
3/2 (2)	1.59 (2179)	1.577 (2162)	--	1.540 (2359)	-- (2349)[e]
1/2 (2)	1.58 (2021)	1.590 (2097)	--	1.562 (2225)	--

a) Balasubramanian and Feng[6]: RECP-CASSCF-MRSCI + spin-orbit(RECP).

b) Dyall[8]: DHF.

c) Present work.

d) Scullman et al.[45]

e) Calculated using the formula $\omega_e = \Delta G_{1/2} - 2\omega_e x_e$, in which the $\Delta G_{1/2}$ value obtained by McCarthy et al.[47] and our calculated value for $\omega_e x_e$ were used.

The excitation energies calculated by Balasubramanian and Feng[6] agree rather well with our CI results, although their two upper states appear rather low indicating that spin-orbit splitting is somewhat underestimated. Their calculated bond lengths are appreciable longer and harmonic frequencies smaller than ours, a feature that is probably explained by insufficient correlation particularly due to their lack of correlating f-functions. The neglect of off-diagonal spin-orbit matrix elements by Gropen et al.[7] is hardly justifiable on the basis of the strong mixing of $\Lambda\Sigma$ - states through the spin-orbit interaction. We have therefore recalculated the spin-orbit splitting from their results using the semi-empirical method of Rohlfing et al.[4]. The results obtained using this semi-empirical method agree rather well with our CI results and indicate that platinum retains much of its atomic character in PtH. This is in accordance with our bonding model and justifies the assignment of the $5d^4_{3/2}\ 5d^5_{5/2}\ \sigma^2_{1/2}$ and $5d^3_{3/2}\ 5d^6_{5/2}\ \sigma^2_{1/2}$ electronic configuration for the three lower and two upper states of PtH respectively. The electronic configurations invites a comparison with the d^9s^2 negative platinum ion and indicates an analogy between the binding of an electron and of a hydrogen atom to platinum. Squires[49] has investigated the possible correlation of transition-metalelectron affinity EA(M) and the dissociation energy D[M-H] of the corresponding transition metal hydride. The study was motivated by the near constant gas-phase acidity observed for these hydrides. Squires obtains an empirical formula linking the two above quantities (D[M-H] = EA(M) + 1.19eV). The electron affinity of platinum is 2.13 eV which is almost twice the corresponding value for nickel (1.16 eV)[50]. The much larger

value for platinum can be understood in terms of relativistic stabilisation of the 6s orbital[10]. The unusual stability of the Pt-H bond may then be explained in an analogous fashion.

The analogy between the PtH molecule and the Pt negative ion further suggests that the spin-orbit parameter of the semi-empirical method used by Rohlfing et al.[4] should be derived from the fine structure splitting of the negative rather than the positive platinum ion. Both the negative ion and the PtH molecule can be well represented with a single configurational (d^9s^2 or $d^9\sigma^2$) wave function. In the positive ion the contribution of the d^8s configuration is non-negligible and decreases the spin-orbit coupling. The use of a spin-orbit parameter that was derived from the Pt^+ experimental splitting will thus underestimate the splitting in the molecule. A better choice is to obtain the spin-orbit parameter either from an experiment or calculation on the negative ion or from a calculation on Pt^+ that includes only the d^9 configuration. Unfortunately the $^2D_{5/2} - {}^2D_{3/2}$ splitting of the d^9s^2 negative platinum ion has not been experimentally determined. The recommended value[51] 10000 (±1000) cm^{-1} obtained by isoelectronic extrapolation gives a spin-orbit parameter A = 0.50 eV from the Landé interval rule. Numerical calculations on the d^9, d^9s and d^9s^2 configurations of Pt^+, Pt and Pt^- give values for A of 0.49, 0.50 and 0.47 eV respectively. We have used the latter value to obtain spin-orbit splitted excitations energies from the preliminary all-electron CASSCF-MRSDCI results of Gropen[42]. The results are listed in table 9 and agree well with our CI results.

5.7. Conclusions

The electronic structure and bonding of the five lower states of the PtH molecule have been investigated using fully relativistic CI based on DHF references. Spectroscopic properties have been obtained by fitting of a Morse potential tending asymptotically to the Pt [J = 3 ($5d^9(^2D_{5/2})6s^1$)] + H($6s^1$) and Pt [J = ($5d^9(^2D_{3/2})6s^1$)] + H($6s^1$) energies for the three lower and two upper states respectively. At the DHF level the effect of relativistic corrections (Gaunt interaction) to the Coulomb electron-electron interaction has been evaluated and found to be hardly significant for the properties mentioned above. At the CI level the wave functions are found to have only one dominant configuration. This indicates a lack of static correlation and is quite contrary to the results obtained for the platinum atom. Dynamic correlation in the d-shell is important for the spectroscopic properties of PtH and the inclusion of correlating f-functions in the basis appears to give considerable improvement of the results.

Our CI as well as DHF results indicate that bonding is essentially the same in all five states of PtH. The results are in accordance with a bonding scheme in which the electronic configuration of the three lower and two upper states of PtH are assigned the electronic configurations $5d^4_{3/2}\,5d^5_{5/2}\,\sigma^2_{1/2}$ and $5d^3_{3/2}\,5d^6_{5/2}\,\sigma^2_{1/2}$ respectively. The ground state of the PtH molecule is found to be an Ω=5/2 state strongly bound with a D_e value of 2.98 eV and a bondlength of 1.52 Å. The assigned electronic configurations suggest an analogy between the PtH molecule and the platinum d^9s^2 negative ion. The stability of the Pt-H bond may then be explained by the relativistic stabilisation of the platinum 6s orbital. The strong atomic character of platinum in the molecule may explain the success of more approximative approaches to the spin-orbit splitted states of PtH. On the basis of the analogy with the negative Pt ion we recommend the use of a spin-orbit parameter that is derived from the spin-orbit splitting of the negative Pt ion in the semi-empirical approach used by Rohlfing et al.[4].

The results show good agreement with experimental data and illustrate the value of 4-component relativistic CI calculations to provide accurate benchmark results for systems in which both relativistic and correlation effects are important.

5.9. Appendix A: Hydrogen basis

The hydrogen basis used in the calculations was derived from a 6s1p primitive basis and contracted to 3s1p. The basis is given in table A1.

Table A1. The hydrogen basis set.

Large components:

	Exponents	Contraction coefficients		
s	79.99016053	.00209389	-.00976942	-.00289511
	11.96435285	.01607826	-.07501606	-.02223054
	2.72256964	.07868258	-.36710784	-.10879011
	.77282765	.26323087	-1.22815136	-.36395498
	.25176829	.49709674	2.45234858	-.83562669
	.08842324	.28627156	-1.33565187	1.43031543
p	.80000000	1.00000000		

Small components:

	Exponents	Contraction coefficients		
s	.80000000	1.00000000		
p	79.99016053	.03242534	-.05733506	.00695649
	11.96435285	.09632089	-.17025340	.02069124
	2.72256964	.22487392	-.39743861	.04832367
	.77282765	.40083334	-.70839556	.08614912
	.25176829	.43204906	1.26704631	-1.13946020
	.08842324	.14745373	-.26058929	1.48212854
d	.80000000	1.00000000		

References

1) F. R. Hartley, "Chemistry of the Platinum Group Metals", (Elsevier Science Publishers: Amsterdam 1991).

2) H. Basch and S. Topiol, J. Chem. Phys. **71**, 802 (1979).

3) S. W. Wang and K. S. Pitzer, J. Chem. Phys. **79**, 3851 (1983).

4) C. M. Rohlfing, P. J. Hay and R. L. Martin, J. Chem. Phys. **85**, 1447 (1986).

5) G. Rasch and S. Tobisch, Chem. Phys. Lett. **166**, 311 (1990).

6) K. Balasubramanian and P. Y. Feng, J. Chem. Phys. **92**, 541 (1990).

7) O. Gropen, J. Almlöf and U. Wahlgren, J. Chem. Phys. **96**, 8363 (1992).

8) K. Dyall, J.Chem. Phys. (1993).

9) S. R. Langhoff and C. W. Bauschlicher, Ann. Rev. Phys. Chem. **39**, 181 (1988).

10) P. Pyykkö, Chem.Rev. **8**, 563 (1988).

11) O. Gropen, in: "Methods of computational chemistry". vol. 2, ed. S. Wilson (Plenum Press: New York, 1988) p.1.

12) R. D. Cowan and D. C. Griffin, J. Opt. Soc. Am. **66**, 1010 (1976).

13) M. Douglas and N. M. Kroll, Ann. Phys. (N.Y.) **82**, 89 (1974).

14) G. Malli and J . Oreg, J. Chem. Phys. **63**, 830 (1975).

15) P. J. C. Aerts and W. C. Nieuwpoort, proceedings of the 6th Seminar on Computational Methods in Quantum Chemistry, Schloss Ringberg (Tegernsee), September 4-7, 1984.

16) S. Okada and O. Matsuoka, J. Chem. Phys. **91**, 4193 (1989).

17) K. G. Dyall, K. Fægri, Jr. and P. R. Taylor, in : The effects of relativity in atoms, molecules and the solid state, ed. I. P. Grant, B. Gyorffy and S. Wilson, (Plenum: New York, 1991).

18) A. K. Mohanty and E. Clementi, Int. J. Quantum Chem. **39**, 487 (1990).

19) T. Saue, Thesis, University of Oslo (1991).

20) A detailed description of the MOLFDIR program package is to be published soon. MOLFDIR is scheduled to be available in the MOTECC'94 suite of programs.

21) R. E. Moss, Advanced Molecular Quantum Mechanics, (W. A. Benjamin, Inc.: London, 1968).

22) M. E. Rose, Relativistic Electron Theory, (Wiley & Sons: New York, 1961).

23) G. Breit, Phys. Rev. **34**, 553 (1929).

24) Y.-K. Kim, Phys. Rev. **154**, 17 (1967).

25) J. A. Gaunt, Proc. Roy. Soc. A **122**, 513 (1929).

26) C. C. J. Roothaan, Rev. Mod. Phys. **32**, 179 (1960).

27) L. Visscher, P. J. C. Aerts and O. Visser, in "The Effects of Relativity in Atoms, Molecules and the Solid State ", ed. S. Wilson, I. P. Grant and B. Gyorffy, (Plenum: New York, 1991).

28) O. Visser, L. Visscher, P. J. C. Aerts and W. C. Nieuwpoort, J. Chem. Phys. **96**, 2910 (1992).

29) J. Olsen, B. O. Roos, P. Jørgensen and H. J. Aa. Jensen, J. Chem. Phys. **89**, 2185 (1988).

30) E. R. Davidson, J. Comput. Phys. **17**, 87 (1975).

31) C. E. Moore, Circular of the National Bureau of Standards **467**, 181 (1958).

32) K.G Dyall, I. P. Grant, C. T. Johnson, E. P. Plummer and F. Parpia, Computer Phys. Commun. **50**, 375 (1998).

Basis set extension: K. G. Dyall, K. Fægri, P. R. Taylor and H. Partridge, J. Chem. Phys. **95**, 2583 (1991).

33) K. Fægri, Theoretical Chemistry, University of Oslo, Technical Note, June 1987.

34) O. Matsuoka and S. Okada, Chem.Phys.Lett. **155**, 547 (1989).

35) O. Visser, P. J. C. Aerts, D. Hegarty and W. C. Nieuwpoort, Chem. Phys. Letters **134**, 34 (1987).

36] O. Gropen, M. Sjøvoll, H. Strømsnes, E. Karlsen, O. Swang and K. Fægri, Theo. Chim. Acta 1993, to be published.

37) L. Visscher, P. J. C. Aerts, O. Visser and W. C. Nieuwpoort, Int. Journal of Quantum Chemistry: Quantum Chemical Symposium **25**, 131-139 (1991).

38) P. J. Hay, J. Chem. Phys. **66**, 4377-84 (1977).

39) R. S. Mulliken, Rev. Mod. Phys. **4**, 1 (1932).

40) O. Visser, L. Visscher, P. J. C. Aerts and W. C. Nieuwpoort, Theo. Chim. Acta **81**, 405 (1992).

41) R. Mulliken, J. Chem. Phys. **23**, 1833 (1955).

42) O. Gropen, Invited Lecture at the 1st Congress of the International Society for Theoretical Chemical Physics, Gerona, Spain, June 1993, to appear in Int. J. Quantum. Chem.

43) K. S. Pitzer, Int. J. Quantum Chem. **25**, 131 (1984).

44) This assumption is supported by the fact that a recalculation by Christel Marian (personal communication) using this parameter gives exactly the same excitation energies.

45) a) H. Neuhaus and R. Scullman, Z. Naturforsch. A **19**, 659 (1964);

b) R. Scullman, Ark. Fys. **28**, 255 (1964);

c) B. Kaving and R. Scullman, Can. J. Phys. **49,** 2264 (1971);

d) B. Kaving and R. Scullman, Phys. Scr. **9**, 33 (1974);

e) R. Scullman and P. Cederbalk, J. Phys. B **10**, 3659 (1977);

f) G. Gustafsson and R. Scullman, Mol. Phys. **67**, 981 (1989).

46) V. A. Loginov, Optics and Spectroscopy (USSR) **20**, 88 (1966).

47) M. C. McCarthy, R. W. Field, R. Engleman Jr. and P. F. Bernath, J. Mol. Spectr. **158**, 208 (1993).

48) R. Scullman, personal communication.

49) R. R. Squires, J. Am. Chem. Soc. **107**, 4385 (1985).

50) R. D. Mead, A. E. Stevens and W. C. Lineberger, in "Gas Phase Ion Chemistry", Vol. 3, ed. M. T. Bowers (Academic Press: New York, 1984), chapter 22.

51) H. Hotop and W. C. Lineberger, J. Phys. Chem. Ref. Data **4**, 539 (1975).

6. Relativistic and electron correlation effects on the d-d spectrum of transition metal fluorides

6.1. Abstract

The electronic spectra of the transition metal complexes CoF_6^{2-}, RhF_6^{2-} and IrF_6^{2-} that occur in the solids Cs_2MeF_6 are calculated. Hartree-Fock and Dirac-Fock calculations followed by non-relativistic and relativistic CI calculations respectively are used to study the influence of relativity and electron correlation. The calculated transitions are found to agree fairly well with experiment, the largest discrepancies arising from the neglect of differential dynamical electron correlation effects.

6.2. Introduction.

Ab initio computational methods based on the non-relativistic Schrödinger equation are nowadays applied quite routinely to describe the electronic structure of 3d and 4d transition metal complexes. In such calculations the main problem is to give an accurate description of the large electron-electron correlation that is present in partly filled d-shells. The most conspicuous errors that arise from the use of a non-relativistic theory instead of a relativistic theory are caused by the neglect of spin-orbit coupling. This deficiency can, however, in most cases be accounted for by the use of a perturbative spin-orbit operator.

In 5d transition metal complexes relativity leads to significant changes in the electronic wave functions compared to non-relativistically calculated wave functions. In these systems relativistic corrections are no longer small and the use of perturbation theory based on non-relativistically determined wave functions is more difficult. Methods that use non-relativistically determined orbitals as a one-electron basis for (approximate) relativistic Configuration Interaction (CI) calculations may need larger expansions to converge than methods that include relativity from the outset.

In this work such a more rigorous approach is followed by employing a relativistic formalism throughout. The basic equation that we use is the Dirac-Coulomb-Gaunt equation that implicitly includes all one-electron relativistic effects and the magnetic (Gaunt) correction to the Coulomb two-electron interaction. We use the Dirac-Fock approach to obtain four-component spinors that are used to set up a determinantal CI space for subsequent relativistic CI calculations. We can thus treat relativity and electron correlation on an equal footing and study the influence and interplay of both on the electronic spectra.

This method has previously been applied to closed shell group IV hydrides[1], a lanthanide complex[2] and recently to the PtH molecule[3] (Chapter 5). We now study the properties of the MeF_6^{2-} complex ions of cobalt, rhodium and iridium as representative examples of transition metal complexes across the periodic table. These ions were chosen because experimental data (structures and electronic spectra) of all three ions are available. Since the metal ions belong to the same column of the periodic table, they have the same valence electron configurations which simplifies the comparison of the results.

6.3. Theory

The Dirac-Fock-RASCI method and its implementation (the MOLFDIR program package) is described in detail in the previous chapters. Here we mention only a few points that are relevant for the present application.

In the RASCI formalism[4] the spinor set is first divided in a core set, an active set and an external or deleted set, after which the active set is further subdivided into three sets (RAS1, RAS2, RAS3). By specifying a minimum number of electrons that has to reside in RAS1 spinors and a maximum number of electrons that may be excited to the RAS3 space, most conventional types of CI spaces can be defined.

In the case of the MeF_6^{2-} ions the RAS1 set consists of the 36 fluorine 2p-like spinors, the RAS2 set consists of the 10 open Me nd-like spinors, and the RAS3 set is formed by the low-lying virtual spinors. A Complete Open Shell CI (COSCI) space is generally defined[2] as the set of determinants that fulfil the constraints that all RAS1 spinors have occupation one, and all RAS3 spinors have occupation zero.

In the present application the COSCI method is equivalent to the well known Ligand Field CI (LFCI) method. Complete diagonalisation of this small CI space is possible and gives a set of intermediary coupled wave functions and a first estimate of the dd-spectrum.

The LFCI reference space is extended in Charge Transfer CI (CTCI) calculations by allowing single, double, triple, or higher excitations from RAS1 to RAS2. These excitations mix low-lying charge-transfer (Me^{3+}, Me^{2+}, Me^{+}) states into the LFCI wave functions. The CTCI method treats the so-called static correlation effects that arise from the low-lying charge-transfer states.

A third sophistication is possible by the relaxation of the obtained wave function by means of single excitations from RAS1 and RAS2 to RAS3. The spinors that were obtained by optimising the d^nL^{36} configuration are not optimal for the $d^{n+1}L^{35}$ and $d^{n+2}L^{34}$ charge-transfer configurations. This deficiency in the spinor basis may in first order be corrected by the inclusion of all singly excited states from these configurations. This type of CI is called First Order CI (FOCI).

In the present application the treatment of dynamical correlation by means of inclusion of double excitations into the RAS3 space is prohibited by the large size of the active space.

6.4. Basis sets

Gaussian type basis sets were optimised to minimise the energy of the Me^{4+} d^5 configurational average. Because no relativistic basis set optimisation program is available at present, we used the non-relativistic code ASCF[5] for this purpose. During the optimisation process the d-exponents were constrained to be a subset of the s-exponents. The advantage of applying these constraints on the d-exponents is that the primitive basis for the small component p-functions, as obtained by kinetic balance, is already contained in the small component functions that arise from the large component s-functions. The f-exponents were similarly constrained to be a subset of the p-exponents, to keep the number of small component d-functions as low as possible.

The non-relativistic exponent optimisation gives quite reasonable results apart from a deficiency in the basis for the $p_{1/2}$ spinors which lacks some steep basis functions. This deficiency was remedied by adding one extra tight p function to the Rh basis and two extra to the Ir basis. The exponents were determined by logarithmic extrapolation of the original set of exponents.

Using these sets of primitive gaussians the atomic spinors of the Me^{4+} ions were determined after which general contracted bases were formed[6] consisting of all occupied spinors. The valence region is described at triple-zeta level by leaving two outer s-functions, one outer p-function and two outer d-functions uncontracted and by adding extra s, p, d and f diffuse functions. The uncontracted functions were kinetically balanced, the contracted functions that were obtained from the occupied spinors were atomically balanced.

To describe the fluorine ions we used Wachters[7] primitive fluorine basis. The general contraction was based on a calculation on the F^- closed shell ion and the resulting triple-zeta valence basis was extended with 1 d polarisation function.

The size of the basis sets is given in table 1. The primitive basis sets of all ions are given in appendix 1. Contraction coefficients are available upon request.

Table 1. : Basis set sizes.

Co	(17s,10p,7d,1f;	nrel.	[6s,4p,4d,1f]
	10s,17p,10d,7f,1g)	rel.	[6s,5p,4d,1f; 5s,9p,7d,5f,1g]
Rh	(18s,14p,11d,1f;	nrel	[7s,5p,5d,1f]
	14s,18p,14d,11f,1g)	rel.	[7s,8p,7d,1f; 5s,12p,9d,7f,1g]

Ir	(21s,15p,13d,7f;	nrel.	[8s,6p,6d,2f]
	15s,21p,15d,13d,7g)	rel.	[8s,10p,9d,3f;
			6s,14p,12d,9f,3g]
F	(10s,6p,1d; 6s,10p,6d,1f)	nrel.	[5s,4p,1d]
		rel.	[5s,4p,1d; 4s,5p,4d,1f]

6.5. Atomic calculations

To investigate the quality of the basis sets we have compared the differences between the absolute energies at Hartree-Fock and at Dirac-Fock level calculated respectively with the contracted basis sets and numerically with the program GRASP[8]. The basis set Hartree-Fock calculations were done with the non-relativistic option of our program package MOLFDIR, the numerical Hartree-Fock limit was obtained by multiplying the speed of light with a value of 10000.

Although the absolute error in the relativistic energies is much larger than the absolute error in the non-relativistic energies, the energy differences between the different configurations are quite satisfactory and accurate to about 0.2 eV (table 2). To study effect of basis set errors on the d-d spectrum we have performed COSCI calculations based both on the numerical spinor set and on the basis set spinor set. If we compare the relative energies of the states in the d^5 manifold we find that the differences between both calculations are small: maximally 26 meV (table 3).

Table 2. Energy differences (eV) between numerical and basis set Dirac-Fock calculations on the d^n averages (n=5,6,7). ΔE = E (Basis set) - E(Numerical).

	Non-Relativistic			Relativistic		
	Co	Rh	Ir	Co	Rh	Ir
$\Delta E\ (Me^{4+})$	0.22	0.56	2.98	0.44	1.79	32.27
$\Delta E\ (Me^{3+})$	0.26	0.54	3.00	0.47	1.78	32.28
$\Delta E\ (Me^{2+})$	0.39	0.53	3.05	0.61	1.76	32.32

Table 3. Energy differences (eV) between numerical and basis set COSCI calculation on the Me^{4+} d^5 average.

	Non-Relativistic			Relativistic		
	Co	Rh	Ir	Co	Rh	Ir
Weighted average error.	0.007	0.013	0.004	0.008	0.009	0.002
Maximum error.	0.013	0.026	0.008	0.015	0.018	0.005

In the optimisation of the Rh^{4+} energy two s- and d-functions ended up with almost the same exponential parameter (0.4435 and 0.3888). Such a close spacing is not very efficient and may give numerical inaccuracies in the molecular calculations. We therefore substituted for the latter primitive function a function with exponent 0.1803 (obtained by logaritmic extrapolation). This explains the somewhat larger deviations from the numerical results in the Rh^{4+} spectrum (table 3).

The tables show that the basis sets give a good description of the different oxidation states of the metal ions, but they do not test the validity of the COSCI approach to calculate accurate spectra. Comparison with experimental data is desirable but is hampered by the scarcity of spectral data for the higher oxidation states of the metal ions. Excitation energies for the 4+ ions are only available for cobalt. Comparison with the Me^{2+} electronic spectrum is possible for both cobalt and rhodium (table 4).

Table 4. Relativistic COSCI spectrum of the Co^{4+}, Co^{2+} and Rh^{2+} free ions. Energies (eV) given relative to the ground state. Intramultiplet splittings (meV) are given in parenthesis.

	Co^{4+}			Co^{2+}		Rh^{2+}	
State	Exp.[9]	COSCI	State	Exp.[10]	COSCI	Exp.[24]	COSCI
$^6S_{5/2}$	0.00	0.00	$^4F_{9/2}$	0.00 (0)	0.00 (0)	0.00 (0)	0.00 (0)
$^4G_{11/2}$	4.61 (0)	5.21 (0)	$^4F_{7/2}$	0.10 (104)	0.10 (103)	0.27 (266)	0.26 (256)
$^4G_{9/2}$	4.62 (9)	5.21 (-1)	$^4F_{5/2}$	0.18 (180)	0.17 (179)	0.43 (432)	0.42 (424)
$^4G_{7/2}$	4.62 (9)	5.20 (-14)	$^4F_{3/2}$	0.23 (231)	0.23 (232)	0.54 (536)	0.53 (532)
$^4G_{5/2}$	4.63 (11)	5.21 (6)	$^4P_{3/2}$	1.88 (0)	2.41 (0)	1.36 (0)	1.85 (0)
$^4P_{3/2}$	5.05 (0)	5.99 (0)	$^4P_{5/2}$	1.91 (28)	2.44 (32)	1.37 (8)	1.85 (-2)
$^4P_{5/2}$	5.07 (17)	6.00 (16)	$^4P_{1/2}$	1.96 (76)	2.48 (78)	1.55 (183)	2.02 (170)
$^4P_{1/2}$	5.09 (34)	6.02 (36)	$^2G_{9/2}$	2.11 (0)	2.40 (0)	1.74 (0)	1.91 (0)
$^4D_{7/2}$	5.54 (0)	6.48 (0)	$^2G_{7/2}$	2.20 (98)	2.50 (99)	1.89 (150)	2.17 (256)
$^4D_{1/2}$	5.57 (25)	6.49 (14)	$^2H_{11/2}$	2.82 (0)	3.20 (0)	2.42 (0)	2.54 (0)
$^4D_{5/2}$	5.58 (34)	6.51 (35)	$^2H_{9/2}$	2.91 (89)	3.28 (82)	2.73 (250)	2.79 (250)
$^4D_{3/2}$	5.58 (34)	6.51 (30)					
$^2I_{11/2}$	6.74 (0)	7.42 (0)					
$^2I_{13/2}$	6.74 (5)	7.44 (16)					

The relativistic COSCI method gives a good description of the intramultiplet spin-orbit splittings, except for the very small splitting of the ^4G excited state of Co^{4+} where it reverses the order of the states. Note, however, that the main feature of d^5 multiplets, virtually vanishing spin-orbit splittings[11], is reproduced correctly. The method does not

deal very well with the intermultiplet splittings. This failure is understandable because at the COSCI level dynamic correlation effects are not accounted for. We may expect the same kind of errors in the molecular calculations.

6.6. Cluster calculations

6.6.1. Introduction

In an ionic model we can describe transitional metal complexes as metal cations that are coordinated by ligand anions. In the complexes studied here we find fourfold oxidised metal ions with the configurations $[Ar]3d^5$, $[Kr]4d^5$ and $[Xe]5d^5$ for Co^{4+}, Rh^{4+} and Ir^{4+} respectively. They are octahedrally coordinated by six fluorine anions. The lowest transitions in the electronic spectra of the complexes originate from excitations within the d^5 manifold of the metal ion. The influence of the surrounding ions is in such a approach accounted for by an electric field that lifts the degeneracy of the metal d-orbitals. Many features of the electronic spectra can then be explained on basis of the symmetry of the crystal field. An assumption that is usually made in Crystal Field theory is that the radial character of the open shell d-like orbitals remains the same. With this assumption the spectrum may be fitted by the use of only a few parameters (10Dq, the Racah two-electron parameters B and C and optionally a spin-orbit parameter ζ). This simple model can be refined[12] by accounting for the radial difference between e_g and t_{2g} orbitals but this adds seven more parameters which is in most cases impractical considering the available experimental data.

The unrealistic high formal charge of the metal ions treated here gives, however, rise to difficulties with the interpretation of the electronic structure of the complexes in a simple ionic model. Covalency will delocalise the ligand electrons and reduce the high formal charge to a more realistic value. In a molecular orbital picture the bonding and anti-bonding combinations of orbitals that are formed from the fluorine p-functions and the metal d-functions in the t_{2g} and e_g representations give rise to charge transfer that makes the metal ion less positive and the fluorines less negative. In contrast to the electrostatic crystal field picture derived from the ionic model, the formation of covalent bonds can now be considered to be the main source of the perturbing field, which led to the development of Ligand Field theory. The covalent bonding will also introduce radial differences between the e_g and t_{2g} open shell orbitals since they contribute to a different type of bonding (σ and π respectively). These differences are again not taken into account, however, so that the parametrisation given above is maintained.

A discussion of the validity of the underlying ideas from an ab initio point of view is given by Vanquickenborne et al[13]. In *ab initio* calculations like the ones presented here, the orbital differences are of course accounted for since the orbitals are determined

variationally. This means that the interpretation of the parameters of the Ligand Field model changes and direct comparison with experimentally derived parameters is difficult. In the relativistic calculations the situation is even more complicated. We now also have to consider the change in character of the orbitals under the influence of spin-orbit coupling. We will therefore in general follow a straightforward approach and compare the observed and calculated transitions directly. In some cases use of a Crystal or Ligand Field model is, however, helpful for a qualitative analysis of the obtained results.

6.6.2. Symmetry and configurations

The five d-orbitals of the central ion are divided in two representations (e_g and t_{2g}) in the octahedral (O_h) point group. The eighteen fluorine p-orbitals span a number of representations including e_g and t_{2g} (table 5).

In the relativistic calculations we will work with one-electron spinors. These functions span the "extra" representations of the full rotational ($O(3)^*$) or the octahedral (O_h^*) double group. For the free ions we find that the d-shell is split into a $d_{3/2}$ and a $d_{5/2}$ subshell while the fluorine p-shells are split into $p_{1/2}$ and $p_{3/2}$ subshells.

The $d_{3/2}$ spinors span the u'_g representation of O_h^* while the $d_{5/2}$ shell is split over its e''_g and u'_g representations. These representations are of course also spanned if we reverse the construction of molecular double group functions and make spinors as products of the e_g and t_{2g} orbitals with α or β spin. We then see that the spinorbitals constructed from the e_g orbitals span the u'_g representation, while the spinorbitals constructed from the t_{2g} orbitals span both the u'_g and the e''_g representation.

Table 5. Orbitals and spinors in different symmetry groups.

	O(3)	O(3)*	O_h	O_h^*
Central Ion	d	$d_{3/2}$, $d_{5/2}$	e_g, t_{2g}	e''_g, $2*u'_g$
Ligands	6*p	$6*p_{1/2}$, $6*p_{3/2}$	a_{1g}, e_g, t_{1g}, t_{2g}, $2*t_{1u}$, t_{2u}	$2*e'_g$, e''_g, $3*u'_g$, $2*e'_u$, e''_u, $3*u'_u$

In figure 1 the relations between the different (spin)orbitals are given. In following discussions on the nature of the spinors and of the splittings we will sometimes loosely speak of t_{2g} (or e_g) *spinors*. This should be read as : "The set of spinors that can be formed from combinations of the e_g (or t_{2g}) *orbitals* multiplied with an α or β spin function".

Figure 1. Relations between orbitals and spinors in different symmetry groups.

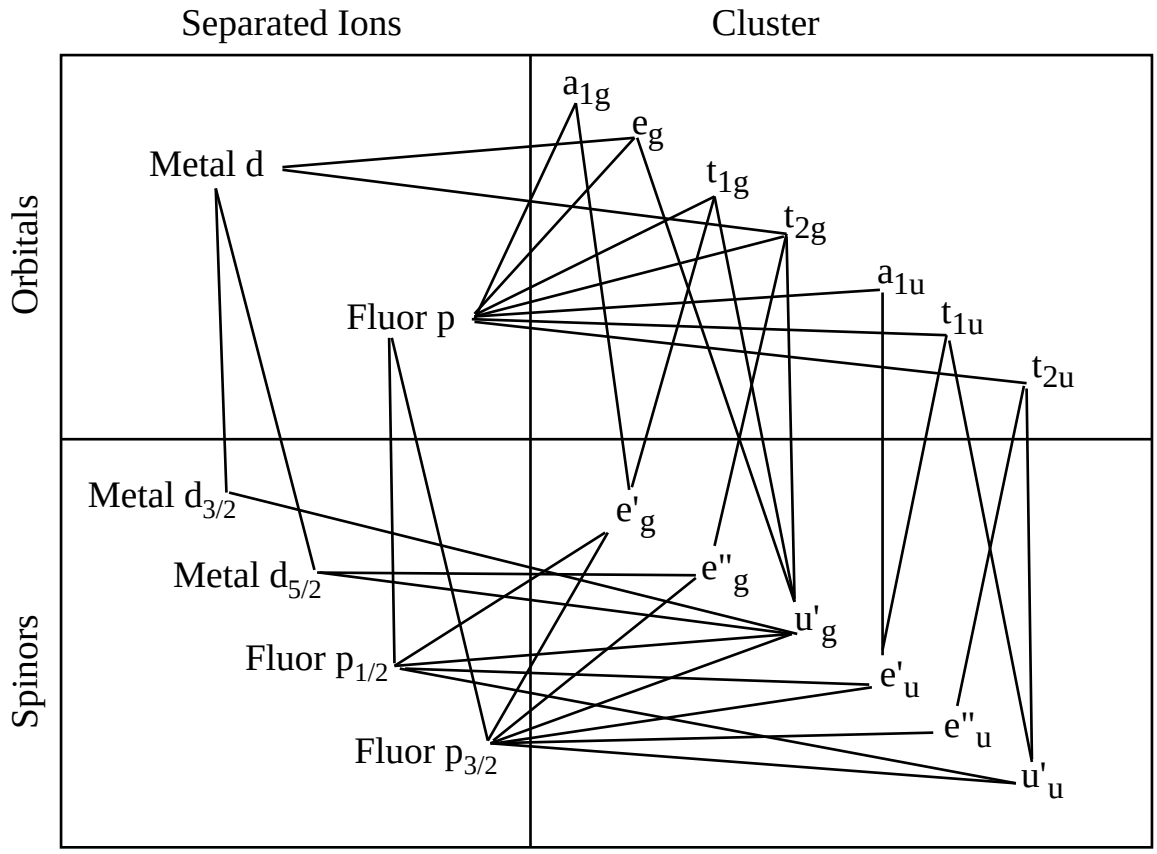

6.6.3. Computational details

The splitting of the d-shell into 2 or 3 groups of spinors gives various ways of dividing the 5 d electrons over the different representations. Optimising the energy of all states arising from the possible configurations by separate SCF calculations is in principle possible but is not feasible in practice. Such a procedure gives different spinor sets for all different states, which means that subsequent CI calculations require separate 4-index integral transformations for all states which would increase the computational effort considerably. The interpretations of such results would furthermore be more cumbersome because of the differences in spinor sets.

Our goal is to obtain one set of spinors that gives a reasonable description of all states. The CI calculations are done (simultaneously) in this molecular spinor basis for all states. To get a balanced description of all states we optimise our spinors for the weighted average energy expression of all configurations that can be made by distributing five electrons over the ten spinors that span the twofold degenerate e''_g and the two four-fold degenerate u'_g representations. This averaged energy expression is equivalent to the non-relativistic weighted average energy expression of the $t_{2g})^{5-x}e_g)^x$ (x = 0, 1,.., 4) configurations.

To check the sensitivity of the results to the choice of the spinor set we have done some non-relativistic calculations on the $^2T_{2g}$ state of CoF_6^{2-}. We studied the energy differences introduced by the use of different one-electron spinor sets for wave functions of different quality. We compare the set of spinors obtained by minimising the energy average of the d^5 configuration (set 1) with the set obtained by minimising the (t_{2g}^5) $^2T_{2g}$ energy expression separately (set 2). Since the t_{2g}^5 configuration has a small weight in the total average we expect these calculations to give maximum values for the spinor relaxation energies that would arise in separate SCF calculations on the various states.

Table 6. $^2T_{2g}$ energy expectation values calculated non-relativistically with different spinor sets and CI spaces. The uncontracted basis without Co f and fluorine d functions was used.

Wave functions	E (Set 1) (a.u.)	E (Set 2) (a.u.)	Difference (eV)
Single determinant	-1992.0945	-1992.1166	-0.60
LFCI	-1992.1105	-1992.1291	-0.51
CTCI	-1992.2005	-1992.2051	-0.13

In table 6 we see that the influence of the spinor set diminishes as the level of CI increases. This can be explained by noting that the most important differences between the two spinor sets can be written as rotations between the closed and open shell t_{2g} (and e_g) spinors. In the CTCI calculations excitations from closed to open shell spinors are allowed, hence the differences between the results obtained with the two spinor sets get much smaller. The influence of the use of average spinors on the final results is probably smaller than 0.1 eV since the other states will also have a non-zero, negative, relaxation energy.

Besides the use of one set of spinors for all states we had to use two other approximations to make the calculations feasible.

The first concerns the level of excitation that is allowed in the Charge Transfer and First Order CI calculations. The maximum excitation level for charge transfer excitations is five, giving wave functions with a filled d-shell and five holes on the ligands. The weights of such configurations in the CTCI or FOCI wave function are likely to be small since the excitation energies involved are of the order of 3-5 eV per excitation level. This assumption was studied by calculating (non-relativistically) the convergence of the correlation energy of CoF_6^{2-} with an increasing level of excitation in the Charge Transfer CI (table 7). We see that beyond the triple excitation level no significant changes in the spectrum occur. In the subsequent calculations we have limited the excitation level in the CTCI and FOCI to doubles. We also performed CTCI

calculations that allowed triple excitations but found these to be insignificant for cases other than CoF_6^{2}.

Table 7. Contributions to CoF_6^{2-} CTCI correlation energies (eV) with increasing level of excitation. The uncontracted basis without Co f and fluorine d functions was used.

State	Correlation	Singles	Doubles	Triples	Quadruples
$^2T_{2g}$	-2.45	-0.63	-1.37	-0.44	-0.01
$^4T_{1g}$	-2.11	-0.42	-1.36	-0.33	-0.01
$^4T_{2g}$	-2.36	-0.50	-1.49	-0.36	-0.01
$^6A_{1g}$	-1.17	-0.16	-0.80	-0.21	-0.01

The second approximation is based on an analysis of the density matrices of the CTCI wave functions. Comparison of the density matrices from the LFCI and the CTCI wave functions showed that the major changes occur in the bonding representations e_g and t_{2g} (figure 2). The density arising from orbitals in the other representations hardly changes, which indicates that excitations that involve these orbitals are not very important. To make this assumption quantitative we performed a calculation in which only the excitations from the e_g and t_{2g} spinors were allowed. This calculation gave a reasonable estimate of the total correlation energies (table 8). We therefore restricted the RAS1 spinor space to this set of bonding spinors in the final CTCI and FOCI calculations. The RAS3 space was chosen to consist of a number of selected spinors that was equal to the number of RAS1+RAS2 spinors to enable possible relaxation for each occupied spinor. Use of all virtual spinors in the RAS3 space to allow more complete relaxation of the wave functions would be desirable, but is not feasible for this system since it would lead to very large sizes ($>10^8$) of the determinantal CI space.

Figure 2. Diagonal elements of the differential (COSCI-LFCI) density matrices. CoF_6^{2-} at the non-relativistic level.

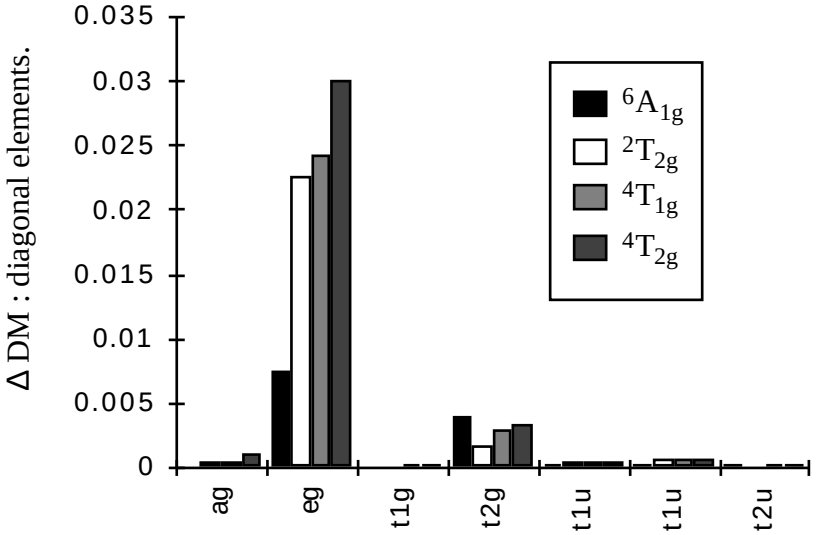

Table 8. Correlation energies (eV) of CoF_6^{2-} with different RAS1 spaces.

State	All fluorine p's	e_g and t_{2g}	Difference
$^2T_{2g}$	-1.67	-1.54	0.13
$^4T_{1g}$	-1.49	-1.38	0.12
$^4T_{2g}$	-1.74	-1.53	0.21
$^6A_{1g}$	-0.76	-0.71	0.05

The final expansion space that was used in the CI calculations consisted of 14 fluorine p-like spinors in RAS1, 10 Metal d-like spinors in RAS2 and 24 virtual spinors. This yielded a number of 13,482 determinants in the CTCI calculations and a number of 562,464 determinants in the FOCI calculation. By the use of abelian point group symmetry is was possible to reduce these spaces to subspaces of at most 3,526 (CTCI) and 140,626 (FOCI) determinants.

6.6.4. Crystal surroundings and cluster geometry

The MeF_6^{2-} ions of cobalt, rhodium and iridium crystallise with a number of alkali cations to form perovskite structures. The compounds have a K_2PtCl_6 like structure in which the MeF_6^{2-} units are separated from each other by about 3.5 Å. The other ions are found at distances slightly larger than 3 Å from the fluorine ions.

Fig 3. Cs_2MF_6 lattice. Plotted is part of a unit cell, extended to show the octahedral surrounding of the transition metal. Drawing is not on scale.

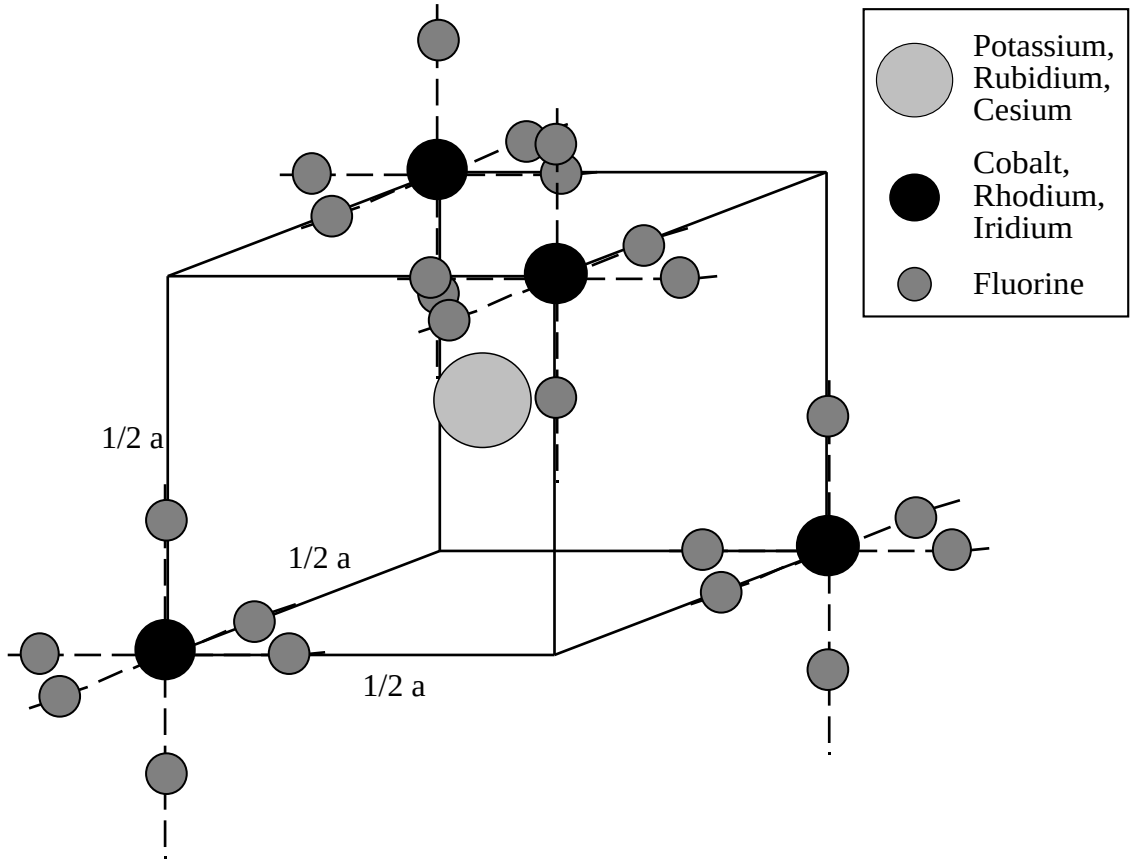

Most experimental spectra available[14,15,16] concern the cesium compounds and are rather poorly resolved. In the case of IrF_6^{2-} more precise values for some transitions were obtained by Magnetic Circular Dichroism (MCD) experiments on Cs_2GeF_6, doped with Cs_2IrF_6[17].

To incorporate the effect of the surrounding ions on the spectra, we have described the surroundings of the IrF_6^{2-} cluster by fitting the Madelung potential of the host (after subtraction of the cluster contributions) to a number of point charges. This fitted potential was also used in the RhF_6^{2-} calculations since no precise value of the lattice parameter (a) of Cs_2RhF_6 was available. In the CoF_6^{2-} calculations we fitted the cluster corrected Madelung potential of the Cs_2CoF_6 lattice.

Both potentials vary slowly over the cluster (table 9) and lower the spinor energies but do not dramatically influence the spectrum. Calculations on the bare clusters give spectra that differed by less than 0.2 eV from spectra calculated with the embedded cluster. Other than electrostatic effects from the surroundings are assumed to be small and are not taken into account.

The fit charges and the accuracy of the fits can be found in appendix 2.

Table 9. Potential at lattice sites (Volts).

Position	Cs_2CoF_6	Cs_2GeF_6
Metal sites	9.25	9.00
Fluorine sites	8.81	8.51
Difference	0.44	0.48

The Me-F distance is not a fixed fraction of the basic lattice parameter (a). So knowledge of this lattice parameter alone is not enough to determine the distances within the MeF_6^{2-} ion. Of the three compounds studied only the Cs_2CoF_6 structure is completely determined experimentally. The Co-F distance was estimated to be 1.73 (±0.05) Å on the basis of X-ray crystallographic data[18]. Of the other two compounds only the Cs-Me distances are known. Recently, however, EXAFS data of the K_2RhF_6 and K_2IrF_6 crystals[19,20] were published that give precise values for the Rh-F and Ir-F distance in these compounds. This distance is found to be 1.93 Å for both Rh-F and Ir-F. Since we did not have these values at the start-up of our calculations we also determined the distances by a geometry optimisation based on a 3 point parabolic fit of LFCI data (table 10). These optimisations were carried out for clusters embedded in potentials as described above. As optimum distance we took the equilibrium distance of the lowest $^2T_{2g}$ (E''_g) state.

For CoF_6^{2-} the optimisation procedure gives a distance of 1.76 Å, which is within the (wide) error range of the experimental distance. Miyoshi and Kashiwagi[21] have done non-relativistic SCF calculations on CoF_6^{2-} ground state using embedded and bare cluster models. Using the bare cluster model they found a distance of 1.79 Å. With their most sophisticated model (which included the effect of the first two layers of surrounding ions as point charges) they found a distance of 1.77 Å. These data show that the potential energy curve is almost entirely determined by the intra-molecular interaction within the isolated CoF_6^{2-} complex and is not influenced much by the surrounding ions.

The independence of the Me-F equilibrium distance on the surrounding ions implies that the optimisation process should give values close to Rh-F and Ir-F distances in K_2RhF_6 and K_2IrF_6. Comparing the calculated values in table 10 with the experimental values we find differences of 0.02 Å. This is indeed the same order of accuracy as was obtained for the Co-F distance. However, the calculated Rh-F distance is shorter than the measured distance, while the calculated Ir-F distance is larger than the measured distance. This indicates that the 2 pm accuracy reached by simple LFCI geometry optimisations is somewhat fortuitous and may be less in other compounds.

In the calculations presented in the next section we have used the experimental metal-fluorine distances of 1.730 Å, 1.934 Å and 1.928 Å for cobalt, rhodium and iridium respectively.

Table 10. Bondlengths (picometers) calculated at the LFCI level.

	CoF_6^{2-}			RhF_6^{2-}			IrF_6^{2-}		
State	non-relat.	relat.	dif.	non-relat.	relat.	dif.	non-relat.	relat.	dif.
$^2T_{2g}$ (E"$_g$)	177	176	-0.3	191	191	-0.6	196	195	-1.4
$^2T_{2g}$ (U'$_g$)		176	-0.2		190	-0.7		194	-1.6
$^4T_{1g}$ (U'$_g$)	179	179	-0.1	195	194	-0.9	201	198	-3.0
$^4T_{1g}$ (E"$_g$)		179	0.1		194	-1.0		198	-2.8
$^4T_{1g}$ (U'$_g$)		179	0.0		194	-0.8		198	-3.4
$^4T_{1g}$ (E'$_g$)		179	-0.1		194	-0.8		198	-3.4
$^4T_{2g}$ (E'$_g$)	179	179	-0.2	195	195	-0.5	201	198	-3.5
$^4T_{2g}$ (U'$_g$)		179	-0.2		195	-0.5		198	-3.2
$^4T_{2g}$ (U'$_g$)		179	-0.1		195	-0.4		198	-3.3
$^4T_{2g}$ (E"$_g$)		179	-0.2		195	-0.4		198	-3.5
$^6A_{1g}$ (U'$_g$)	181	181	-0.1	198	199	1.0	205	200	-5.6
$^6A_{1g}$ (E"$_g$)		181	-0.1		199	1.0		200	-5.5
Exp.[29,30,31]	173 (5)			193.4 (0.2)			192.8 (2)		

6.6.5. Analysis of the spinor set

To get insight in the amount of covalency that is present in the complexes we have analysed the individual valence e_g and t_{2g} spinors by means of the Mulliken population analysis scheme[22]. Since we used the same average of configuration energy expression to optimise spinors for the clusters as for the bare metal ions, we can also compare the calculated spinor energies to study trends in the spin-orbit splitting. The open and closed shell spinor energies can, however, not be compared directly with each other because the definition of the closed shell Fock operator differs from the one in that is used for the open shell spinors. The shifts that are found in the open shell spinor energies, going from Co to Ir, reflect the shifts found in the Me^{4+} bare ions.

Table 11a : Energies and Mulliken population analysis of the highest closed shell e_g (u'_g) spinors.

	Energy (eV)	% Me (d)	% F (s)	% F (p)
CoF_6^{2-} (NR)	-19.04	28.2	2.9	70
CoF_6^{2-} (R)	-18.93	27.6	2.8	69.6
RhF_6^{2-} (NR)	-18.40	26.6	2.4	70.9
RhF_6^{2-} (R)	-18.24	25.2	2.3	72.1
IrF_6^{2-} (NR)	-18.44	23.6	2.8	73.5
IrF_6^{2-} (R)	-18.06	21.7	2.5	75.7

Table 11b : Energies and Mulliken population analysis of the open shell e_g (u'_g) spinors.

	Energy (eV)	% Me (d)	% F (s)	% F (p)
CoF_6^{2-} (NR)	-18.26	74.3	0.6	25.1
CoF_6^{2-} (R)	-18.14	75.0	0.6	24.4
RhF_6^{2-} (NR)	-12.10	73.0	0.3	27.0
RhF_6^{2-} (R)	-11.74	74.3	0.3	25.7
IrF_6^{2-} (NR)	-9.09	74.6	-0.3	25.6
IrF_6^{2-} (R)	-7.98	77.8	-0.5	22.5

Table 11c : Energies and Mulliken population analysis of the highest closed shell t_{2g} (e''_g, u'_g) spinors.

	Energy (eV)	% Me (d)	% F (p)	% F (d)
CoF_6^{2-} (NR)	-17.44	10.7	88.5	0.8
CoF_6^{2-} (R,e"g)	-17.37	10.3	88.9	0.8
CoF_6^{2-} (R,u'g)	-17.42	10.4	88.8	0.8
RhF_6^{2-} (NR)	-16.88	13.9	85.3	0.8
RhF_6^{2-} (R,e"g)	-16.76	12.8	86.4	0.7
RhF_6^{2-} (R,u'g)	-16.83	13.1	86.2	0.8
IrF_6^{2-} (NR)	-17.01	14.4	84.6	1.0
IrF_6^{2-} (R,e"g)	-16.76	10.9	88.1	1.0
IrF_6^{2-} (R,u'g)	-16.87	11.8	87.2	1.0

Table 11d : Energies and Mulliken population analysis of the open shell t_{2g} (e''_g, u'_g) spinors.

	Energy (eV)	% Me (d)	% F (p)	% F (d)
CoF_6^{2-} (NR)	-21.98	90.9	8.9	0.2
CoF_6^{2-} (R,e"g)	-21.73	91.2	8.6	0.2
CoF_6^{2-} (R,u'g)	-21.86	91.1	8.7	0.2
RhF_6^{2-} (NR)	-15.84	87.2	12.4	0.4
RhF_6^{2-} (R,e"g)	-15.30	88.3	11.2	0.5
RhF_6^{2-} (R,u'g)	-15.57	87.8	11.7	0.4
IrF_6^{2-} (NR)	-13.40	86.0	13.9	0.2
IrF_6^{2-} (R,e"g)	-11.87	89.0	10.6	0.4
IrF_6^{2-} (R,u'g)	-12.69	87.4	12.3	0.3

From the population analysis (table 11) it is clear that the e_g orbitals show more metal-fluorine mixing than the t_{2g} orbitals. This confirms the stronger covalency of the e_g orbitals due to their capacity of forming σ-bonds. The open and closed shell populations are almost complementary which supports the molecular orbital picture that is used in the Ligand Field model. The differences between the different compounds are too small to permit interpretation in terms of changes in covalency.

The differences between the relativistic and the non-relativistic results may be explained by considering the symmetry aspects of the bonding. In the relativistic case there are two representations in which metal-fluorine d-p bonds may be formed. The u'_g representation is spanned twice by the metal d-functions which means that different combinations can be formed depending on the strength of the spin-orbit coupling.

In the case of weak spin-orbit coupling and strong bonding the u'_g spinors will be combined into e_g and t_{2g} spinors and thus into σ and π-bonds as in the non-relativistic case. Alternatively, in the case of a strong spin-orbit coupling at the central atom and weak bonding, the functions will tend to localise and resemble the atomic double group functions. The open shell u'_g spinors will now be combined to form the $d_{3/2}$ and four of the $d_{5/2}$ spinors. The e''_g representation then contains the remaining two $d_{5/2}$ spinors.

In other words: the construction of strong σ-bonds is accompanied by a relativistic hybridisation energy that depends on the spin-orbit splitting of the d-shell. From the spinor energies of table 11 we can see that the first case applies here. The relativistic treatment splits the open shell t_{2g} spinors into two groups but this splitting is much smaller than the t_{2g}-e_g splitting. If we compare this splitting with the splitting within the d-shell in the Me^{4+} ions , we find that the atomic splitting is reduced to 54% in CoF_6^{2-},

52% in RhF_6^{2-} and 54% in IrF_6^{2-}. The figures are close to the value of 60% that is obtained if pure t_{2g} metal d-combinations are formed.

The decrease relative to this theoretical value gives information on the covalency of the compounds. If we use a simple Crystal Field model[23] to incorporate the effect of spin-orbit coupling we find that values of 62, 64 and 68% for Co, Rh and Ir, respectively might be expected. This model is based on the assumption that the open shell orbitals consist of metal d-functions only. In practise the open shell spinors are, however, partly spread out over the fluorines where a much smaller spin-orbit splitting (ζ_{2p} = 0.05 eV) is found. This delocalisation effect counteracts the increase of the percentage of the atomic splitting that would be expected from the increasing strength of the spin-orbit coupling. Since the actual values remain fairly constant one can see that the iridium complex is somewhat more covalent than the cobalt and rhodium complexes.

6.6.6. Configuration Interaction

The spinor sets presented above are used for various types of CI calculations that were described above. In addition we have done some calculations on the specific configurations $t_{2g}^{5-x}e^x$ (x = 0, 1,.., 4). A theoretical value for the crystal field parameter 10Dq was determined by the formula $10Dq = (E(t_{2g}^5) - E(t_{2g}1e_g^4))/4$.

Table 12. Average energies (eV) for the $t_{2g}^{5-x}e^x$ (x = 0, 1,.., 4) configurations, relative to the t_{2g}^5 average energy.

	CoF_6^{2-}		RhF_6^{2-}		IrF_6^{2-}	
	N-Rel.	Rel.	N-Rel.	Rel.	N-Rel.	Rel.
t_{2g}^5	0.00	0.00	0.00	0.00	0.00	0.00
$t_{2g}4e_g^1$	2.05	2.06	2.93	2.96	3.76	3.93
$t_{2g}3e_g^2$	4.64	4.65	6.16	6.21	7.74	8.08
$t_{2g}2e_g^3$	7.77	7.76	9.67	9.75	11.95	12.45
$t_{2g}1e_g^4$	11.44	11.40	13.48	13.57	16.38	17.03
10Dq	2.86	2.85	3.37	3.39	4.10	4.26
10Dq (Experimental)	2.52		2.54		3.04	

The calculated values for 10Dq can be compared with experimental fits and show a rather large discrepancy. This may (partly) be explained by the invalidity of the simple crystal field model in covalent ions. The experimental fit has been done on assignments of states from the lower two configurations, since these are the only states that can be indentified. The other transitions lie at higher energies where the much more intense

charge transfer type excitations occur that obscure the weak (parity forbidden) d-d transitions. Among the observed transitions at low energy there is none that can be written in terms of only 10Dq. One always needs to fit the other ligand field parameters B and C as well. In this fit the ratio between B and C is usually fixed which means that a spectrum that in principle would need 12 parameters (the 10 Griffith parameters, 10Dq and ζ) is fitted with three free parameters. Calculation of B and C from our results gave rather different results depending on the energy-differences that were fitted. In CoF_6^{2-} for instance, the ratio C/B varied from 4.7 to 6.0 while in the experimental fit a value of 4.9 was taken.
In order to calculate the splittings between the individual states one has to account for the configurational mixing within the d-shell. This mixing is included in all (LF, CT, FO) CI calculations that we have done.

In tables 13 a-c the results of these CI calculations are presented. We used the Coulomb operator to represent the two-electron interaction, except in the second series of LFCI (C+G) calculations in which the Coulomb-Gaunt operator was used. The column NR + SO gives the results of a non-relativistic calculation in which the spin-orbit coupling was accounted for in an approximate way. In the other non-relativistic columns we have shifted the energies of the states by ζ_d. This allows for a better comparison with the experimental and relativistic figures where the zero-point of energy is the $^2T_{2g}$ (E''_g) state instead of the weighted average of $^2T_{2g}$ (E''_g) and $^2T_{2g}$ (U'_g).

The energy lowerings and the thereby induced changes in the spectrum that are found upon increasing the level of CI are most prominent for the CoF_6^{2-} complex. A multiconfigurational description is essential here, in order to obtain a correct representation of the lowest states. In IrF_6^{2-} the dominant changes occur if we go from a description without spin-orbit coupling to one were this effect is included. The lowest states can thus be described by a simple LFCI wave function, provided that the spin-orbit coupling is accounted for.

Table 13a. CI results for the lowest states of CoF_6^{2-}. Energies (eV) given relative to the $^2T_{2g}$ (E''_g) state.
Intramultiplet splittings (eV) given in parentheses. Spin-orbit parameter ζ_{3d} = 0.095 eV was used in the perturbative SOCI calculations.

		Non-Relativistic			NR + SO	Relativistic			
State	Exp.[26]	LFCI	CTCI	FOCI	Repr.	SOCI	LFCI(C)	LFCI(C+G)	CTCI	FOCI
$^2T_{2g}$	0	0.10	0.10	0.10	E''_g	0	0	0	0	0
	--				U'_g	0.15 (0.15)	0.14 (0.14)	0.14 (0.14)	0.14 (0.14)	0.14 (0.14)
$^4T_{1g}$	0.79	0.22	0.38	0.46	U'_g	0.32 (0)	0.28 (0)	0.27 (0)	0.41 (0)	0.49 (0)
					E''_g	0.39 (0.07)	0.33 (0.05)	0.31 (0.04)	0.43 (0.02)	0.51 (0.02)
					U'_g	0.38 (0.07)	0.33 (0.05)	0.31 (0.04)	0.43 (0.02)	0.51 (0.02)
					E'_g	0.35 (0.02)	0.31 (0.02)	0.29 (0.02)	0.43 (0.03)	0.52 (0.03)
$^4T_{2g}$	1.28	1.19	1.21	1.27	E'_g	1.26 (0)	1.25 (0)	1.24 (0)	1.22 (0)	1.28 (0)
					U'_g	1.27 (0.00)	1.25 (0.00)	1.24 (0.00)	1.22 (0.00)	1.28 (0.00)
					U'_g	1.31 (0.05)	1.26 (0.01)	1.25 (0.01)	1.24 (0.03)	1.31 (0.03)
					E''_g	1.33 (0.07)	1.26 (0.01)	1.26 (0.01)	1.26 (0.04)	1.32 (0.04)
$^6A_{1g}$	> 0	-1.32	-0.50	-0.32	U'_g	-1.24 (0)	-1.29 (0)	-1.29 (0)	-0.53 (0)	-0.35 (0)
					E''_g	-1.24 (0.00)	-1.29 (0.00)	-1.29 (0.00)	-0.53 (0.00)	-0.35 (0.00)

The absolute energies of the $^2T_{2g}$ (E"g) states in Hartrees are given below to make comparison of results possible. The energies contain a constant (spurious) contribution from the interactions between the point charges of the fitted potentials of appendix 2. Note that the nuclei in the clusters are represented by a gaussian charge distribution with exponent 0.256207E+9 for Co and 0.544946E+9 for F.

	LFCI	SOCI	LFCI (C+G)	CTCI	FOCI
Non-Relativistic	-1992.199236	-1992.206122	--	-1992.255795	-1992.270679
Relativistic	-2003.456999	--	-2002.799990	-2003.509464	-2003.524783

Table 13b. CI results for the lowest states of RhF_6^{2-}. Energies (eV) given relative to the $^2T_{2g}$ (E''_g) state.
Intramultiplet splittings (eV) given in parentheses. Spin-orbit parameter ζ_{4d} = 0.209 eV was used in the perturbative SOCI calculations.

		Non-Relativistic				NR + SO	Relativistic			
State	Exp.[27]	LFCI	CTCI	FOCI	Repr.	SOCI	LFCI(C)	LFCI(C+G)	CTCI	FOCI
$^2T_{2g}$	0	0.21	0.21	0.21	E''_g	0	0	0	0	0
	< 0.5				U'_g	0.34 (0.34)	0.32 (0.32)	0.31 (0.31)	0.31 (0.31)	0.31 (0.31)
$^4T_{1g}$	1.44	1.70	1.81	1.80	U'_g	1.57 (0)	1.58 (0)	1.59 (0)	1.72 (0)	1.71 (0)
					E''_g	1.62 (0.04)	1.62 (0.03)	1.62 (0.03)	1.76 (0.04)	1.74 (0.04)
					U'_g	1.82 (0.24)	1.76 (0.18)	1.75 (0.17)	1.85 (0.13)	1.84 (0.13)
					E'_g	1.87 (0.30)	1.80 (0.22)	1.79 (0.21)	1.89 (0.18)	1.88 (0.17)
$^4T_{2g}$	1.98	2.48	2.51	2.48	E'_g	2.51 (0)	2.48 (0)	2.48 (0)	2.50 (0)	2.46 (0)
					U'_g	2.53 (0.02)	2.50 (0.01)	2.49 (0.01)	2.52 (0.02)	2.48 (0.01)
					U'_g	2.63 (0.12)	2.53 (0.05)	2.52 (0.05)	2.57 (0.07)	2.53 (0.06)
					E''_g	2.66 (0.15)	2.54 (0.06)	2.53 (0.06)	2.58 (0.08)	2.55 (0.08)
$^6A_{1g}$		1.98	2.39	2.39	U'_g	2.23 (0)	2.12 (0)	2.10 (0)	2.43 (0)	2.43 (0)
					E''_g	2.25 (0.02)	2.13 (0.01)	2.11 (0.01)	2.44 (0.01)	2.44 (0.01)

The absolute energies of the $^2T_{2g}$ (E"g) states in Hartrees are given below to make comparison of results possible. The energies contain a constant (spurious) contribution from the interactions between the point charges of the fitted potentials of appendix 2. Note that the nuclei in the clusters are represented by a gaussian charge distribution with exponent 0.176688E+9 for Rh and 0.544946 E+9 for F.

	LFCI	SOCI	LFCI (C+G)	CTCI	FOCI
Non-Relativistic	-5296.886858	-5296.897584	--	-5296.920006	-5296.923705
Relativistic	-5394.294470	--	-5390.801552	-5394.323816	-5394.327505

Table 13c. CI results for the lowest states of IrF_6^{2-}. Energies (eV) given relative to the $^2T_{2g}$ (E''_g) state.
Intramultiplet splittings (eV) given in parentheses. Spin-orbit parameter ζ_{5d} = 0.603 eV was used in the perturbative SOCI calculations.

		Non-Relativistic			NR + SO	Relativistic				
State	Exp.[28, 29]	LFCI	CTCI	FOCI	Repr.	SOCI	LFCI(C)	LFCI(C+G)	CTCI	FOCI
$^2T_{2g}$	0.00	0.60	0.60	0.60	E''_g	0	0	0	0	0
	0.82				U'_g	0.96 (0.96)	0.93 (0.93)	0.91 (0.91)	0.91 (0.91)	0.91 (0.91)
$^4T_{1g}$	2.45	2.99	3.06	3.05	U'_g	2.84 (0)	2.71 (0)	2.72 (0)	2.77 (0)	2.76 (0)
					E''_g	3.07 (0.23)	2.98 (0.27)	2.97 (0.26)	3.03 (0.27)	3.03 (0.26)
					U'_g	3.39 (0.55)	3.19 (0.48)	3.18 (0.46)	3.22 (0.46)	3.21 (0.46)
					E'_g	3.56 (0.72)	3.34 (0.63)	3.32 (0.61)	3.37 (0.60)	3.36 (0.60)
$^4T_{2g}$	3.09	3.74	3.77	3.74	E'_g	4.02 (0)	3.83 (0)	3.82 (0)	3.82 (0)	3.79 (0)
					U'_g	4.09 (0.07)	3.85 (0.02)	3.84 (0.02)	3.86 (0.04)	3.83 (0.04)
					E''_g	4.38 (0.36)	3.89 (0.06)	3.88 (0.06)	3.91 (0.09)	3.89 (0.10)
					U'_g	4.41 (0.39)	3.92 (0.08)	3.90 (0.08)	3.92 (0.10)	3.90 (0.11)
$^6A_{1g}$		4.19	4.21	4.20	U'_g	5.05 (0)	4.65 (0)	4.63 (0)		
					E''_g	5.05 (-0.01)	4.67 (0.03)	4.65 (0.02)		

The absolute energies of the $^2T_{2g}$ (E"g) states in Hartrees are given below to make comparison of results possible. The energies contain a constant (spurious) contribution from the interactions between the point charges of the fitted potentials of appendix 2. Note that the nuclei in the clusters are represented by a gaussian charge distribution with exponent 0.116194E+9 for Ir and 0.544946 E+9 for F.

	LFCI	SOCI	LFCI (C+G)	CTCI	FOCI
Non-Relativistic	-17416.517161	-17416.553167	--	-17416.539945	-17416.544430
Relativistic	-18456.812764	--	-18434.619602	-18456.829331	-18456.833325

The calculated states of all three compounds can be described within an L-S coupling scheme. The spin-orbit splitting of the lowest doublet and quartet states in IrF_6^{2-} is considerable but remains smaller than the inter-multiplet distances. The relativistic treatment lowers the doublet state relative to the quartet and sextet states. This is caused by interaction between the e_g and the t_{2g} (u'_g) spinors. The spin-orbit coupling pushes these two levels apart and thus lowers the energy of the t_{2g}^5 configuration relative to the $t_{2g}^{5-x}e_g^x$ ($x \neq 0$) configurations.

The latter effect can also be modelled with a perturbative Ligand Field model for the spin-orbit coupling. In this model we assume that the spin-orbit coupling matrix elements between the $^2T_{2g}$, $^4T_{1g}$, $^4T_{2g}$ and $^6A_{1g}$ can be expressed in terms of the atomic spin-orbit parameter ζ_d. This spin-orbit parameter is obtained from a relativistical calculation on Me^{4+} by the relation $\zeta_d = 0.4\ (\varepsilon(d_{3/2}) - \varepsilon(d_{5/2}))$ with ε the Dirac-Fock spinor energy. We add this spin-orbit coupling matrix[24] to the diagonal matrix given by the LFCI energies of these states and rediagonalise. The results show good agreement with our relativistic LFCI results of CoF_6^{2-} and RhF_6^{2-}. The influence of the spin-orbit coupling is overestimated, because covalency effects were neglected in this model. In this simple model we furthermore neglected interaction with other d^5 states which may also decrease the spin-orbit splitting of the higher multiplets.

The effect of the inclusion of the Gaunt operator in the hamiltonian was studied perturbation wise at the LFCI level. We used the set of spinors that were determined at the Dirac-Coulomb level and thus neglected the effect of the Gaunt operator on the form of the spinors. The influence on the calculated splittings is small, giving as most significant result a decrease of the IrF_6^{2-} $^2T_{2g}$ spin-orbit splitting of 0.025 eV

6.7. Discussion

Experimentally all compounds are found to have a $^2T_{2g}$ low-spin ground state. Our calculations confirm this assignment except for CoF_6^2, where the $^6A_{1g}$ state is found to be the lowest state. This discrepancy with experiment is probably due to the neglect of dynamical electron correlation that also lead to the discrepancies with experiment in the atomic calculations. The sextet state is described significantly better at the Hartree-Fock-LFCI level than the doublet or quartet states, because the Pauli correlation is incorporated whereas the Coulomb correlation is not, at this level of theory[13]. Miyoshi et al.[25] have published non-relativistic calculations on this system that support this assumption. In their LFCI calculations they find the $^6A_{1g}$ state lowest at 0.91 eV below the $^2T_{2g}$ state. When they incorporate a semi-empirical correction for the atomic

correlation energies, employing the method of Pueyo and Richardson[26], they find the $^6A_{1g}$ state 0.12 eV above the $^2T_{2g}$ state.

An additional source of errors in the CoF_6^{2-} calculations is the uncertainty of 0.05 Å in the used experimental bondlength. Variation of the bondlength with 0.02 Å gives rise to variations in the calculated intermultiplet splittings of the order of 0.2 to 0.3 eV.

For the Rh and Ir fluorides we can not give an estimate of dynamical correlation effects on basis of atomic results because no experimental spectra of Rh^{4+} and Ir^{4+} are available. It is, however, likely that dynamical correlation effects will also influence the spectrum of these compounds.

6.8. Conclusions

The excitation energies of the cobalt (IV), rhodium (IV) and iridium (IV) hexafluorides can be fairly well described by First Order CI. The electron-electron interaction dominates the spin-orbit coupling for all complexes, so the calculated states can be interpreted as (spin-orbit split) LS-coupled multiplets.

Calculated intermultiplet energy differences agree with experimental data to about 0.4 eV in CoF_6^{2-} and to about 0.8 eV in IrF_6^{2-}. For these energy differences, static correlation effects that arise from low-lying charge transfer states are found to be most important in CoF_6^{2-}, while spin-orbit effects dominate in IrF_6^{2-}. The discrepancies with experiment can be explained by the influence of differential dynamic electron correlation effects that are largely neglected at the level of theory that we use here.

The intramultiplet spin-orbit splittings are not much influenced by correlation corrections. These splittings can be calculated to good accuracy in a Ligand Field CI calculation. Use of a perturbative model to calculate the spin-orbit coupling is also possible in these d^5 ions and gives good results for the CoF_6^{2-} and RhF_6^{2-} ions, but overestimates the splittings in the quartets of IrF_6^{2-}.

6.9. Appendix 1 : Basis sets

Table A1.1. Exponents of the primitive gaussian functions.

Cobalt		Rhodium		Iridium		Fluorine	
s	1084972.40	s	2731601.66	s	26668729.1	s	18648.5
s	162536.244	s	408859.481	s	3655468.76	s	2790.77
s	36991.6658	s	93307.3527	s	799486.001	s	633.258
s	10477.4164	s	26379.9304	s	223307.569	s	178.599
s	3418.40523	s	8563.26613	s	72755.3847	s	57.7896
s	1234.48863	s	3069.80285	s	26195.5709	s	20.4555
s	481.364201	s	1177.65743	s	10153.5021	s	7.58796
s	198.728746	s	472.694052	s	4066.33469	s	1.99213
s	20.7965155	sd	195.613241	sd	1660.71803	s	0.749854
s	0.145	sd	83.0173165	sd	695.762587	s	0.241845
sd	84.1211960	sd	35.8644033	sd	300.316974	p	63.1253
sd	25.1128635	sd	15.7285857	sd	131.207017	p	14.5012
sd	9.18340049	sd	6.92795231	sd	59.8738317	p	4.38233
sd	3.70926232	sd	3.01827958	sd	28.3242236	p	1.45355
sd	1.49235456	sd	1.19601332	sd	13.0883983	p	0.463237
sd	0.56778468	sd	0.44353579	sd	5.96839221	p	0.126578
sd	0.36051148	sd	0.18032814	sd	2.62206777	d	0.241845
p	2344.78030	sd	0.073	sd	1.06750738		
p	555.647128	p	54250.6937	sd	0.4219794		
p	178.863068	p	12847.3483	sd	0.13458954		
p	67.1082327	p	3042.43775	sd	0.0429		
p	27.3476842	p	986.433555	p	630825.605		
p	11.6614996	p	375.207531	p	150637.678		
p	4.77240079	p	157.689216	p	35971.4473		
p	1.99067313	p	70.4823506	p	8589.78338		
pf	0.79864849	p	32.7196868	p	2791.38561		
p	0.32	p	14.6128764	p	1066.37478		
		p	6.75523649	p	446.084374		
		p	3.06574636	pf	161.628290		
		p	1.34905790	pf	58.0553565		
		pf	0.56425188	pf	25.2728514		
		p	0.236	pf	11.3439089		
				pf	4.89293799		
				pf	1.85277206		
				pf	0.78292625		
				p	0.27559172		

6.10. Appendix 2 : Fitted Madelung potentials

Table A2.1. Potential of the Cs_2CoF_6 lattice.

Atom	Position in lattice coordinates	Number of equivalent positions	Formal Charge	Fit Charge	Distance to central Co (Å)
Co	(0.00, 0.00, 0.00)	1	4+	In cluster	0.0
F	(0.20, 0.00, 0.00)	6	1-	In cluster	1.73
Cs	(0.25, 0.25, 0.25)	8	1+	0.9811	3.86
F	(0.50, 0.30, 0.00)	24	1-	-0.7679	5.22
Co	(0.50, 0.50, 0.00)	12	4+	1.9598	6.30
F	(0.80, 0.00, 0.00)	24	1-	1.1527	7.18
Cs	(0.75, 0.25, 0.25)	24	1+	-0.7872	7.39

Table A2.2. Potential of the Cs_2GeF_6 lattice.

Atom	Position in lattice coordinates	Number of equivalent positions	Formal Charge	Fit Charge	Distance to central Ge (Å)
Ge (Rh, Ir)	(0.00, 0.00, 0.00)	1	4+	In cluster	0.0
F	(0.20, 0.00, 0.00)	6	1-	In cluster	
Cs	(0.25, 0.25, 0.25)	8	1+	0.9811	3.91
F	(0.50, 0.30, 0.00)	24	1-	-0.7718	5.26
Ge	(0.50, 0.50, 0.00)	12	4+	2.0358	6.38
F	(0.80, 0.00, 0.00)	24	1-	1.1269	7.22
Cs	(0.75, 0.25, 0.25)	24	1+	-0.8195	7.48

Table A2.3. Accuracy (V) of the point charge fits of the Madelung potential.

Crystal	maximum error	average error
Cs_2CoF_6	0.0025	0.00004
Cs_2GeF_6	0.0024	0.00004

References

1) O. Visser, L. Visscher, P.J.C. Aerts and W. C. Nieuwpoort, Theoretica Chimica Acta **81**, 405 (1992).

2) O. Visser, L. Visscher, P. J. C. Aerts and W. C. Nieuwpoort, J. Chem. Phys. **96**, 2910 (1992).

3) Chapter 5.

4) J. Olsen, B. O. Roos, P. Jørgensen and H. J. Aa. Jensen, J. Chem. Phys. **89**, 2185 (1988).

5) ASCF: Atomic Self Consistent Field code, developed by the theoretical chemistry group in Groningen.

6) L. Visscher, P.J.C. Aerts and O. Visser, in : "The Effects of Relativity in Atoms, Molecules and the Solid State ", ed. S. Wilson, I. P. Grant and B. Gyorffy, (Plenum: New York, 1991).

7) A. J. H. Wachters, Ph. D. Thesis, Rijks Universiteit Groningen 1971.

8) K.G Dyall, I. P. Grant, C. T. Johnson, E. P. Plummer and F. Parpia, Computer Phys. Commun. **50**, 375 (1998).

9) J. Sugar and C. Corliss, J. Phys. Chem. Ref. Data **101**, 1097 (1981).

10) C. E. Moore, Circular of the National Bureau of Standards **467**, 181 (1958).

11) E. U. Condon and G. H. Shortley, The Theory of Atomic Spectra, (Cambridge 1953).

12) J. S. Griffith, The Theory of transition metal ions, (Cambridge University Press: London, 1971).

13) L. G. Vanquickenborne, M. Henderickx, D. Postelmans, I. Hyla-Krispin and K. Pierloot , Inorg. Chem. **27**, 900 (1988).

14) G. C. Allen and K. D. Warren, Inorganic Chemistry **8**, 1902 (1969).

15) G. C. Allen, G. A. M. El-Sharkawy and K. D. Warren, Inorganic Chemistry **10**, 2231 (1973).

16) G. C. Allen, R. Al-Mobarak, G. A. M. El-Sharkawy and K. D. Warren, Inorganic Chemistry **11**, 787 (1972).

17) L. C. Weiss, P. J. McCarthy, J. P. Jainski and P. N. Schatz, Inorganic Chemistry **17**, 2689 (1978).

18) J. W. Quail and G. A. Rivett, Can. Journal of Chem. **50**, 2447 (1972).

19) A. K. Brisdon, J. Holloway, E. G. Hope, W. Levason, J. S. Ogden and A. K. Saad, J. Chem. Soc. Dalton Trans., 447, 1992.

20) A. K. Brisdon, J. Holloway, E. G. Hope, W. Levason, J. S. Ogden and A. K. Saad, J. Chem. Soc. Dalton Trans., 139, 1992

21) E. Miyoshi, H. Kashiwagi, Int. J. of Quantum Chemistry **24**, 85 (1983).

22) R. Mulliken, J. Chem. Phys. **23**, 1833 (1955).

23) See C. J. Ballhausen, "Introduction to Ligand Field Theory" , (McGraw-Hill, New York : 1962), page 118-119.

24) See reference 12, page 421.

25) E. Miyoshi, T. Takada, S. Obara, H. Kashiwagi and K. Ohno, Int. J. of Quantum Chem. **19**, 451 (1981).

26) L. Pueyo and J. W. Richardson, J. Chem. Phys. **67**, 3577 (1977).

7. Summary and conclusions

7.1. Summary

In this thesis we describe a method for relativistic quantum mechanical calculations on molecules. We obtain relativistic zero order wave functions by the use of the Dirac-Fock method and improve these by relativistic Configuration Interaction. This opens the way for an accurate *ab initio* treatment of both relativity and electron correlation in molecules or clusters that contain one or more heavy nuclei.

In the first chapters we describe the fundamental physical background of the method that is based on the Dirac-Coulomb-(Gaunt) equation. Use of variational methods to obtain the eigenvalues and eigenfunctions that correspond to the lowest electron states is possible, even though the hamiltonian is unbound from below. Collapse into "spurious" or positronlike states of lower energy is on the effective one-electron Dirac-Fock level prevented by the use of kinetic or atomic balance. Use of the no-pair approximation avoids problems with lower-lying states in the many-electron CI-calculations.

The implementation of the method (MOLFDIR) is described in chapter 3. This set of computer programs enables a thorough study of the properties of small molecules. Its performance is dominated by the large numbers of two-electron integrals that arise from the use of four-spinor one-electron functions. The range of possible applications of the Dirac-Fock part is mainly determined by the total number of electrons that need to be included in the calculation. The feasibility of CI calculations depends on the number of active valence spinors and electrons. The limitations of both methods are of a technical nature, we did not encounter any fundamental problems with the use of the Dirac-Coulomb-Gaunt hamiltonian.

In chapter 5 we describe the PtH molecule. If ω-ω coupling is used (Hunds case c), the bonding in this molecule can be clearly understood in a simple single configurational model. Attempts to describe the bond in a non-relativistic Λ-Σ coupling formalism (Hunds case a) give rise to large mixings between the states. Due to the atomic nature of the spin-orbit splitting, such approaches may, however, give good results provided that the spin-orbit parameter that is used in a perturbation treatment is chosen carefully. Accurate calculation of the bond length of this molecule requires a good treatment of both relativity and electron correlation. Neglect or approximate treatment of either one of them may give errors in the order of 0.05 Å. Excitation energies are less sensitive to electron correlation but are strongly influenced by the spin-orbit coupling.

In chapter 6 we study the influence of relativity and electron correlation on the d-d spectrum of CoF_6^{2-}, RhF_6^{2-} and IrF_6^{2-}. The first peaks in the electronic spectrum of these ions arise from interconfigurational transitions from the $t_{2g}^5\ ^2T_{2g}$ ground state to the $t_{2g}^4e_g^1\ ^4T_{1g}$ and $^4T_{2g}$ states. The effect of relativity is largest for the IrF_6^{2-} where the ground state is split by an amount of 0.91 eV. The calculated spin-orbit splittings do not vary much with the level of CI that is used and agree well with experiment. In all ions the LS-coupling scheme may still be used to assign the states since the intermultiplet splittings are larger than the intramultiplet spin-orbit splittings. The inclusion of charge transfer configurations in the wave functions lowers the $^2T_{2g}$ ground state relative to the excited states. These charge transfer states are most important in CoF_6^{2-} , where a multiconfigurational description is essential for the calculation of the excitation energies.

7.2. Conclusions

Relativity and electron correlation can now be treated on an equal footing using the method and computer programs that are presented in this thesis. Both are found to be important in the description of heavy transition metal complexes.

In addition to the use of a relativistic one-electron operator, relativistic corrections to the Coulomb two-electron interaction operator may be included. The influence of the largest of such corrections, the magnetic Gaunt interaction, is found to be insignificant for most molecular properties calculated.

The present implementation of the method is suitable for benchmark calculations on relatively small molecules of general shape. Although the computational requirements are still large, calculations may be done in a routine fashion. The modular set-up of the computer program allows for an easy incorporation of new methods and (technical) improvements of the existing algorithms.

In the transition metal compounds that were treated in this thesis, the most important manifestation of relativity found is the large spin-orbit coupling in the 5d shell. The thereby induced splittings in the electronic spectra are well described in both the Dirac-Fock and the Dirac-Fock-CI method.

7.3. Suggestions for further research

The discussions in this thesis have focused on energy differences between electronic states and on energy dependent quantities like bond lengths and harmonic frequencies. The wave functions that are obtained from the calculations may, however, also be used for calculation of electronic properties like dipole moments and transition probabilities. This asks for the derivation of operators that can be used in a

relativistic formalism and for the implementation of new algorithms to perform the actual calculations.

Besides the use of direct Configuration Interaction one can apply most of the other accurate methods that were developed to solve the Schrödinger equation to the Dirac equation. The development of relativistic versions of methods like the Coupled Cluster method, the Multi Configurational Self Consistent Field method and the Density Functional method can give computer programs that are as accurate for calculations on heavy elements as the present ab initio programs are for the lighter atoms. The new relativistic algorithms may use Kramers' symmetry in order to reach the same computational reductions as are obtained by the separation of spin and space coordinates that is possible in the non-relativistic calculations.

Apart from these further technical developments, more research on the relativistic corrections to the Coulomb interaction is desirable. The effect of the Gaunt interaction can be studied more extensively than is done in this thesis and the effect of the Breit retardation term and of other quantum electrodynamical corrections on molecular properties should be investigated.

Samenvatting

Chemie is een molekulaire wetenschap. Kennis van de molekulaire struktuur van een stof wordt gebruikt om haar chemische reakties en eigenschappen te verklaren. Deze struktuur wordt meestal weergegeven met behulp van de atoomsymbolen, verbonden door streepjes die de chemische bindingen aangeven. Hierbij gelden regels zoals de bekende oktetregel: een atoom wordt altijd omgeven door 4 streepjes. Op deze wijze kunnen de meeste (organische) molekulen goed worden weergegeven en geklassificeerd in klassen (carbonzuren, alcoholen, aromaten , etc.) die op gelijksoortige wijze reageren.
Voor een grondiger begrip van chemische reakties, waarbij men de verschillen in reaktiesnelheid tussen molekulen uit eenzelfde klasse wil verklaren of het mechanisme van de reaktie wil begrijpen is dit model te simpel. Uitbreiding kan enerzijds gebeuren door extra regels in te voeren op basis van experimentele informatie. Anderszijds is het mogelijk om een stapje verder te gaan in de ontleding van de stof tot steeds kleinere deeltjes. We beschouwen dan een atoom als een verzameling elektronen die in banen rond de atoomkern bewegen. Chemische bindingen komen tot stand door de vorming van molekulaire banen waarin elektronenparen gedeeld worden door verschillende atomen. Door te berekenen voor welke samenstelling van atomen de elektronen de meest gunstige (laagst energetische) banen bezetten is het mogelijk om de molekuulstruktuur en reaktiemechanismen te begrijpen.
Anders dan de beweging van planeten rond de zon, kunnen elektronenbanen niet worden beschreven met behulp van klassieke (Newtoniaanse) mechanica. De elektronen zijn dusdanig klein en licht dat ze niet alleen als deeltje zijn te beschouwen maar ook golfverschijnselen vertonen. Een ander belangrijk verschijnsel is de quantisatie van energieniveaus: slechts bepaalde energieën zijn toegestaan zodat slechts een beperkt aantal banen rond een atoom mogelijk is.
Dit gedrag wordt beschreven door de quantum mechanica. Door het oplossen van de quantummechanische Schrödinger vergelijking kunnen elektronen golffunkties en daarbij horende energiewaarden worden gevonden. Deze golffunkties bevatten alle informatie over de beweging en distributie van de elektronen in een molekuul zodat molekulaire eigenschappen als bijvoorbeeld het dipoolmoment kunnen worden bepaald. Door de energieën van begin- en eindprodukten uit te rekenen kunnen reaktie-energieën worden berekend. Om golffunkties en energieën te berekenen kan men experimentele informatie als atomaire ionisatiepotentialen en electronaffiniteiten in de berekeningen verwerken. Deze semi-empirische aanpak wordt meestal gecombineerd met een vereenvoudigde

voorstelling van de Schrödinger vergelijking en golffunktie zodat de berekeningen relatief eenvoudig blijven. Nadelen van deze methode zijn dat door het werken met een vereenvoudigde vergelijking belangrijke effekten over het hoofd kunnen worden gezien en dat voldoende accurate experimentele gegevens beschikbaar moeten zijn.

Dit laatste nadeel is niet aanwezig in een zogenaamde *ab initio* aanpak. Hierbij wordt getracht zo weinig mogelijk experimentele informatie in de berekeningen te verwerken. De enige experimentele informatie die in deze aanpak noodzakelijk is betreft fundamentele fysische konstanten zoals de massa en lading van elektronen en protonen en de konstante van Planck. Berekeningen worden zo een numeriek experiment dat onafhankelijk is van de beschikbaarheid en nauwkeurigheid van experimentele gegevens. Dit maakt het mogelijk om bijvoorbeeld nog niet gesynthetiseerde verbindingen te onderzoeken. Een nadeel van de aanpak is het grote aantal variabelen (de posities van alle elektronen in de driedimensionale ruimte) dat voor komt in een molekulaire Schrödingervergelijking. Door de electromagnetische wisselwerking tussen de elektronen wordt de beweging van een elektron beïnvloed door de beweging van de hem omringende elektronen: de elektronenbeweging is gecorreleerd. Hierdoor dient de beweging van alle elektronen gelijktijdig te worden beschouwd. Mathematisch gezien blijkt dit uit de onmogelijkheid om de molekulaire Schrödingervergelijking te reduceren tot een stelsel van 1-electron vergelijkingen. Dit maakt het onmogelijk om langs analytische weg of via standaard numerieke integratie technieken de golffunktie te bepalen.

Een andere weg moet dus worden gekozen als men in een *ab initio* aanpak tot zo goed mogelijk benaderde oplossingen wil komen. Meestal wordt hierbij begonnen met de zogenaamde Hartree-Fock methode waarbij een eenvoudige vorm voor de golffunktie wordt gekozen. Fysisch gezien wordt door deze keuze de expliciete elektron-elektron interaktie vervangen door een gemiddeld elektrisch veld, waarin de elektronen onafhankelijk van elkaar bewegen. De golffunkties die in deze benadering worden verkregen dienen als basis voor meer geavanceerde methoden die het gebrek aan correlatie in elektronen beweging compenseren. Een voorbeeld van zo'n methode is de Configuratie Interaktie (CI) methode die in dit proefschrift wordt beschreven. Hoewel deze "gecorreleerde" methoden in het algemeen zeer rekenintensief zijn is het tegenwoordig mogelijk om berekeningen uit te voeren en quantitatief korrekte resultaten te bereiken voor niet al te grote molekulen.

Als men *ab initio* berekeningen wil doen voor molekulen die "zware" atomen bevatten, d.w.z. atomen met hoge kernlading zoals bijvoorbeeld platina, goud of uranium, dienen zich nieuwe problemen aan. De elektronen krijgen in het sterke elektrische veld van de kern een snelheid die in de buurt komt van de lichtsnelheid (300000000 m/s). Dit zorgt

voor zogenaamde relativistische korrekties op de beweging die de golffunktie en energie van de elektronen belangrijk veranderen. Om dit in rekening te brengen dient men een vergelijking te nemen die zowel voldoet aan de eisen der quantum mechanica als aan de eisen van de (speciale) relativiteitstheorie. Zo'n vergelijking is de in 1928 geponeerde Dirac vergelijking. Behalve dat deze op natuurlijke wijze het voorkomen van het intrinsieke magnetische moment van het elektron, de spin, bleek te beschrijven, voorspelde zij ook het bestaan van het anti-elektron : het positron. Het bestaan van deze anti-deeljes maakt het vinden van de laagst energetische elektronen golffunkties lastiger daar ook positron golffunkties oplossingen zijn van de Dirac vergelijking. Een andere complicatie is het feit dat deeltjesbehoud niet is gegarandeerd omdat een positron-elektron paar kan worden gecreëerd onder toevoeging van een energie van $2mc^2$ (m: massa van het elektron of positron, c: de lichtsnelheid). In de chemie is dit laatste verschijnsel echter van geen belang omdat chemische reaktie energieën in de orde van enkele electronvolts liggen, hetgeen een miljoen maal kleiner is dan de paarcreatie energie.

Met deze punten in het achterhoofd kan men nu de Diracvergelijking nemen als basis voor relativistische *ab initio* berekeningen. De golffunkties en energieën die gevonden worden kunnen op dezelfde wijze worden gebruikt voor het bepalen van molekulaire eigenschappen en spectra als de golffunkties en energieën die gevonden worden op basis van de Schrödinger vergelijking. Om benaderde oplossingen te vinden worden methodes gebruikt die analoog zijn aan de methodes die worden toegepast in niet-relativistische *ab initio* aanpakken. De rekentijd die nodig is om zulke oplossingen te vinden is echter een orde groter (minimaal 16 maal) dan in de conventionele, niet relativistische aanpak. Dit heeft lange tijd verhinderd dat een volledig relativistisch formalisme werd toegepast om golffunkties te berekenen.

Veelal worden uitgaande van de Dirac vergelijking korrekties op de Schrödinger vergelijking afgeleid, die dan kunnen worden gebruikt in een verder niet relativistisch model. Het voordeel daarvan is dat conventionele algoritmen en computer programmatuur kunnen worden gebruikt, een nadeel is dat de invloed van relativiteit slechts gedeeltelijk wordt meegenomen. Het is daarom zinvol om de uitkomsten van deze quasi-relativistische berekeningen te toetsen aan de resultaten van berekeningen in een volledig relativistisch formalisme. Immers, pas als voor een klein maar representatief testmolekuul beide typen berekeningen goede overeenstemming vertonen kunnen met enig vertrouwen de benaderde, goedkopere, methoden worden gebruikt voor grotere molekulen. Dit type calibratie berekeningen in een relativistisch formalisme was door de benodigde rekeninspanning tot voor kort slechts mogelijk voor atomen. De komst van

krachtige supercomputers in de laatste tien jaar maakt het nu echter in principe ook mogelijk om molekulaire berekeningen te doen. De hiertoe benodigde algoritmen en computerprogrammatuur zijn nog volop in ontwikkeling, maar op dit moment worden al op enkele plaatsen in de wereld volledig relativistische berekeningen aan chemisch interessante systemen gedaan.

In dit proefschrift wordt de zgn. Dirac-Fock-CI methode beschreven die het relativistische analogon is van de bekende niet-relativistische Hartree-Fock-CI techniek. De Dirac-Fock methode berust op een vereenvoudiging van de veel-deeltjes golffunktie tot een antisymmetrisch produkt (determinant) van één-deeltjes funkties. Deze golffunktie wordt later verfijnd door configuratie interaktie (CI) met andere determinanten, zodat de correlatie tussen de elektronenbeweging in rekening wordt gebracht.

In hoofdstukken 1 en 2 worden de achtergronden van het onderzoek en de gebruikte vergelijkingen beschreven. In hoofstuk 3 volgt een gedetailleerde beschrijving van het in Groningen ontwikkelde MOLFDIR programma pakket, dat als eerste pakket ter wereld de mogelijkheid biedt om molekulaire Dirac-Fock-CI berekeningen uit te voeren.

Om ingewikkelde golffunkties te beschrijven expandeert men deze vaak in een set van eenvoudige exponentiële funkties, de zogenaamde basis set. Hoofdstuk 4 behandelt de kinetische en atomaire balans procedure die noodzakelijk is om deze basis set expansie techniek op een betrouwbare wijze te kunnen toepassen in een vergelijking die zowel elektronen als positronen beschrijft.

In hoofdstuk 5 wordt het molekuul platinahydride behandeld. Dit simple twee-atomige molekuul is het eenvoudigst denkbare model voor de binding van waterstof aan platina oppervlakken. Aangezien een goed begrip van deze binding belangrijk is om de katalytische eigenschappen van platina te begrijpen, is veel onderzoek verricht aan dit molekuul. De Dirac-Fock-CI berekeningen zijn in goede overeenstemming met experimentele data en blijken bij uitstek geschikt om de de kwaliteit van de meer benaderende (goedkopere) berekeningen te bepalen.

In hoodstuk 6 worden berekeningen aan een groep van drie overgangsmetaal fluoriden gepresenteerd. Door drie systemen met dezelfde valentie elektronenconfiguratie, maar met een verschillend centraal ion te nemen, is het belang van relativistische en elektronencorrelatie effekten in verschillende rijen van het periodiek systeem bestudeerd en vergeleken.

Een algemene conclusie is dat vooral de zogenaamde spinbaankoppelingseffekten goed worden beschreven met de in dit proefschrift beschreven aanpak. Voor de systemen die hier behandeld zijn blijken electronencorrelatie en relativistische effekten elkaar weinig te beïnvloeden.

Appendix. Evaluation of CI coupling constants

The coupling constants $\gamma_{ij}^{IJ} = \langle I \mid E_{ij} \mid J \rangle$ that were introduced in equation 37 of chapter 3, may be calculated using the graphical representation of the CI space[1]. A description of the method for non-symmetry adapted graphs will be given first, after which the evaluation of coupling constants in symmetry adapted CI spaces is considered. Finally the separation of external space[2] in CI-SD calculations is discussed.

A.1. Coupling coefficients in non-symmetry adapted graphs

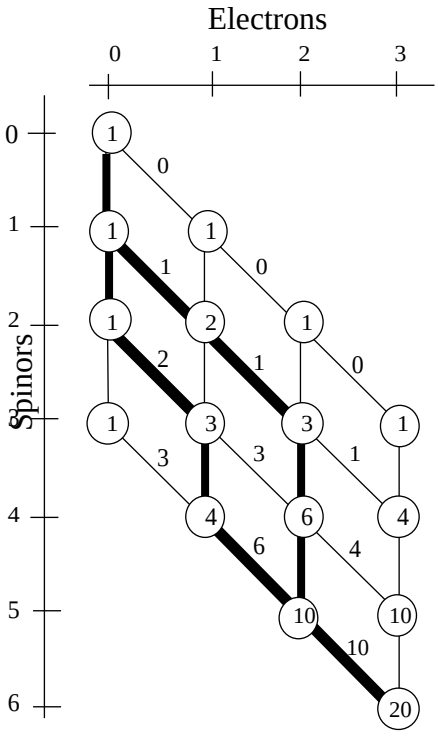

Non-zero one-electron coupling coefficients connect two determinants that differ by at most one spinor. In the graphical representation of the CI space this difference in spinor occupation looks like a loop in the graph. Figure 1 gives an example of such a loop in the (6 spinor, 3 electron) Full CI space that was given in figure 1 of chapter 2.

Figure 1. Loop formed by the determinants |236| and |356| in a (6 spinor, 3 electron) space.

We can subdivide the figure, that is indicated by two different paths, into three parts. A head part in which both paths overlap, the loop part where the paths separate, run parallel and finally meet again, and a tail part in which the paths again overlap. The value of the coupling coefficients is solely determined (Slater's rule) by the number of simultaneously occupied spinors (n_{Loop}) in the loop part of the diagram

$$\gamma_{ij}^{IJ} = (-1)^{n_{Loop}} \qquad (1)$$

In the example that is given in figure 1, this number is 1 since we have one set of diagonal arcs: $(2,0) \rightarrow (3,1)$ and $(2,1) \rightarrow (3,2)$. The value of the coupling coefficient is therefore $(-1)^1 = -1$· From inspection of the diagram one may also find the values for i,

j, I and J for this loop. I and J are the sums of arc weights of the paths, i and j are the arcs where the paths separate and reunite again. In the example we obtain I=13, J=19, i=2 and j=5, or I=19, J=13, i=5 and j=2, depending on whether we take the upper part of the loop as belonging to I or the lower part, respectively.

The information contained in the diagram is used in the calculation of the sigma vector (chapter 3, formula 47). In the example we find for instance that the one-electron integral g_{25} has to be multiplied with CI coefficient 19 to contribute to sigma vector element 13.

Using the diagrams to evaluate the coupling coefficients individually is, however, not very efficient. The great strength of the method is the possibility of simultaneous evaluation of large groups of coupling coefficients.

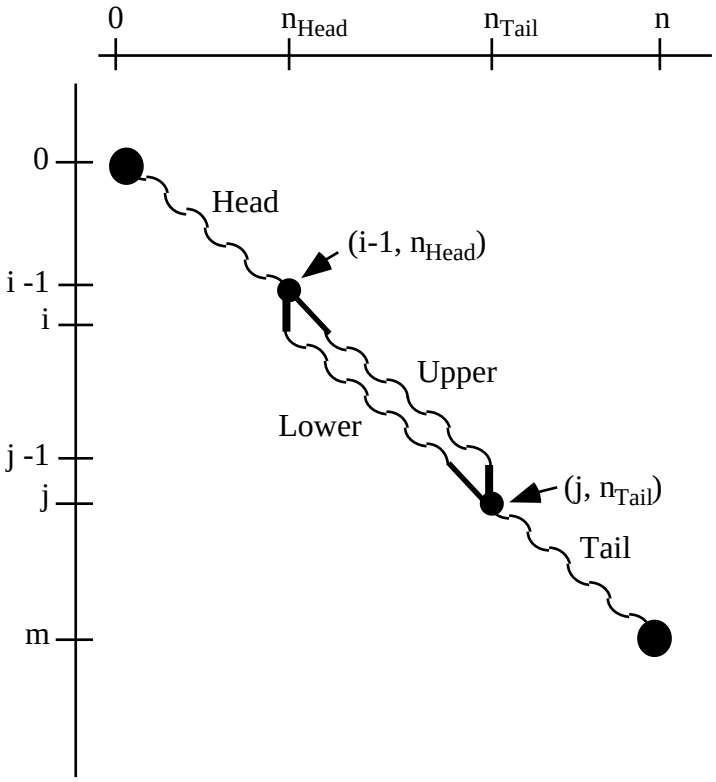

Figure 2. Representation of loops in a graph.

We can write pairs that are connected by coupling coefficients with the same value of i and j, schematically as indicated in figure 2.

The wiggly lines stand for all possible paths that may connect the begin and end vertex of the line. This means that given a certain combination of i and j we may calculate the whole range of values of I and J for which γ_{ij}^{IJ} is non-zero simultaneously. If we take i < j then the indices I and J are given by $1 + Y_{Head} + Y_{Tail} + Y_{Upper}$ and $1 + Y_{Head} + Y_{Tail} + Y_{Lower}$, respectively. The value of the coupling coefficient is easily calculated as the difference between the number of electrons as $(-1)^{n_{Loop}}$, with $n_{Loop} = n_{Tail} - n_{Head} - 1$.

To get all coupling coefficients we now have to vary n_{Head} and n_{Tail} such that all possible combinations of vertices (i-1, n_{Head}) and (j, n-n_{Tail}) are considered. This results in a list of values for γ_{ij}^{IJ} and addresses (indices) I and J that can be used directly in the CI code.

To make the amount of data that has to be handled as small as possible the factorisation of the addresses into three parts that was described above is used. For each ij combination one needs a list of possible vertex pairs {(i-1, n_{Head})-(j, n_{Tail})} and the sign of the coupling coefficient for this vertex pair. For each vertex pair one than has a list of combinations {Y_{Lower}, Y_{upper}} and a list of contributions {Y_{Tail}}. It is easily verified that the contributions to the index coming from Y_{Head} are numbered consecutively from 0 to W(i-1, n_{Head})-1, so this range can be represented by a single number.

To illustrate the procedure we take the calculation of the non-zero coupling coefficients with i=2 and j=5 for the diagram given in figure 1. We see that the vertex combinations (1,0)-(5,2), (1,0)-(5,3), (1,1)-(5,2) and (1,1)-(5,3) give possible loops. The coupling coefficients that arise from these vertices are given in table 1.

Table 1. Breakdown of coupling coefficients in parts.

i=2, j=5	(1,0)-(5,2)	(1,0)-(5,3)	(1,1)-(5,2)	(1,1)-(5,3)
Sign γ	-1	1	1	-1
Y_{Head}	0	0	0	0
Y_{Upper}	2, 4	3	0	0, 1
Y_{Lower}	8, 9	9	6	5, 7
Y_{Tail}	10	0	10	0
Sign γ	-1	1	1	-1
Y_I	13, 15	4	11	1, 2
Y_J	19, 20	10	17	6, 8

We get 6 non-zero coupling coefficients, that are represented by 24 numbers (Signs and the partial Y-values). In this case representation by the summed numbers as is done in the last three lines would be more advantageous since it gives only 16 numbers. One can easily imagine, however, that in larger spaces the former representation becomes more favourable.

A.2. Coupling coefficients in symmetry adapted graphs.

In symmetry adapted graphs the evaluation of the coupling coefficients can be done analogous to the way it is done in the non-symmetry adapted case. A difference is the representation of the Y_{Tail} part. We have to consider the case that the spinors i and j belong to different representations. This means that E_{ij} connects determinants that belong to different symmetry representations. The paths that represent these determinants hence end in different vertices. Graphically this is seen in the fact that the paths no longer join at the Tail vertex (Figure 3). This implies that although the

occupation of their Tail parts is identical we obtain different contributions to their index. In the example shown in figure 3, we find that I has index 6 in representation Γ_1 while J has index 5 in representation Γ_3. Y_{Tail} is now different, which means that we need an additional number to represent I-J pairs.

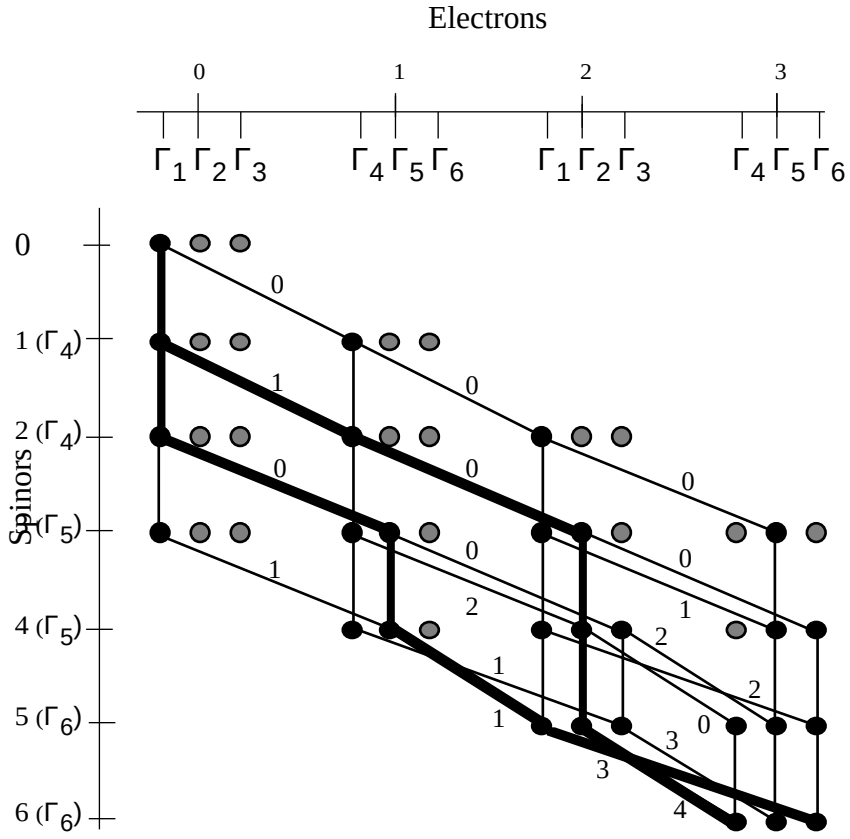

Figure 3. Loops in symmetry-adapted graphs.

We can use the symmetry-adapted graph to specify the representation that we want to calculate coupling coefficients for. If we do a CI calculation on a number of states that belong to representation Γ_λ than we only need coupling coefficients γ_{ij}^{IJ} with either I or J belonging to representation Γ_λ. This reduces the number of coupling coefficients that we have to calculate.

For example, if we specify the constraint that J belong to Γ_5 for the excitation E_{25} of the example of the previous paragraph, we find that the only vertex combination that remains is the (1, 1, Γ_4) - (5, 3, Γ_5) combination. The other possible vertex combinations can either not be connected to each other, the Head vertex can not be reached from the (0, 0, Γ_1) vertex or the Tail vertex can not be connected to the (6, 3, Γ_5) vertex. The number of coupling coefficients is now two, a reduction of the original number with a factor of three.

A.3. Separation of external space

In singles and doubles type CI-calculations the spinor space is divided into basically two sets, an internal space consisting of a small number of spinors that is almost completely occupied and an external space consisting of a large number of virtual spinors that is occupied by at most 2 electrons. In the RASCI formalism this corresponds to a large RAS3 space and a maximum excitation level $n_{E3} = 2$.

These constraints give rise to a simple form of the diagram in the RAS3 part. The possible loops that may be formed in this space are simple, since only two diagonal arcs may be occupied. We can especially use this simplicity to evaluate the coupling coefficients in the case of two-electrons integrals (ij | kl) with 3 or more external indices. This class is the most abundant one in these type of CI calculations, so reduction in the number and evaluation time of the coupling coefficients will give important reductions in the CPU-time involved with the calculation.

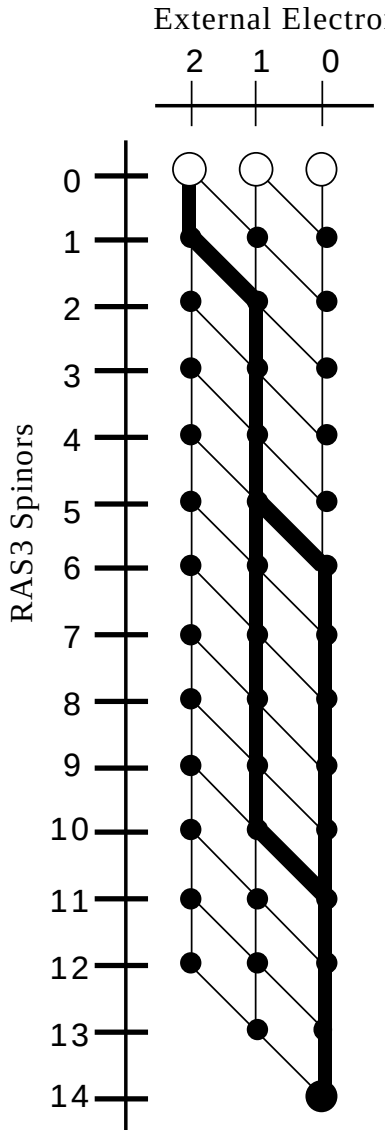

As an example wetake the case in which j > i > k > l, with i, j, k RAS3. In the second quantised hamiltonian this integral is connected to the double excitation $E_{ij}E_{kl}$. In the expression for the sigma vector (chapter 3, formula46) we operate first with E_{kl} on a determinant |J> to obtain determinant |K>, after which we operate with E_{ij} on |K> to obtain determinant |I>. We can now simplify the calculation of the coupling coefficients γ_{ij}^{IK} that are connected with the second excitation, E_{ij}. Since k belongs to RAS3 we know that the determinants |I> and |K> have a fixed, occupied arc in the RAS3 part of the diagram. The other arcs are determined by the restriction that i must be occupied in I and that j must be occupied in |K>. This means that only one single loop is possible. The situation is sketched in figure 4 for the integral (611 | 2 x), with x representing an arbitrary spinor in RAS1 or RAS2.

Figure 4. Separation of external space. Only the external part of the diagram is drawn.

The coupling coefficients γ_{ij}^{IK} that are needed by the evaluation of integrals with 3 or 4 external spinors hence can be evaluated with a few operations and need not be fetched from computer memory or disk. Their number is also reduced relative to the complete set of one-electron coupling coefficients since we used the constraint that spinor k was occupied.

In the symmetry adapted graphs one can also use this technique. The diagrams and formulas are a little more complicated but no fundamental difficulties arise.

References

1) W. Duch, GRMS or Graphical Representation of Model Spaces, Lecture Notes in Chemistry **42**, (Springer: Berlin 1986).

2) P. E. M.Siegbahn, J. Chem. Phys. **72**, 1647 (1980).